

Springer Theses

Recognizing Outstanding Ph.D. Research

Jérôme Gleyzes

Dark Energy and the Formation of the Large Scale Structure of the Universe



Springer

Springer Theses

Recognizing Outstanding Ph.D. Research

Aims and Scope

The series “Springer Theses” brings together a selection of the very best Ph.D. theses from around the world and across the physical sciences. Nominated and endorsed by two recognized specialists, each published volume has been selected for its scientific excellence and the high impact of its contents for the pertinent field of research. For greater accessibility to non-specialists, the published versions include an extended introduction, as well as a foreword by the student’s supervisor explaining the special relevance of the work for the field. As a whole, the series will provide a valuable resource both for newcomers to the research fields described, and for other scientists seeking detailed background information on special questions. Finally, it provides an accredited documentation of the valuable contributions made by today’s younger generation of scientists.

Theses are accepted into the series by invited nomination only and must fulfill all of the following criteria

- They must be written in good English.
- The topic should fall within the confines of Chemistry, Physics, Earth Sciences, Engineering and related interdisciplinary fields such as Materials, Nanoscience, Chemical Engineering, Complex Systems and Biophysics.
- The work reported in the thesis must represent a significant scientific advance.
- If the thesis includes previously published material, permission to reproduce this must be gained from the respective copyright holder.
- They must have been examined and passed during the 12 months prior to nomination.
- Each thesis should include a foreword by the supervisor outlining the significance of its content.
- The theses should have a clearly defined structure including an introduction accessible to scientists not expert in that particular field.

More information about this series at <http://www.springer.com/series/8790>

Jérôme Gleyzes

Dark Energy and the Formation of the Large Scale Structure of the Universe

Doctoral Thesis accepted by
the Institute for Theoretical Physics-CEA Saclay, France

 Springer

Author
Dr. Jérôme Gleyzes
Jet Propulsion Laboratory
Pasadena, CA
USA

Supervisor
Dr. Filippo Vernizzi
CEA, IPhT
Gif-sur-Yvette
France

ISSN 2190-5053

Springer Theses

ISBN 978-3-319-41209-2

DOI 10.1007/978-3-319-41210-8

ISSN 2190-5061 (electronic)

ISBN 978-3-319-41210-8 (eBook)

Library of Congress Control Number: 2016943810

© Springer International Publishing Switzerland 2016

This work is subject to copyright. All rights are reserved by the Publisher, whether the whole or part of the material is concerned, specifically the rights of translation, reprinting, reuse of illustrations, recitation, broadcasting, reproduction on microfilms or in any other physical way, and transmission or information storage and retrieval, electronic adaptation, computer software, or by similar or dissimilar methodology now known or hereafter developed.

The use of general descriptive names, registered names, trademarks, service marks, etc. in this publication does not imply, even in the absence of a specific statement, that such names are exempt from the relevant protective laws and regulations and therefore free for general use.

The publisher, the authors and the editors are safe to assume that the advice and information in this book are believed to be true and accurate at the date of publication. Neither the publisher nor the authors or the editors give a warranty, express or implied, with respect to the material contained herein or for any errors or omissions that may have been made.

Printed on acid-free paper

This Springer imprint is published by Springer Nature

The registered company is Springer International Publishing AG Switzerland

Supervisor's Foreword

In the last 30 years, cosmology has witnessed much progress mostly spurred by a positive interplay between theoretical developments and observational discoveries. Thanks to high-precision data such as the cosmic microwave background anisotropies, we have been able to reconstruct the evolution of the universe and of the structures that we observe today with an exquisite accuracy. For instance, we know that large-scale structures formed by the gravitational collapse of dark matter around some small initial inhomogeneities. According to our current understanding, the initial seeds of these inhomogeneities were generated during inflation, an early universe phase characterised by an accelerated expansion, triggered by the vacuum energy of a scalar field. The quantum fluctuations of this field, converted into density perturbations, are imprinted in the observable sky. By studying their statistical distribution we have been able to confirm inflationary predictions. Despite these confirmations, inflation remains a paradigm awaiting for a convincing proof and lacking robust connections with known high energy physics.

Even more mysterious, the current accelerated expansion of the universe, discovered in 1998, has triggered enormous interest in both the communities of observational cosmologists and theoretical physicists. The simplest explanation, a cosmological constant is consistent with observations. However, given the theoretical difficulties traditionally associated to this possibility, most of the efforts of the scientific community are now devoted to rule it out. Alternatively, the acceleration may be due to some dynamical component called dark energy or to some modification in the laws of gravity on very large scales. Many models have been proposed, each of them leading to specific effects on the evolution of structures formation. As for inflation, the knowledge of the statistical properties of the large-scale structures and their evolution may be critical to help to better understand the origin of the current acceleration. For this reason, the major science agencies are currently planning large field cosmic surveys. The main scientific driver of these ground based and space telescopes is a precise determination of the statistical properties of the cosmic fields and their evolution, with the primary goal of constraining dark energy and the origin of cosmological perturbations.

Jérôme Gleyzes started to work on his Ph.D. thesis in this scientific context. He first focused his research on bridging theoretical models of dark energy with observations. It should be emphasised that the number and variety of proposed models of dark energy and modified gravity is rather impressive, which represents a challenge for future observations. Jérôme developed an approach to characterise most models in a unified way, in terms of a few number of parameters corresponding to particular observational effects on cosmological scales. This is based on the construction of a general theory of cosmological perturbations around a cosmological background in terms of all possible Lagrangian operators satisfying certain symmetries, dictated by the class of models under consideration. This approach has rapidly become popular in the scientific community under the name of effective field theory of dark energy and will likely play an important role in years to come in attempts to constrain deviations from general relativity on cosmological scales.

In developing this approach, to avoid models with instabilities Jérôme restricted to the quadratic operators leading at most to two derivatives in the equations of motion for the propagating degrees of freedom. However, he discovered that the quadratic operators satisfying these properties were one more than those needed to describe the so-called Horndeski theories. This came as a surprise, because such theories, developed by Horndeski in the seventies and recently rediscovered, were long believed to be the most general ones being free from dangerous instabilities. By completing the Lagrangian of the quadratic operators at the full non-linear level, he was able to construct theories beyond Horndeski. These theories allow higher derivatives in the equations of motions. However, due to their degeneracy they only contain propagating degrees of freedom whose order of derivatives is never higher than two, as required for a healthy theory without instabilities. This discovery led to a very rich activity in the literature, with many studies of the phenomenological consequences of theories beyond Horndeski and several theoretical developments on their extensions.

In 2014, triggered by the exciting—but unfortunately incorrect—conclusions that the BICEP2 telescope had observed primordial gravitational waves from inflation, Jérôme turned to the study of inflationary predictions. As I mentioned above, current observations confirm inflation. However, incontestable evidence could only come from observing primordial tensor modes. In this context, Jérôme demonstrated that the predictions for the gravitational wave spectrum from inflation are completely robust. In particular, despite some claims in the literature, he showed that it is not possible to alter the standard predictions of inflation by modifying the speed of propagation of tensors. In contrast to what happens for scalar fluctuations, a scale-invariant spectrum of tensor fluctuations can only arise in inflation. Thus, the measurement of the gravitational wave amplitude would unambiguously determine the energy scale of inflation.

Finally, the last part of the thesis is devoted to the so-called consistency relations, relations between correlation functions of the cosmic fields (e.g. the dark matter density contrast or the galaxy number density), valid in the limit in which one of the wavelength modes is much longer than the others. These relations are

non-perturbative for the short-scale modes; in other words they automatically incorporate short-scale baryonic effects and the bias between galaxies and dark matter. For this reason, they can be employed as a test of standard cosmology. Moreover, Jérôme showed that since they are based on the equivalence principle, their breaking can be used to test the presence of a fifth force, which arises in some modified gravity models.

In conclusion, Jérôme's thesis covers many aspects of modern cosmology. It provides an innovative and pedagogical introduction to each of them and contains cutting-edge results, rare to be found in a unique research manuscript. It should be clear that Jérôme's research has already made a large impact in the community and will surely continue to do so in the future.

Gif-sur-Yvette, France
April 2016

Dr. Filippo Vernizzi

Acknowledgements

This Ph.D. has been a great adventure, where I interacted with a number of excellent people, for which I am extremely grateful. A special mention to the students at ICTP, like Marko and Gabriele, whom I visited numerous times. To Michele, I say thank you for sharing the work, writing notes, and being there to compare our codes.

I have learnt a lot from many great scientists. In particular, I would like to thank Claudia de Rham, Andrew Tolley, Justin Khoury and Mark Trodden for the time I had with them where our interactions were very fruitful. I would also like to give many thanks to Pedro Ferreira and Tessa Baker. My visits to Oxford were always enriching.

Finally, I would like to give special thanks to the people that played a crucial role during my Ph.D. and have shaped the researcher I am today: Paolo Creminelli, David Langlois, Federico Piazza. The most important of them is Filippo Vernizzi, my advisor. Thanks for always being there to answer my questions, for treating me like an equal, for giving me so many opportunities to travel and present our work, and for guiding me through many aspects of the world of physicists.

Contents

1	Introduction	1
1.1	The Homogeneous Universe	1
1.1.1	The Friedmann-Lemaître-Robertson-Walker Metric	2
1.1.2	Comoving Distance and Redshift	3
1.1.3	The Friedmann Equations	4
1.1.4	Observations and the Discovery of Dark Energy	5
1.2	The Large Scale Structure of the Universe	8
1.2.1	Growth of Perturbation in Λ CDM	10
1.2.2	Galaxy Surveys	12
1.2.3	Weak Lensing	14
1.3	This Thesis	18
	References	19
2	The Effective Field Theory of Dark Energy	21
2.1	The Unitary Gauge Action	22
2.2	ADM Formalism and the Effective Field Theory of Dark Energy	24
2.2.1	Background Evolution	25
2.2.2	The Quadratic Action	27
2.3	Going from Models to the EFT of DE	32
2.4	Stability and Theoretical Consistency	35
2.5	Evolution of Cosmological Perturbations	37
2.5.1	Vector Sector	37
2.5.2	Tensor Sector	38
2.5.3	Scalar Sector	38
2.6	Conclusions	46
	Appendix	48
	References	50
3	Beyond Horndeski	53
3.1	Horndeski Theories	53
3.2	General Considerations on Higher Order Derivatives	55

- 3.3 Generalized Generalized Galileons G^3 57
- 3.4 Hamiltonian Analysis 58
- 3.5 Field Redefinitions 61
- 3.6 Linear Analysis and Coupling to Matter 64
 - 3.6.1 Stability and Ghosts 64
 - 3.6.2 Newtonian Gauge and Einstein Frame 65
- 3.7 Conclusions 68
- References 68
- 4 Predictions for Primordial Tensor Modes 71**
 - 4.1 Introduction to Inflation 71
 - 4.1.1 The Horizon Problem 72
 - 4.1.2 The Predictions of Inflation 73
 - 4.1.3 Characteristics of the Fluctuations 74
 - 4.2 Tensor Sound Speed and Quadratic Action 79
 - 4.3 Other Operators 81
 - 4.4 Conclusions 83
 - References 83
- 5 Consistency Relations of the Large Scale Structure 85**
 - 5.1 Deriving Consistency Relations 86
 - 5.1.1 Several Soft Legs 89
 - 5.1.2 Soft Loops 91
 - 5.1.3 Soft Internal Lines 92
 - 5.2 Going to Redshift Space 95
 - 5.3 Violation of the Equivalence Principle 96
 - 5.3.1 A Toy Model 97
 - 5.3.2 Estimate of the Signal to Noise 101
 - 5.4 Conclusions 104
 - References 105
- 6 Conclusion 107**
 - 6.1 Summary 107
 - 6.2 Outlook 108
 - References 109
- Curriculum Vitae 111**

Abbreviations

GR	General Relativity
EFT of DE	Effective Field Theory of Dark Energy
EOM	Equation(s) Of Motion
DOF	Degree(s) Of Freedom
FLRW	Friedmann–Lemaître–Robertson–Walker
ADM	Arnowitt–Deser–Misner
EP	Equivalence Principle
WEP	Weak Equivalence Principle
EFTI	Effective Field Theory of Inflation

Notations

Φ	00 part of the metric
Ψ	Trace of the spatial metric
$f_A \equiv \frac{\partial f}{\partial A}$	A subscript denotes a partial derivative
$\phi_\mu \equiv \nabla_\mu \phi,$	Covariant derivatives are denoted by an greek index
$\phi_{\mu\nu} \equiv \nabla_\nu \nabla_\mu \phi, \dots$	Generalization to several covariant derivatives
$X \equiv \phi_\mu \phi^\mu$	X will be the contraction of $\nabla_\mu \phi$
$R \equiv {}^{(3)}R$	When not specified, the Ricci scalar is the spatial one
$x \equiv \vec{x}$	A quantity in bold will signify it is a vector

Chapter 1

Introduction

I feel particularly lucky to have been working on my Ph.D. at such an exciting time for cosmology. With the fantastic results of the Planck mission [1], our picture of the Universe and its history has become much clearer. The precision of these observations, as well as that of future large scale structure missions such as EUCLID [2] and LSST [3], has also highlighted the challenges that cosmology faces. One of them is that theorists need to build efficient ways to compare theory and observations to say anything quantitative about potential deviations from the standard model of cosmology, Λ CDM (for Λ , cosmological constant, + Cold Dark Matter). Secondly, to make sure no theoretically consistent model is overlooked, the conditions to have stable theories need to be further investigated. After reviewing briefly the basis of cosmology¹ and the problem of dark energy, I will go into details on the work I've conducted, which was motivated by these two ideas. For a more detailed introduction to cosmology and dark energy, the reader is referred to Scott Dodelson's book [4], or to shorter reviews [5, 6]. You can also find online [7] the notes from Daniel Baumann's lectures on cosmology at Cambridge.

1.1 The Homogeneous Universe

In Astronomy, there does not seem to be a privileged direction in space: when looking up at the sky, stars are found in every direction (at least in a statistical sense). Based on this observation, we can deduce that, from our place in the Universe, it appears isotropic. We can then reach two conclusions; either we are in a special place of the Universe, or the Universe is isotropic from every point. Since Copernicus and Galileo, we have been used to the fact that the Earth is not a special place. Thus, it is on the second conclusion that cosmologists base their study of the Universe. We can thence go one step further, because if the Universe is isotropic from every

¹A brief introduction to the theory of inflation will be presented in Sect. 4.1.

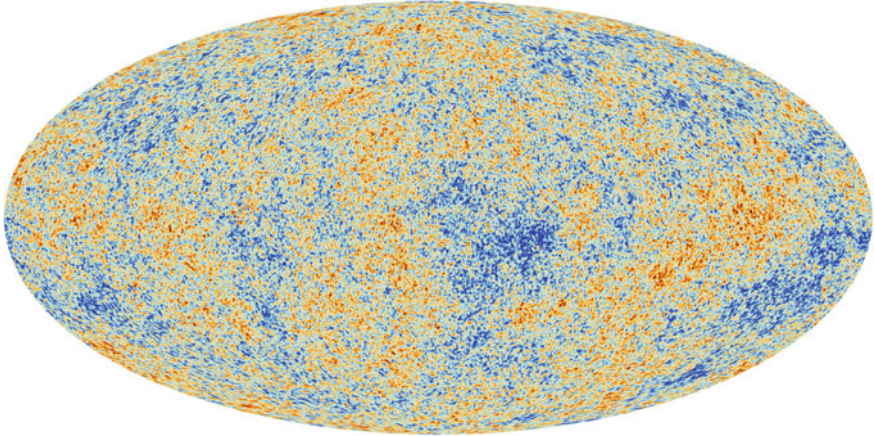


Fig. 1.1 Map of the CMB. The colder parts (*blue*) differ from the hotter (*red*) by less than 1 part in 10^5 . *Credit* ESA and the Planck Collaboration

point, it is also homogeneous. This hypothesis was later confirmed by the discovery of the Cosmic Microwave Background, a 2.725 K blackbody radiation relic of the early Universe [8], which is highly homogeneous, as illustrated in Fig. 1.1.

On such large scales (much bigger than e.g. the galaxy), the only force that is relevant is gravity. Therefore, the theoretical framework that we will use in cosmology is Einstein’s theory of General Relativity (GR). The reader is referred to textbooks on General Relativity, such as [9, 10], or Sean Carroll’s notes [11], for more details. One of the key ingredient in GR is the metric, the 4-D tensor $g_{\mu\nu}$, that describes how distances are measured in the Universe. Einstein’s field equations then relates this metric (more precisely, its derivatives) to the energy content of the Universe, hence the common saying that in GR, matter “curves” spacetime, which then affects how test-particles move in this spacetime.

1.1.1 *The Friedmann-Lemaître-Robertson-Walker Metric*

In the 1920s, both Alexander Friedmann [12] and George Lemaître [13] independently found a metric for a homogeneous, isotropic Universe. Later, Howard Robertson [14] and Arthur Walker [15] proved that this metric was in fact the only solution for such a Universe. The line element (i.e. the infinitesimal distance measure in four dimensions) for this metric is :

$$ds^2 = g^{\mu\nu} dx_\mu dx_\nu = c^2 dt^2 - a^2(t) \left[\frac{dr^2}{1 - \kappa r^2} + r^2 (d\theta^2 + \sin^2 \theta d\phi^2) \right]. \quad (1.1)$$

Here, $\kappa \in (-1, 0, 1)$ depending whether the spatial part of the Universe is, respectively, negatively curved, flat, or positively curved. $a(t)$ is the scale factor, which characterizes the expansion/contraction of the Universe.

It follows from (1.1) that even if two objects are at a constant dr , the distance between them increases because of $a(t)$. Indeed, $(r, \theta$ and $\phi)$ are spherical coordinates called comoving, because they “move along” with the expansion of the Universe. A famous (and useful although not entirely perfect) analogy to this consists of raisins in a pudding being baked. As the dough expands, the raisins move along with it, without having a movement of their own. Their comoving coordinates are not changing, but only the equivalent of $a(t)$.

1.1.2 Comoving Distance and Redshift

How can one then determine the comoving distance? One can use a photon which would travel from a distance r to an observer at the origin (since the Universe is isotropic at every point, the origin can be chosen freely) between t_{emit} and t_{obs} . Photons travel along geodesics $ds = 0$, thus (1.1) gives:

$$c dt = \pm a(t) dr . \quad (1.2)$$

Since the photon is traveling towards the origin, one has to choose the negative sign. Therefore :

$$r = c \int_{t_{\text{emit}}}^{t_{\text{obs}}} \frac{dt}{a(t)} . \quad (1.3)$$

Moreover, repeating the same calculation for a photon from r emitted at $t_{\text{emit}} + \delta t_{\text{emit}}$ and received at $t_{\text{obs}} + \delta t_{\text{obs}}$ one finds that

$$\int_{t_{\text{emit}}}^{t_{\text{obs}}} \frac{dt}{a(t)} = \int_{t_{\text{emit}} + \delta t_{\text{emit}}}^{t_{\text{obs}} + \delta t_{\text{obs}}} \frac{dt}{a(t)} , \quad (1.4)$$

in the limit where the frequency ν of the photon is much smaller than $t_{\text{obs}} - t_{\text{emit}}$, one can take $\delta t = \nu^{-1}$, which leads to $a(t_{\text{emit}})\nu_{\text{emit}} = a(t_{\text{obs}})\nu_{\text{obs}}$. Using $\lambda\nu = c$ and defining the redshift $z = \frac{(\lambda_{\text{obs}} - \lambda_{\text{emit}})}{\lambda_{\text{emit}}}$ one obtains that:

$$\frac{a(t_{\text{emit}})}{a(t_{\text{obs}})} = \frac{1}{1+z} . \quad (1.5)$$

This is a very important result because it links the scale factor to an observable quantity, the redshift z .

1.1.3 The Friedmann Equations

Having the form of the metric, one needs to apply Einstein's field equations of General Relativity (GR) to actually describe the dynamics of the Universe. These equations link the derivatives of the metric $g_{\mu\nu}$ to the energy-momentum tensor of the Universe, $T_{\mu\nu}$

$$G_{\mu\nu} + \Lambda g_{\mu\nu} = 8\pi G T_{\mu\nu}. \quad (1.6)$$

Here, $G_{\mu\nu}$ is the Einstein tensor, which characterizes the curvature of Universe (see [11] for the exact definition), Λ is the cosmological constant which appears from mathematical considerations, and G is the Newtonian gravitational constant. Under the assumption that the Universe is homogeneous and isotropic, $T_{\mu\nu}$ is the energy-momentum tensor of a perfect fluid, of density $\rho(t)$ and pressure $p(t)$, and takes the following form

$$T_{\mu\nu} = \left(\rho(t) + \frac{p(t)}{c^2} \right) u_\nu u_\mu + p(t) g_{\mu\nu}, \quad (1.7)$$

with $g_{\mu\nu}$ the metric tensor and u_μ the velocity four-vector.² Friedmann showed in 1922 [12] that combining the metric from (1.1) with (1.6) yields two independent equations, which are now named after him,

$$H^2(t) = \frac{8\pi G}{3} \rho(t) - \frac{k}{a^2(t)} + \frac{\Lambda}{3}, \quad (1.8)$$

$$\frac{\ddot{a}(t)}{a(t)} = -\frac{4\pi G}{3} (\rho(t) + 3p(t)) + \frac{\Lambda}{3}, \quad (1.9)$$

where $H = \frac{\dot{a}}{a}$. The conservation of the energy-momentum tensor³ gives a third equation related to the two previous ones,

$$\dot{\rho}(t) = -3H(t)(p(t) + \rho(t)). \quad (1.10)$$

If the Universe is composed of different fluids, labelled i , then $\rho = \sum_i \rho_i$ and $p = \sum_i p_i$. In order to simplify those equations, people usually define $\rho_{\text{crit}} = \frac{3H^2(t)}{8\pi G}$, $\Omega_i = \frac{\rho_i}{\rho_{\text{crit}}}$, and $w_i(t) = \frac{p_i}{\rho_i}$. In (1.8) and (1.9) the Λ -term has been moved to the other side of the equation and is considered as one of the fluids composing the Universe, with $\rho_\Lambda = \frac{\Lambda}{8\pi G}$ and $T'_{\mu\nu} = T_{\mu\nu} + \rho_\Lambda g_{\mu\nu}$. For the new fluid to satisfy (1.9), one has to set $p_\Lambda = -\rho_\Lambda$.

²In the rest of this thesis, unless specified, we take $c = 1$.

³This results from the invariance of the matter action under coordinate transformations, as we will see later in Sect. 2.5.3.

1.1.4 Observations and the Discovery of Dark Energy

In order to see how far a source is, one starts by measuring how much known spectrum lines of the source are redshifted. Once calibrated with sources which have known distances (e.g. sources with known intrinsic luminosities), astronomers can have access to the distance of the source. This distance redshift relation is crucial, as it is one of the few ways to measure the distance of very far objects.

However, as seen in the previous section, the redshift is linked to the scale factor, whose dynamics is dictated by the Friedmann equations. Thus, different cosmological models will give a different distance-redshift relations, which can then be compared to the actual data. The luminosity distance $r_L(z)$ is defined as $r_L^2(z) = \frac{L}{4\pi l}$, where L is the intrinsic luminosity and l is the apparent luminosity, the one actually measured by an observer. This distance can be related to the geometry (and cosmology) through

$$r_L = (1+z) \times \begin{cases} \sinh r & \text{if } \kappa = 1, \\ r & \text{if } \kappa = 0, \\ \sin r & \text{if } \kappa = -1, \end{cases} \quad (1.11)$$

where κ is the spatial curvature in Eq.(1.1) and r is given in Eq.(1.3).

Traditionally, astronomers use magnitudes instead of luminosities, and they define the distance modulus μ as:

$$\mu = m(z) - M = 25 + 5 \log_{10} \left(\frac{r_L}{10\text{pc}} \right). \quad (1.12)$$

where m is the apparent magnitude, and M the absolute magnitude of the source and pc means parsec.⁴

The problem is that, to compute the distance modulus, one needs to know the intrinsic luminosity of the source. There is one candidate that has been found : Type Ia Supernovae (SN Ia). Those sources are the result of the explosion of dying stars. They don't always have the same luminosity, but they have a characteristic light curve (i.e. the luminosity as a function of time after the explosion): the faster they fade, the fainter they were. By calibrating this relation, one can have access to the absolute magnitude [17]. Using these standard candles, astronomers ([18–20]) found that the simplest model which best fitted the observations was a flat universe filled with non-relativistic cold matter and a non zero cosmological constant, see Fig. 1.2.

Nevertheless, there is no observation of these candles for redshifts higher than $\simeq 2$. To probe at higher redshift, another standard ruler for the distance-redshift relation can be found in the CMB. Indeed, there must have been small inhomogeneities in the matter distribution just after the Big Bang, otherwise, there would not be the large scale structure seen today. Those overdensities gravitationally attracted more matter. However, before the Universe cooled down to below 3000 K (recombination

⁴1 parsec (pc)= 3.1×10^{16} m = 3.3 lightyears (ly).

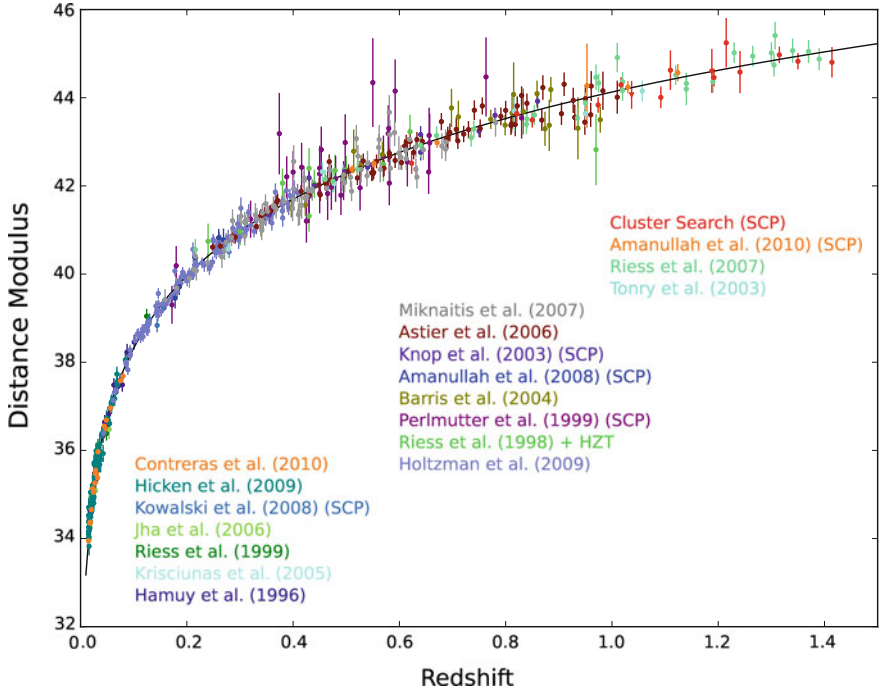


Fig. 1.2 The distance modulus of Eq.(1.12) as a function of redshift. The *solid line* represents the best-fit cosmology for a flat Λ CDM Universe for supernovae alone. *Credit* Suzuki et al. [16] ©AAS. Reproduced with permission

epoch, $z \simeq 1100$), photons interacted tightly with baryonic matter. Thus, overdense regions for matter were also overdense regions for photons, and the pressure from the compressed photons resulted in an outward force on the baryons, expulsing them with a determined velocity. As the Universe expanded and cooled, photons stopped interacting with baryons, and the baryonic waves stopped expanding, imprinting a characteristic length scale χ on the Universe at the recombination epoch, i.e. on the CMB [21]. This length scale, known as the BAO (baryon acoustic oscillations) scale, appears in correlation functions of the density field (such as the power spectrum, see Fig. 1.3, where the oscillations are due to the BAO) and can be compared to the one computed from acoustic physics. This is why the CMB gives us the angular distance $d_A = \frac{\chi}{\Delta\theta}$ at $z \simeq 1100$ [22]. This d_A can also be related to cosmology since $d_A = r_L/(1+z)^2$.

Combining these different probes yields likelihood contours in the $(\Omega_{m,0}, \Omega_{\Lambda,0})$ map, overlapping at $\sim (0.3, 0.7)$, shown in Fig. 1.4.

This is why the Λ CDM model is also called the concordance model (see [22] for the value of the parameters). However, this model may be in good agreement with the Supernovae Ia data and CMB, but there are still problems with it :

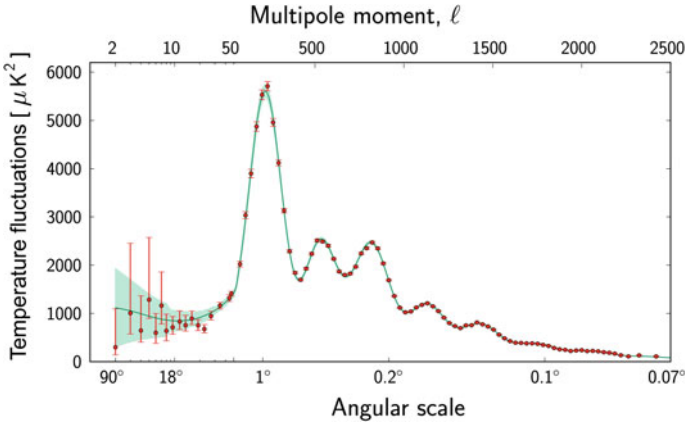
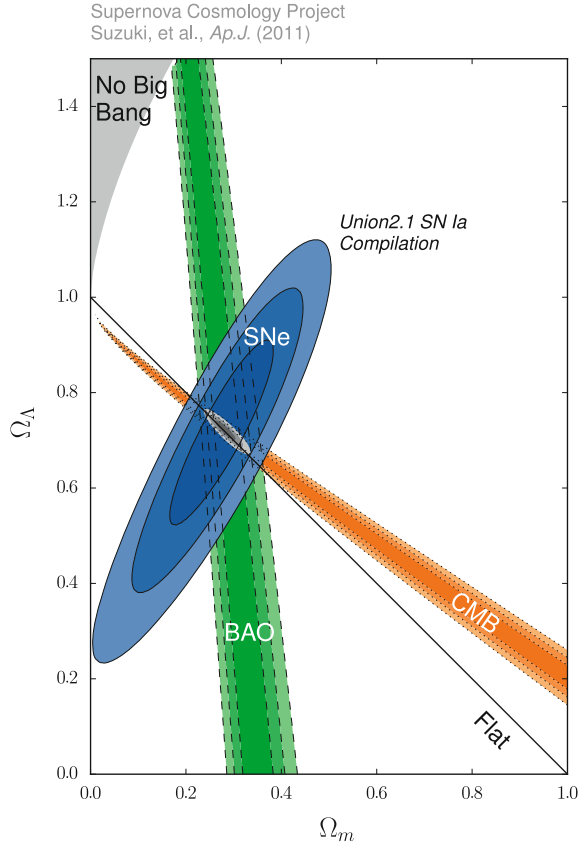


Fig. 1.3 Power Spectrum (i.e. the variance) of the fluctuations in Fig. 1.1, which are proxies for the matter overdensities discussed above, as measured by Planck [22]. It is plotted as a function of the multipole moment l (high l 's correspond to small angles in the sky). The *red dots* are the measurements and the *green* is the best-fit Λ CDM prediction. *Credit* ESA and the Planck Collaboration

- We do not really know what dark energy is. In the standard cosmological model, it is assumed to be a cosmological constant. However, the value that we get from observations is deeply puzzling: it is many orders of magnitude smaller than the expected contribution from the vacuum energy (that behaves also as a cosmological constant). Even worse, if by some amazing coincidence, the contributions from the vacuum energy and the bare cosmological constant in Eq. (1.6) were to cancel and give the small value of Λ_{obs} that is measured, quantum fluctuations would spoil that cancellation and bring Λ_{obs} to a much higher value [23, 24]. In theorist's terms, the smallness of the cosmological constant is not technically natural. This problem is called the old cosmological constant problem.
- In this model, the Universe is matter dominated in the past, and dark energy dominated in the future. It is thus somewhat odd that we find ourselves in the short lapse of time where the two densities are of the some order. This is known as the new cosmological constant problem.

Due to the limited number of probes and their relative lack of precision, a vast range of cosmological models agrees with the observational data behind Fig. 1.4. They are all pretty much indistinguishable from each other (and from a cosmological constant) at the background level, but significant differences can arise when considering the perturbed Universe, particularly in the way structures (such as clusters of galaxies) evolve. This is why a lot of effort is put into better measuring and characterizing the large scale structure of the Universe.

Fig. 1.4 Combination of results for different probes.
 Credit Suzuki et al. [16]
 ©AAS. Reproduced with permission



1.2 The Large Scale Structure of the Universe

The history of the large scale structure of the Universe starts with Fig. 1.1, in particular with the small fluctuations that one can see by eye (although the differences in temperature are at the order of one part in 10^5). Those fluctuations, which are thought to origin from quantum fluctuations during inflation (this will be discussed in more detailed in Sect. 4.1), are the seeds of the galaxies that we observe in the sky. In the standard picture, Λ CDM, one then uses the laws of general relativity (GR) to evolve the fluctuations from early times to today. The picture is simple: overdense region in matter create potential wells for gravity, which in term attract more matter.

In practice, because GR is non linear, following the history down to very small scales (such as that of galaxies) is extremely hard. One often has to use N -body simulations, which recreate (parts of) the Universe on a supercomputer and trace the behavior of matter, from large scales to small (Fig. 1.5). What theorists can do is work in a perturbative framework, on the scales where the non linearity from GR

are not yet playing in important role. The scale of reference is anything larger than roughly tens of megaparsecs, while a galaxy is typically tens of kiloparsecs.

For a detailed introduction to the subtleties of cosmological perturbations, the reader is referred to e.g. [25, 26].

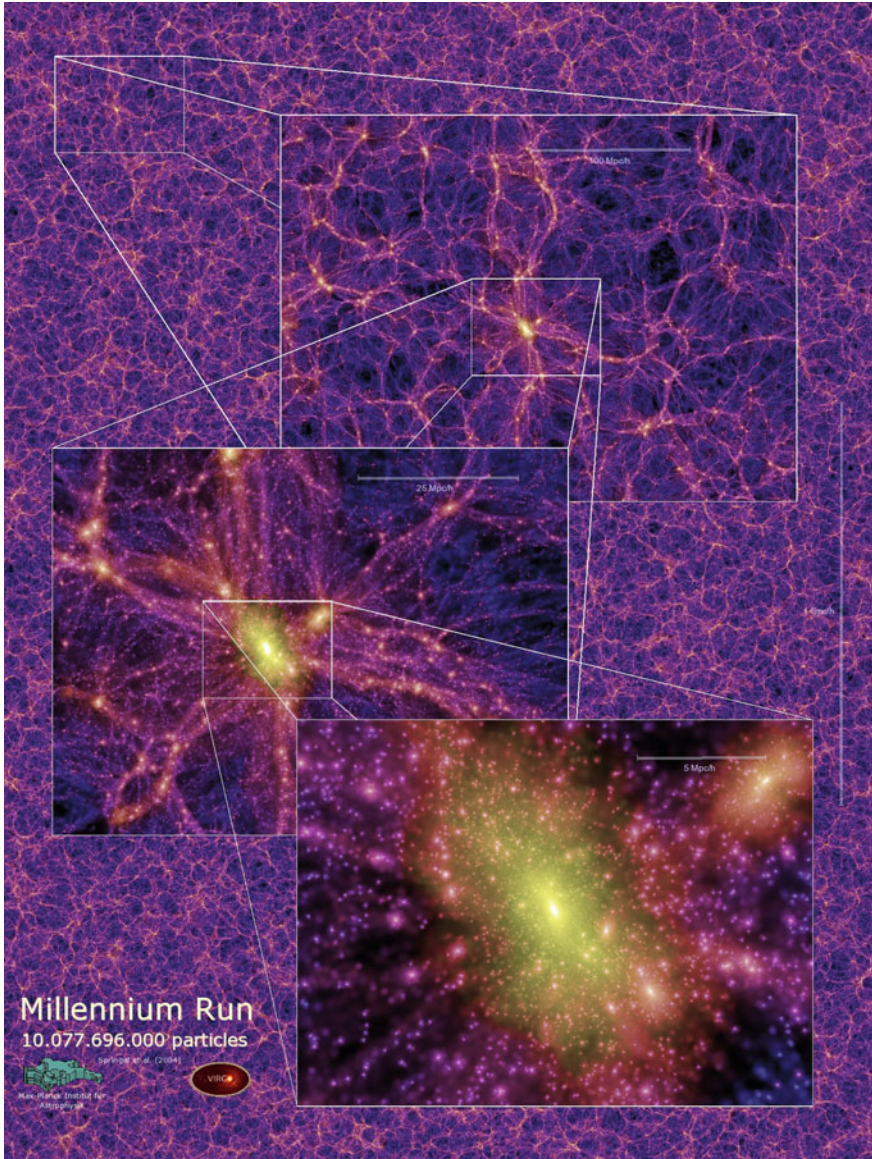


Fig. 1.5 The simulated Universe at different scales. *Credit Millennium simulation–Virgo [27]*

1.2.1 Growth of Perturbation in Λ CDM

The dynamics of the Universe are captured by two sets of equations. First, Einstein's equations

$$G_{\mu\nu} + \Lambda g_{\mu\nu} = 8\pi G T_{\mu\nu}, \quad (1.13)$$

and secondly, the conservation of the stress energy tensor of the Universe

$$\nabla_\mu T^{\mu\nu} = 0. \quad (1.14)$$

The latter comes from the invariance under coordinate transformations (see Sect. 2.5.3 for more details). This symmetry also implies that we are free to choose the coordinate system we want to describe the system. This is called choosing a gauge, i.e. a specific form for the metric $g_{\mu\nu}$. A convenient one for the studies of growth is the Newtonian gauge, whose name comes from the fact that the equations take a form very similar to that of Newtonian gravity. The metric can be cast as (at linear order in perturbations)

$$g_{\mu\nu} = \begin{pmatrix} -(1+2\Phi) & 0 \\ 0 & a^2(1-2\Psi)\delta_i^j \end{pmatrix}, \quad (1.15)$$

where a is the scale factor, and δ_i^j is the Kronecker delta symbol.

With this metric and in Fourier space, the dynamics in the Newtonian limit (which corresponds to focusing on wavenumber $k \gg aH$) is governed by

$$-\frac{k^2}{a^2}\Phi = 4\pi G \sum_i \bar{\rho}_i \delta_i, \quad (1.16)$$

where for each fluid i with background density $\bar{\rho}_i$ I have defined the density contrast $\delta_i = (\rho_i - \bar{\rho}_i)/\bar{\rho}_i$. Since the effect of dark energy becomes manifest only after matter-radiation equality, I will focus in the following on matter only. The conservation of the stress energy tensor of matter yields two equations (one for the temporal part, one from the spatial part), which are the standard continuity and Euler equations. In Fourier space, they read

$$\dot{\delta}_m - \frac{k^2}{a^2}v_m = 0, \quad (1.17)$$

$$\dot{v}_m + \Phi = 0, \quad (1.18)$$

v_m is the velocity potential, defined such that $\mathbf{v}_m = \nabla v_m$. The two equations above can be combined to give a single equation for the evolution of δ_m .

$$\ddot{\delta}_m + 2H\dot{\delta}_m - \frac{k^2}{a^2}\Phi = 0. \quad (1.19)$$

Therefore, the growth of matter perturbation depends critically on gravity. If it obeys the standard equation (1.16), then this can be written as⁵

$$\ddot{\delta}_m + 2H\dot{\delta}_m + 8\pi G\bar{\rho}_m\delta_m = 0. \quad (1.20)$$

Equation (1.16) can be modified in two ways. Either by having perturbations in the dark energy (which could be the case if it were not just a cosmological constant) and thus modifying the l.h.s. or by modifying the way the potential responds to an overdensity, i.e. by modifying gravity. In practice, the two approaches are not really separate, as anything additional on the r.h.s. of Eq. (1.16) can be put on the l.h.s. and be seen as an extra fluid (see Sect. 2.5.3.2 for details).

Let me stress that the presence of a pure cosmological constant also modifies the growth since it modifies H . The typical effect is to suppress the growth compared to a case with matter only. It is easy to understand: dark energy is “repulsive”, which is why the Universe is undergoing accelerated expansion. Therefore, overdensities are less attracted when dark energy is present.

Notice that for Λ CDM, the coefficients in Eq. (1.20) are independent of k . Thus, one can look for solutions in the form $\delta_m(t, \mathbf{k}) = D_m(t) \delta_0(\mathbf{k})$, with D_m satisfying

$$\ddot{D}_m + 2H\dot{D}_m + 8\pi G\bar{\rho}_m D_m = 0, \quad (1.21)$$

and $\delta_0(\mathbf{k})$ characterizes the initial conditions. According to the inflationary scenario, this $\delta_0(\mathbf{k})$ is a (nearly) gaussian random variable (that originates from quantum fluctuations), whose two-point function reads

$$\langle \delta_0(\mathbf{k})\delta_0(\mathbf{k}') \rangle = (2\pi)^3 \delta_D(\mathbf{k} + \mathbf{k}') P_0(k). \quad (1.22)$$

The Dirac delta arises from the invariance under translation of the model, while the homogeneity and isotropy impose that P_0 depends only on the norm of \mathbf{k} . P_0 is often decomposed as follows

$$P_0(k) = A_S \left(\frac{k}{k_\star} \right)^{n_s-1} T(k)^2. \quad (1.23)$$

A_S is the amplitude of the primordial power spectrum, the one of the fluctuations at the end of inflation, at a given pivot scale k_\star (usually one takes $k_\star = 0.05 \text{ Mpc}^{-1}$). n_s is the scalar spectral index, which is very close to one: $n_s = 0.968 \pm 0.006$ (68 %C.L.) according to the Planck mission [28]. $T(k)$ is called the transfer function, and encodes the physics from the end of inflation to matter domination (see Sect. 7 of [4] for more details).

Thus, by measuring the evolution of power spectrum of δ_m with time, one can in principle access the quantity D_m , which characterizes the growth of structures. This is the goal of many cosmological experiments, such as SDSS [29], CFHTLenS

⁵Note that by definition of a cosmological constant, it does not have perturbations: $\delta_\Lambda = 0$.

[30], Euclid [2], LSST [3] and WFIRST [31]. In the following, I will give a brief introduction to two major probes of the large scale structure: galaxy surveys and weak lensing.

1.2.2 Galaxy Surveys

As I said above, there is much information to be gained in measuring correlation functions of the density field, either of a primordial nature (like the spectral index n_s) or concerning the growth of structures, and therefore gravity. However, this density field is mainly cold dark matter⁶ (hence the CDM in Λ CDM), which, as its name implies, does not emit light. Thus, one needs a tracer of the total matter field, something that can be seen with a telescope and that correlates with the density field.

Galaxies (and clusters of galaxies) meet these criteria. They are composed of ordinary matter (generically called baryons by cosmologists) so they can be seen, and they form in deep enough potential wells, which corresponds to peaks of the matter density field. Therefore, by cataloging galaxies and their positions, one can compute correlations functions and hope to relate them to correlation functions of the underlying density field (Fig. 1.6).

In order to do so, one introduces a bias parameter b so that the overdensity of galaxies, δ_g , is directly proportional to δ_m ,

$$\delta_g = b \delta. \quad (1.24)$$

In the simplest cases, b is just a constant. However, N -body simulations indicate that the story is more complex: b depends on redshift (i.e. on time), on the scale k , on the mass of the dark matter halo where the galaxy lives, etc. In the presence of primordial non gaussianity, it also depends on the non gaussianity parameter f_{NL} [32]. See [33, 34] for a systematic study of the bias parameter.

In practice, b is a nuisance parameter, an unknown, and needs to be fixed with N -body simulations or data, which weakens the constraining power of galaxy surveys, although there is still enough constraining power to say something about cosmology [35]. A complimentary way out of this is with redshift space distortion (RSD).

In galaxy surveys, the spatial coordinates of a galaxy are obtained through its 2-D coordinates on the sphere, while the radial coordinates is obtained through its redshift, which is related to its distance away from us (see Fig. 1.2). However, just like in the standard Doppler effect, the wavelength of photons, and therefore the redshift, is affected by the peculiar velocity of galaxies, v_g . The mapping from redshift space to real space therefore includes these peculiar velocities. The nice thing about velocities is that there is no bias on scale much larger than galaxies: both CDM and baryons feel

⁶According to Planck [22], CDM represents $\sim 85\%$ of the matter content.

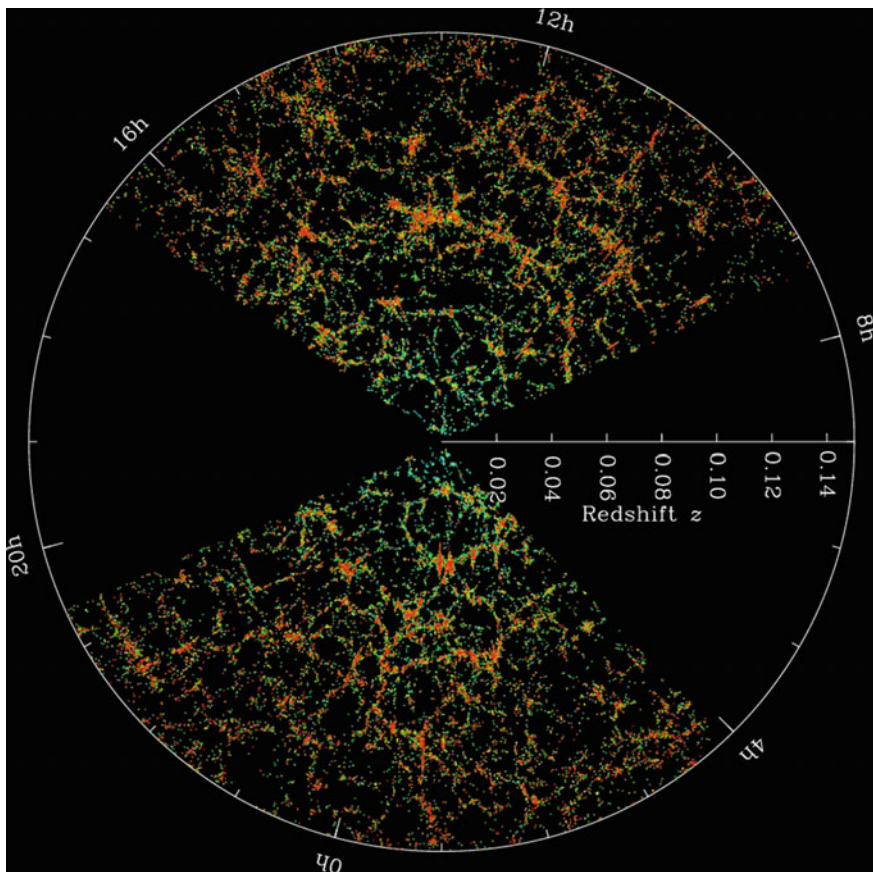


Fig. 1.6 Distribution of galaxies as measured by SDSS [29]. The *colors* correspond to the age of the stars inside the galaxies, with *red* being old stars. The *black regions* represent the parts that are masked by our own galaxy. *Credit* M. Blanton and the Sloan Digital Sky Survey

the same force, as given in the Euler equation (1.18).⁷ Using the continuity equation as well, one can show that the velocity potential verifies

$$v_g = \frac{a^2 H}{k^2} f \delta_m, \quad f \equiv \frac{d \ln D_m}{d \ln a}. \quad (1.25)$$

Combining all this leads to the Kaiser formula [38]

$$P_{\text{obs}}(\mathbf{k}) = (b + f \mu^2)^2 P_\delta(k), \quad \mu \equiv \frac{\mathbf{k} \cdot \hat{\mathbf{z}}}{k}. \quad (1.26)$$

⁷This assumes the validity of the equivalence principle. This is no longer true otherwise, see [36, 37].

Here, P_δ is the power spectrum of the underlying density field, and μ is the angle between \mathbf{k} and the direction of the line of sight, $\hat{\mathbf{z}}$. This dependence comes from the fact that RSD are only along the line of sight. Thus, there is an angular dependence in the observed power spectrum, and the μ^4 term is independent of the bias. It is however degenerate with the overall amplitude of the power spectrum of δ (related to the amplitude of the primordial fluctuations), that also need to be measured. This is why people often quote constraints on the combination $f\sigma_8$, where σ_8 is the amplitude of the power spectrum smoothed on a $R = 8$ Mpc scale,

$$\sigma_8^2 \equiv \int \frac{d^3k}{(2\pi)^3} W(kR)^2 P_\delta(k), \quad W(x) \equiv 3 \frac{\sin x - x \cos x}{x^3}. \quad (1.27)$$

For an analysis of RSD in actual data, see e.g. [39].

Another way to get information of the growth that does not depend on the galaxy bias is through weak lensing. In GR, since matter curves spacetime, light from distance sources is deflected by the *total* matter distribution along the line of sight. Those deflections modify the shape of observed galaxies, and introduce magnification and shear in the galaxy distribution, which give information on the underlying matter distribution.

1.2.3 Weak Lensing

In general relativity, photons follow geodesics, which are given by the metric $g_{\mu\nu}$. More precisely, in Newtonian gauge, photons are sensitive to the sum of the two potentials $\Psi + \Phi$ of Eq. (1.15). In GR, $\Phi = \Psi$, but in modified gravity theories this is not necessarily the case, so I will keep them separate. The derivation that follows is inspired by the review [40], that the reader is encouraged to consult for more details. The key equation is⁸

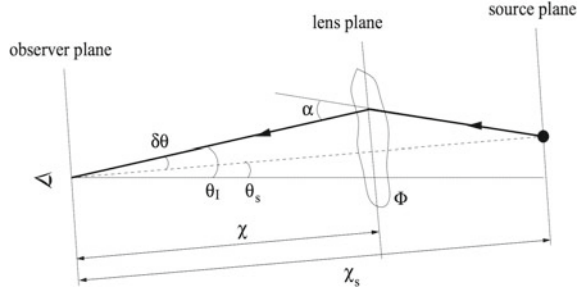
$$\delta\theta \equiv \theta_I - \theta_s = \int_0^{\chi_s} d\chi \frac{\chi_s - \chi}{\chi_s} \nabla_\perp(\Phi + \Psi). \quad (1.28)$$

$\chi = \int dz/H(z)$ is the radial comoving distance, and a subscript s means that it is measured at the source. ∇_\perp is the gradient perpendicular to the line of sight. See Fig. 1.7 for a visual representation.

The integral over χ means that we sum over all the possible sources which deflect the light ray along its trajectory. However, since one does not know the initial θ_s , $\delta\theta$ is not an observable. We need some more work to relate the deflection to something that can actually be measured. From Eq. (1.28), one can compute the shear matrix Ψ_{ij} for a source j with an observed angle θ_i

⁸For simplicity, I will assume a flat spatial metric.

Fig. 1.7 Light ray deflected by an overdensity, acting as a lens. θ_s is the original angle, while θ_I is the one observed. Courtesy of Patrick Valageas and collaborators [40]



$$\Psi_{ij} \equiv \frac{\partial \delta\theta_i}{\partial \theta_{s,j}} = \int_0^{\chi_s} d\chi \frac{\chi(\chi_s - \chi)}{\chi_s} \nabla_i \nabla_j (\Phi + \Psi). \quad (1.29)$$

This allows to construct the mapping between the image area of the source (s) and the observed area (I)

$$\begin{aligned} A &\equiv \frac{\partial \theta_s}{\partial \theta_I} = (\delta_{ij} + \Psi_{ij})^{-1} \\ &= \begin{pmatrix} (1 - \kappa - \gamma_1) & -\gamma_2 \\ -\gamma_2 & (1 - \kappa + \gamma_1) \end{pmatrix}. \end{aligned} \quad (1.30)$$

κ is called the convergence, and is related to the magnification of the source $\mu = \det[A]^{-1} \simeq 1 + 2\kappa$, while $\gamma = \gamma_1 + i\gamma_2$ is the shear, whose norm describes the distortions that conserve the area of the light bundle.

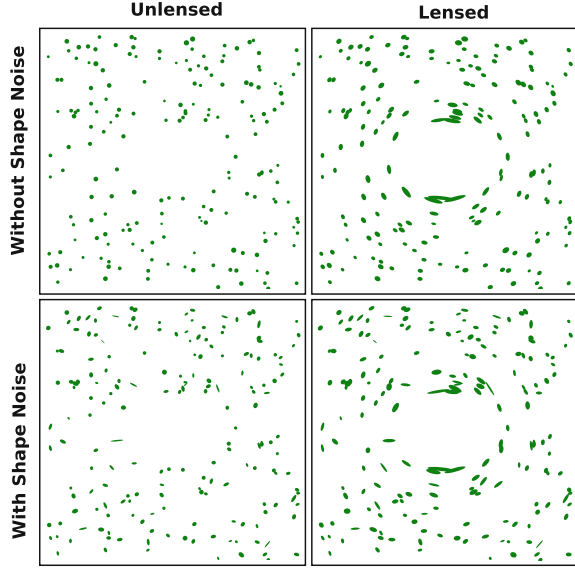
Since the original flux at the source is rarely known, it is very hard to measure the convergence κ . What can be measured is the cosmic shear. Indeed, one expects that on average, there is no correlation between the shape of galaxies (i.e. their ellipticity). This is illustrated in Fig. 1.8. Therefore, if a correlation is measured, it should be due to cosmic shear. Things are not so easy in practice, as galaxies are intrinsically aligned, because they typically reside in clusters. In the weak lensing limit, the observed ellipticity can be written as [41]

$$e \equiv \frac{1 - r^2}{1 + r^2} = e_s + 2\gamma, \quad (1.31)$$

where r is the observed axis ratio of the galaxy. Typically, the r.m.s. of e_s is of order $\sqrt{\langle e_s^2 \rangle} \simeq 0.4$, while γ is of order a few 10^{-2} . Therefore, one needs a large number of galaxies to get a sufficient signal to noise ratio [42].

Since γ is related to $\Phi + \Psi$, its power spectrum can be used for two things. Within Λ CDM, $\Phi = \Psi \propto \delta_m$, so that the power spectrum for γ give information directly on the growth. It can also be used to test gravity directly, by looking for a deviation from $\Phi = \Psi$.

Fig. 1.8 Effect of a lens on the shapes of nearby galaxies. The effect of intrinsic alignment is illustrated on the bottom panels. *Credit* Wikipedia



Let me stress that there is also another way to measure weak lensing using the CMB [43].⁹ The idea is that lensing “shifts” the CMB temperature from a given direction $\hat{\mathbf{n}}$, i.e.

$$T^{\text{lensed}}(\hat{\mathbf{n}}) = T^0(\hat{\mathbf{n}} + \mathbf{d}) = T^0(\hat{\mathbf{n}}) + \nabla T^0 \cdot \mathbf{d}, \quad \mathbf{d} = \nabla\varphi. \quad (1.32)$$

T^0 is the unlensed temperature, and φ is the lensing potential

$$\varphi \equiv - \int_0^{\chi_s} d\chi \frac{\chi(\chi_s - \chi)}{\chi_s} (\Phi + \Psi). \quad (1.33)$$

Therefore, if T^0 is statistically isotropic and homogeneous, T^{lensed} is not because of \mathbf{d} . Indeed, working in small patches of the sky where one can decompose the angular dependence in standard 2-D Fourier modes \mathbf{l} (see [44] for a generalization to the full sky),

$$T(\hat{\mathbf{n}}) = \int \frac{d^2l}{(2\pi)^2} T_l e^{i\hat{\mathbf{n}} \cdot \mathbf{l}}, \quad (1.34)$$

we have that

$$\langle T_l^0 T_{\mathbf{l}'}^0 \rangle = (2\pi)^3 \delta_D(\mathbf{l} + \mathbf{l}') C_l^0, \quad (1.35)$$

⁹I am thankful to Emmanuel Schaan for a great explanation of CMB lensing.

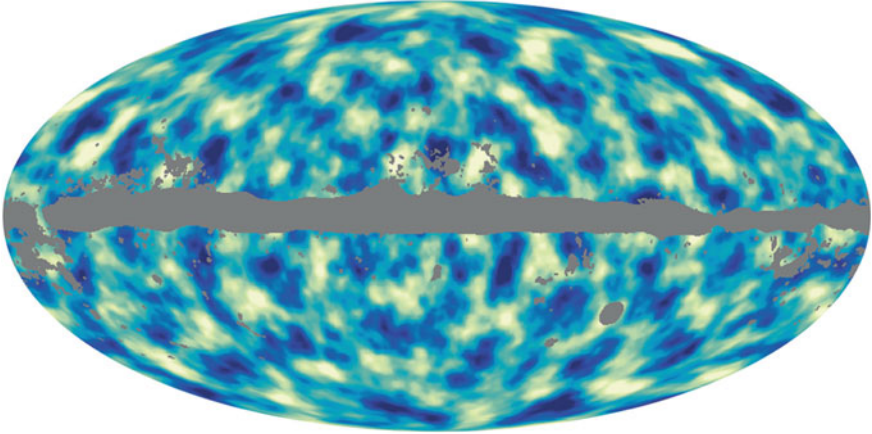


Fig. 1.9 Distribution of the dark matter in the sky, projected along the line of sight. Darker regions are denser. The grey parts were removed because of foreground contamination. *Credit ESA and the Planck Collaboration*

which is zero for $\mathbf{l} \neq -\mathbf{l}'$. However, because \mathbf{d} and T^0 are correlated (they both originate from primordial fluctuations), for $\mathbf{l} \neq -\mathbf{l}'$

$$\langle T_{\mathbf{l}}^{\text{lensed}} T_{\mathbf{l}'}^{\text{lensed}} \rangle = f(\mathbf{l}, \mathbf{l}') \varphi(\mathbf{l} + \mathbf{l}') \neq 0. \quad (1.36)$$

f is related to the statistics of the unlensed temperature [43],

$$f(\mathbf{l}, \mathbf{l}') = (\mathbf{l} + \mathbf{l}') \cdot (\mathcal{C}_l^0 \mathbf{l} + \mathcal{C}_{l'}^0 \mathbf{l}'). \quad (1.37)$$

Thus, by measuring the power spectrum between different \mathbf{l} 's, one can access the lensing potential φ , and thus, the underlying dark matter distribution. The Planck mission used this to produce a map of dark matter, see Fig. 1.9.

Note that the combination of weak lensing and galaxy surveys helps breaking degeneracies. Indeed, one now has three power spectra: galaxy-galaxy P_{gg} , galaxy-weak lensing $P_{\delta g}$, and weak lensing-weak lensing $P_{\delta\delta}$. They all scale differently with the bias parameter b , so that it can be constrained.

I hope through this rapid overview I've convinced the reader of the need to better understand our Universe on cosmological scales. In particular, I think we are now at a very interesting time, where efforts both from the theoretical and observational community are shifting. From the study of the expansion history of the Universe, where dark energy was initially discovered, we are headed into the study of the large scale structure, which contains even more information about dark energy and/or modifications of gravity. There is much work to be done on the theory side, such as better defining criteria for sensible theories from a purely formal point of view, as well as providing easier, more practical ways of relating theories to observations.

1.3 This Thesis

In particular, this has led me to develop a way to parametrize deviations from Λ CDM at the level of linear perturbations, which is called the Effective Field Theory of Dark Energy (EFT of DE). While the background evolution of the Universe is now quite constrained by distance measurements, much less is known about the evolution of the inhomogeneities that give rise to the large scale structure. Studying their behavior in the linear regime, where theoretical control is still reachable, should prove very informative. I will show in Chap. 2 that the EFT of DE allows for a systematic and quantitative exploration of deviations from Λ CDM, because of its model independence and minimal number of parameters.

While working on the EFT of DE, we realized that what was thought to be the largest class of stable theories for gravity plus a scalar, Horndeski theories [45], could actually be extended. Usually, the stability of theories is obtained by imposing that the equations of motion do not contain terms with more than two derivatives. In Chap. 3, I will argue that this is actually not a necessary condition for scalar-tensor theories. This means that before discarding higher derivatives theories, a more careful analysis needs to be performed. As we shall see, this opens the gate to new models.

Although most of cosmology has been focused on scalar perturbations since they have been actually observed, the precision reached by BICEP2 [46] seems to indicate that detecting primordial gravitational waves might well be within our grasp. They are potentially a great source of information on the early universe, since the standard predictions for tensor modes from inflation give straightforward access to its energy scale. In Chap. 4, I will present why, contrarily to the scalar case, the predictions for tensor modes are very robust. In particular, this implies that it is difficult to get a scale invariant power spectrum for gravitational waves without a period of inflation.

The final subject that I will discuss is the work I have done on consistency relations. These relations allow to express $(n + 1)$ -point correlation functions of the cosmic density fields in term of the n -point ones in the limit where one density field is slowly varying in space. As I will show in Sect. 5.1, their strength comes from the fact that very little information on the n others fields is needed: only that they have Gaussian initial conditions and that they obey the Equivalence Principle. This is a huge advantage since taking correlation functions in the large scale structure typically requires to deal with non linear evolutions that are hard to control theoretically. This control is further limited by the poorly known relation between the galaxy distribution, that we observe, and the underlying dark matter distribution, that we predict. The lack of an accurate understanding of these phenomena reduces the amount of information that can be extracted from galaxy surveys. Since consistency relations do not rely on the knowledge of short scales physics, they do not suffer from this problem. In particular, this gives access to new ways of probing the Equivalence Principle on very large scales, where gravity is less tested.

References

1. **Planck Collaboration** Collaboration, R. Adam et al., Planck 2015 results. I. Overview of products and scientific results. 1502.01582
2. **EUCLID Collaboration** Collaboration, R. Laureijs et al., Euclid Definition Study Report. 1110.3193
3. **LSST Science, LSST Project** Collaboration, P.A. Abell et al., LSST Science Book, Version 2.0. 0912.0201
4. S. Dodelson, *Modern Cosmology* (Academic Press, Amsterdam, 2003)
5. M. Trodden, S.M. Carroll, TASI lectures: introduction to cosmology, in *Progress in String Theory. Proceedings, Summer School, TASI 2003*, Boulder, USA, 2–27 June 2003, pp. 703–793 (2004). astro-ph/0401547
6. E.J. Copeland, M. Sami, S. Tsujikawa, Dynamics of dark energy. *Int. J. Mod. Phys. D* **15**, 1753–1936 (2006). hep-th/0603057
7. D. Baumann, Lecture notes on cosmology. <http://www.damtp.cam.ac.uk/user/db275/Cosmology/Lectures.pdf>
8. D.J. Fixsen, E.S. Cheng, J.M. Gales, J.C. Mather, R.A. Shafer, E.L. Wright, The cosmic microwave background spectrum from the full COBE FIRAS data set. *Astrophys. J.* **473**, 576 (1996). astro-ph/9605054
9. S. Weinberg, *Gravitation and Cosmology: Principles and Applications of the General Theory of Relativity* (Wiley, New York, NY, 1972)
10. R.M. Wald, *General Relativity* (Chicago University Press, Chicago, IL, 1984)
11. S.M. Carroll, Lecture Notes on General Relativity. gr-qc/9712019
12. A. Friedman, Über die krümmung des raumes. *Z. Phys.* **10**(1), 377–386 (1922)
13. G. Lemaitre, The expanding universe. *Mon. Not. Roy. Astron. Soc.* **91**, 490–501 (1931)
14. H.P. Robertson, Kinematics and world-structure. *Astrophys. J.* **82**, 284–301 (1935)
15. A.G. Walker, On Milne’s theory of world-structure, in *Proceedings of the London Mathematical Society*, vol. s2-42, no. 1, pp. 90–127 (1937)
16. N. Suzuki, et al., The hubble space telescope cluster supernova survey: V. Improving the dark energy constraints above $z > 1$ and building an early-type-hosted supernova sample. *Astrophys. J.* **746**, 85 (2012). 1105.3470
17. M.M. Phillips, The absolute magnitudes of type IA supernovae. *Astrophys. J.* **413**, L105–L108 (1993)
18. **Supernova Search Team Collaboration**, A.G. Riess et al., Observational evidence from supernovae for an accelerating universe and a cosmological constant. *Astron. J.* **116**, 1009–1038 (1998). astro-ph/9805201
19. **Supernova Cosmology Project** Collaboration, S. Perlmutter et al., Measurements of Omega and Lambda from 42 high redshift supernovae. *Astrophys. J.* **517**, 565–586 (1999). astro-ph/9812133
20. **Supernova Cosmology Project** Collaboration, R.A. Knop et al., New constraints on Omega(M), Omega(lambda), and w from an independent set of eleven high-redshift supernovae observed with HST. *Astrophys. J.* **598**, 102 (2003). astro-ph/0309368
21. W. Hu, N. Sugiyama, J. Silk, The physics of microwave background anisotropies. *Nature* **386**, 37–43 (1997). astro-ph/9604166
22. **Planck Collaboration** Collaboration, P. Ade et al., Planck 2015 results. XIII. Cosmological parameters. 1502.01589
23. J. Khoury, Les Houches Lectures on Physics Beyond the Standard Model of Cosmology. 1312.2006
24. A. Padilla, Lectures on the Cosmological Constant Problem. 1502.05296
25. C.-P. Ma, E. Bertschinger, Cosmological perturbation theory in the synchronous and conformal Newtonian gauges. *Astrophys. J.* **455**, 7–25 (1995). astro-ph/9506072
26. F. Bernardeau, S. Colombi, E. Gaztanaga, R. Scoccimarro, Large scale structure of the universe and cosmological perturbation theory. *Phys. Rep.* **367**, 1–248 (2002). astro-ph/0112551

27. V. Springel et al., Simulating the joint evolution of quasars, galaxies and their large-scale distribution. *Nature* **435**, 629–636 (2005). astro-ph/0504097
28. **Planck** Collaboration, P.A.R. Ade et al., Planck 2015 results. XX. Constraints on inflation. 1502.02114
29. **SDSS-III** Collaboration, S. Alam et al., The eleventh and twelfth data releases of the sloan digital sky survey: final data from SDSS-III. *Astrophys. J. Suppl.* **219**(1), 12 (2015). 1501.00963
30. **CFHTLenS** Collaboration, H. Hildebrandt, An overview of the completed Canada-France-Hawaii telescope lensing survey (CFHTLenS), in *Proceedings, 49th Rencontres de Moriond on Cosmology*, pp. 87–94 (2014). 1406.1379
31. J. Green et al., Wide-Field InfraRed Survey Telescope (WFIRST) Final Report. 1208.4012
32. N. Dalal, O. Doré, D. Huterer, A. Shirokov, The imprints of primordial non-gaussianities on large-scale structure: scale dependent bias and abundance of virialized objects. *Phys. Rev. D* **77**, 123514 (2008). 0710.4560
33. V. Assassi, D. Baumann, D. Green, M. Zaldarriaga, Renormalized halo bias. *JCAP* **1408**, 056 (2014). 1402.5916
34. V. Assassi, D. Baumann, F. Schmidt, Galaxy bias and primordial non-gaussianity. *JCAP* **1512**(12), 043 (2015). 1510.03723
35. **SDSS** Collaboration, M. Tegmark et al., Cosmological constraints from the SDSS luminous red galaxies. *Phys. Rev. D* **74**, 123507 (2006). astro-ph/0608632
36. P. Creminelli, J. Gleyzes, L. Hui, M. Simonović, F. Vernizzi, Single-field consistency relations of large scale structure. Part III: test of the equivalence principle. *JCAP* **1406**, 009 (2014). 1312.6074
37. J. Gleyzes, D. Langlois, M. Mancarella, F. Vernizzi, Effective theory of dark energy at redshift survey scales. *JCAP* **1602**(02), 056 (2016). 1509.02191
38. N. Kaiser, Clustering in real space and in redshift space. *Mon. Not. Roy. Astron. Soc.* **227**, 1–27 (1987)
39. B.A. Reid et al., The clustering of galaxies in the SDSS-III baryon oscillation spectroscopic survey: measurements of the growth of structure and expansion rate at $z = 0.57$ from anisotropic clustering. *Mon. Not. Roy. Astron. Soc.* **426**, 2719 (2012). 1203.6641
40. D. Munshi, P. Valageas, L. Van Waerbeke, A. Heavens, Cosmology with weak lensing surveys. *Phys. Rep.* **462**, 67–121 (2008). astro-ph/0612667
41. P. Schneider, C. Seitz, Steps towards nonlinear cluster inversion through gravitational distortions. I. Basic considerations and circular clusters. *Astron. Astrophys.* **294**, 411 (1995). astro-ph/9407032
42. M. Kilbinger, Cosmology with cosmic shear observations: a review. *Rep. Prog. Phys.* **78**, 086901 (2015). 1411.0115
43. W. Hu, T. Okamoto, Mass reconstruction with cmb polarization. *Astrophys. J.* **574**, 566–574 (2002). astro-ph/0111606
44. T. Okamoto, W. Hu, CMB lensing reconstruction on the full sky. *Phys. Rev. D* **67**, 083002 (2003). astro-ph/0301031
45. G.W. Horndeski, Second-order scalar-tensor field equations in a four-dimensional space. *Int. J. Theor. Phys.* **10**, 363–384 (1974)
46. **BICEP2 Collaboration** Collaboration, P. Ade et al., Detection of B -mode polarization at degree angular scales by BICEP2. *Phys. Rev. Lett.* **112**(24), 241101 (2014). 1403.3985

Chapter 2

The Effective Field Theory of Dark Energy

When looking at alternatives to the standard Λ CDM+GR model, the simplest and most common way is to introduce an extra scalar field (see [1] for a review). It can either act as an additional dark energy fluid, or as a modification of the laws of gravity themselves. It is the easiest modification one can make and is as such the first that should be explored: there is only one additional degree of freedom to consider, making it an informative step before looking at more complicated scenarios. Even in some cases where multiple degrees of freedom are added, such as in massive [2] or bimetric gravity [3] for example, one recovers the case of a single scalar field in relevant limits.

This universality is yet more manifest for a second reason. The goal of the modifications at hand are to try and explain the current accelerated expansion of the Universe [4, 5]. Thus, in general, any field added for this purpose will have a background value that is time dependent, since the homogeneous Universe evolves in time. This explicitly breaks the time diffeomorphism invariance, that can be restored as usual with Goldstone modes, which would be a single scalar in this case (see for example [6]). Therefore, the low energy perturbations around a time dependent background will generically be described by this scalar, regardless of the fundamental origin of the theory.

These ideas were first developed in the case of inflation in [7] under the name of the Effective Field Theory of Inflation and then used for example to compute higher order correlation functions, which allow to probe non-Gaussianities [8, 9]. Later, it was applied in the context of late time acceleration in the Effective Field Theory of Dark Energy (EFT of DE) in [10, 11] and also [12].

In this section, I will present the concepts behind such an approach as well as its many advantages, based on the work I did in [13], later summarized in a review [14].

2.1 The Unitary Gauge Action

The first thing I will assume is the Weak Equivalence Principle, namely that there exists a metric that universally couples to the matter sector, even if the formalism I am going to present would apply if species coupled to different metrics (see e.g. [15, 16]).

Next, the goal is to look for a generic action that would describe cosmological perturbations around a FLRW background when looking at cosmology beyond Λ CDM. By this I mean either dark energy and/or modifications of the actual laws of gravity. For concreteness, I will consider the case of an extra scalar field, ϕ . However, the idea is to be as model independent as possible considering these assumptions.

As I mentioned before, this scalar field, in a cosmological context, is naturally expected to be spacelike, i.e. to have a gradient such that $\nabla_\mu \phi \nabla^\mu \phi < 0$. In this case, the hypersurfaces of constant ϕ define a preferred foliation of time. It is convenient to use the gauge freedom in the theory to choose this specific time: this is called the unitary gauge.

By doing so, the perturbation in the scalar field are hidden, since now we have

$$\phi(\vec{t}, \vec{x}) = \phi_0(\vec{t}) + \delta\phi(\vec{t}, \vec{x}) = \phi_0(t), \quad (2.1)$$

where the last equality holds because of the choice of specific time t that is made, see Fig. 2.1. Of course, the perturbation $\delta\phi$ did not disappear, it is part of the perturbations of the metric. For example, the standard kinetic term for ϕ becomes in this gauge

$$X \equiv \nabla_\mu \phi \nabla^\mu \phi = g^{00} \dot{\phi}_0^2, \quad (2.2)$$

so that these quantities still contribute to the perturbative expansion through $g^{00} = -1 + \delta g^{00}$. The unitary gauge has therefore the advantage of having to deal only with the metric, however it has a minor inconvenient. Since a choice of time was made, the invariance under time reparametrization is lost (while leaving the spatial one intact). This means that the theory will not be manifestly covariant, as can be seen already from Eq. (2.2). Indeed, tensors with upper indices set to 0 are allowed in this gauge (they correspond to contractions with the gradient of the scalar field, e.g. $\mathcal{P}^{00} \sim \mathcal{P}^{\mu\nu} \nabla_\mu \phi \nabla_\nu \phi$). This should not be worried over, as a simple redefinition of time

$$t \rightarrow t + \pi(t, \vec{x}), \quad (2.3)$$

allows to explicitly reintroduce the invariance under time reparametrization of the theory [6]. This is known as the Stueckelberg trick and the variable π is the field

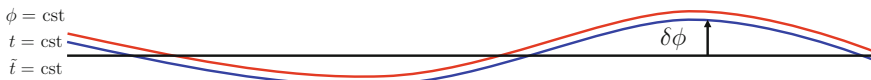


Fig. 2.1 The original time \vec{t} hypersurface in *black*. In *blue*, the new time t in unitary gauge, that is chosen so its constant hypersurfaces match the ϕ hypersurfaces (*red*).

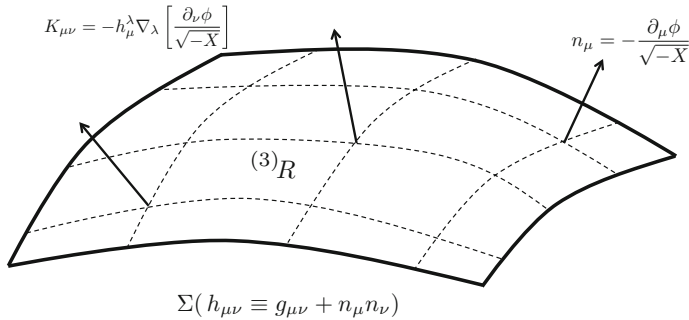


Fig. 2.2 Σ , a constant ϕ hypersurface, and its geometrical quantities: the normal vector n_{μ} , the projected metric $h_{\mu\nu}$, the intrinsic curvature R , as well as the extrinsic curvature $K_{\mu\nu}$.

that non linearly realizes this invariance. This will be useful to change gauge. In particular, to go to Newtonian gauge, where the equations of motion (EOM) have an easier interpretation.

Nevertheless, the unitary gauge will enable us to write the most general action for a scalar-tensor theory, without reference to a specific model. Indeed, in this gauge, all the terms that are invariant under spatial diffeomorphisms are in principle allowed. Further conditions can be imposed, such as second-order EOM for example, but the basic ingredients can be obtained from the geometry of the hypersurfaces illustrated in Fig. 2.2 and are the following:

- The normal vector orthogonal to the surfaces, $n_{\mu} \equiv -\frac{\nabla_{\mu} \phi}{\sqrt{-X}}$. This term is the one responsible for the presence of tensors with 0 as upper indices.
- The extrinsic curvature, $K_{\mu\nu}$. It quantifies the variation of the normal vector

$$K_{\mu\nu} \equiv h_{\mu\sigma} \nabla^{\sigma} n_{\nu}, \quad h_{\mu\sigma} \equiv g_{\mu\sigma} + n_{\mu} n_{\sigma}, \quad (2.4)$$

$h_{\mu\sigma}$ being the induced metric on the hypersurface. The quantity $K_{\mu\nu}$ tells us how the hypersurfaces are embedded in the full 4-D space.

- The final ingredient is the intrinsic curvature, given by the 3-D Ricci tensor R_{ij} of the hypersurface. This is the equivalent¹ of the 4-D Riemann tensor ${}^{(4)}R_{\mu\nu\rho\sigma}$ for the full space. In what follows, unless specified explicitly with a (4), the Ricci tensor R_{ij} and scalar R will always be the 3-D ones.

¹In three dimensions, there is as much information in the Ricci tensor as in the Riemann tensor since

$$R_{\mu\nu\rho\sigma} = R_{\mu\rho} h_{\nu\sigma} - R_{\nu\rho} h_{\mu\sigma} - R_{\mu\sigma} g_{\nu\rho} + R_{\nu\sigma} h_{\mu\rho} - \frac{1}{2} R (h_{\mu\rho} h_{\nu\sigma} - h_{\mu\sigma} h_{\nu\rho}). \quad (2.5)$$

This is because the Weyl tensor vanishes. Another way to see it is to count the independent variables in the Riemann and Ricci tensors using their known symmetries. One obtains the same number for both in three dimensions.

The numbers of combinations of these terms is infinite. This is why in the following I will impose restrictions on the categories of action I will consider. To be more quantitative, I will discuss these restrictions in the formalism of Arnowitt-Deser-Misner (ADM) [17].

2.2 ADM Formalism and the Effective Field Theory of Dark Energy

In order to be more specific about the action, I will go one step further in the distinction between space and time. To make more explicit the 3+1 decomposition, I will use the ADM form of the metric, namely write the line element as

$$ds^2 = -N^2 dt^2 + h_{ij} (dx^i + N^i dt) (dx^j + N^j dt) , \quad (2.6)$$

where N is the lapse, N^i the shift and h_{ij} is the spatial metric on constant time hypersurfaces, which can be decomposed into a scalar part, ζ , and a tensorial one, γ_{ij} as

$$h_{ij} = a^2 e^{2\zeta} (\delta_{ij} + \gamma_{ij}) , \quad \partial_i \gamma_{ij} = \gamma_{ii} = 0 . \quad (2.7)$$

With this metric and in unitary gauge, the basic ingredients I mentioned above take the simpler form

$$n_\mu = -\delta_\mu^0 N , \quad g^{00} = -\frac{1}{N^2} , \quad (2.8)$$

$$K_{ij} = \frac{1}{2N} [\dot{h}_{ij} - D_i N_j - D_j N_i] . \quad (2.9)$$

The other components are not needed. Indeed, $K^{0i} = K^{00} = 0$ since by definition (2.4) the extrinsic curvature is orthogonal to the unit vector, $n_\mu K^{\mu\nu} = 0$. D_i is the covariant derivative associated with the spatial metric h_{ij} . The 3-D Ricci tensor R_{ij} is the standard one constructed from this metric. With this decomposition of the metric, any Lagrangian respecting the spatial diffeomorphisms invariance can be cast into the generic form

$$S_g = \int d^4x \sqrt{-g} L(N, K_{ij}, R_{ij}, h_{ij}, D_i, \partial^0; t) . \quad (2.10)$$

As an example, the Einstein-Hilbert action of standard GR,

$$S_{\text{GR}} = \int d^4x \sqrt{-g} \frac{M_{\text{Pl}}^2}{2} {}^{(4)}R , \quad (2.11)$$

can be rewritten in this form as

$$L_{\text{GR}} = \frac{M_{\text{Pl}}^2}{2} [K_{ij}K^{ij} - K^2 + R], \quad (2.12)$$

using the Gauss Codazzi relation

$${}^{(4)}R = K_{\mu\nu}K^{\mu\nu} - K^2 + R + 2\nabla_\mu(Kn^\mu - n^\rho\nabla_\rho n^\mu). \quad (2.13)$$

Virtually all known models of dark energy involving a single field can be mapped onto a specific form of the Lagrangian (2.10). However, the real strength of this approach is that it allows to generically look at modifications of Λ CDM, without the need to specify a model.

To be quantitative, I will only look at the linearized theory, which means the action will only contain perturbations up to second order. Secondly, I will discuss the case where the three DOF of the theory (the two tensor polarizations and the additional scalar) obey second-order dynamics, to ensure stability. Moreover, I will assume that the full theory is given by an action $S_{\text{full}} = S_g + S_{\text{mat}}$, where S_{mat} is an action that describes minimally coupled matter.

2.2.1 Background Evolution

As I said in the Introduction, it is fairly simple in general to reproduce the same background as that of Λ CDM, even if the perturbations might be different. Nevertheless, I will firstly discuss the background equations by considering a spatially flat FLRW spacetime, whose metric reads

$$ds^2 = -\bar{N}^2(t)dt^2 + a^2(t)\delta_{ij}dx^i dx^j. \quad (2.14)$$

In this spacetime, the intrinsic curvature tensor of the constant time hypersurfaces vanishes, i.e. $R_{ij} = 0$, and the components of the extrinsic curvature tensor are given by

$$K_j^i = \frac{\dot{a}}{Na} \delta_j^i \equiv H \delta_j^i, \quad (2.15)$$

where H is the Hubble parameter. Note that since this is the background level, only a time dependence can appear. Substituting into the Lagrangian L of (2.10), one thus obtains an homogeneous Lagrangian, which is a function of $\bar{N}(t)$, $a(t)$ and of time:

$$\bar{L}(a, \dot{a}, \bar{N}) \equiv L \left[K_j^i = \frac{\dot{a}}{Na} \delta_j^i, R_j^i = 0, N = \bar{N}(t) \right]. \quad (2.16)$$

The variation of the homogeneous action,

$$\bar{S}_g = \int dt d^3x \bar{N} a^3 \bar{L}, \quad (2.17)$$

leads to

$$\delta \bar{S}_g = \int dt d^3x \left\{ a^3 (\bar{L} + \bar{N} L_N - 3H\mathcal{F}) \delta \bar{N} + 3a^2 \bar{N} \left(\bar{L} - 3H\mathcal{F} - \frac{\dot{\mathcal{F}}}{\bar{N}} \right) \delta a \right\}, \quad (2.18)$$

where L_N denotes the partial derivative $\partial L / \partial N|_{\text{bgd}}$, evaluated on the homogeneous background. We have also introduced the coefficient \mathcal{F} , which is defined from the derivative of the Lagrangian with respect to the extrinsic curvature, evaluated on the background

$$\left(\frac{\partial L}{\partial K_{ij}} \right)_{\text{bgd}} \equiv \mathcal{F} \bar{g}^{ij}, \quad (2.19)$$

where $\bar{g}^{ij} = a^{-2} \delta^{ij}$ are the spatial components of the inverse background metric.

If we add some matter minimally coupled to the metric $g_{\mu\nu}$, the variation of the corresponding action with respect to the metric defines the energy-momentum tensor,

$$\delta S_m = \frac{1}{2} \int d^4x \sqrt{-g} T^{\mu\nu} \delta g_{\mu\nu}. \quad (2.20)$$

In a FLRW spacetime, this reduces to

$$\delta \bar{S}_m = \int d^4x \bar{N} a^3 \left(-\rho_m \frac{\delta \bar{N}}{\bar{N}} + 3p_m \frac{\delta a}{a} \right). \quad (2.21)$$

Consequently, variation of the total homogeneous action $\bar{S} = \bar{S}_g + \bar{S}_m$ with respect to N and a yields, respectively, the first and second Friedmann equations in a very unusual form:

$$\bar{L} + \bar{N} L_N - 3H\mathcal{F} = \rho_m \quad (2.22)$$

and

$$\bar{L} - 3H\mathcal{F} - \frac{\dot{\mathcal{F}}}{\bar{N}} = -p_m. \quad (2.23)$$

These two equations, which are the generalization of the Friedmann equations, also imply

$$\frac{\dot{\mathcal{F}}}{\bar{N}} + \bar{N} L_N = \rho_m + p_m. \quad (2.24)$$

It is easy to check that one recovers the usual Eqs.(1.8)–(1.9) when gravity is described by general relativity only. Indeed, in this case,

$$\frac{\partial L_{\text{GR}}}{\partial K_j^i} = M_{\text{pl}}^2 \left(K_i^j - K \delta_i^j \right), \quad (2.25)$$

which, after substituting $K_j^i = H \delta_j^i$, yields,

$$\mathcal{F}_{\text{GR}} = -2M_{\text{pl}}^2 H, \quad (2.26)$$

whereas $\bar{L}_{\text{GR}} = -3M_{\text{pl}}^2 H^2$ and $L_N = 0$. In the rest of this thesis, I will set $\bar{N} = 1$, which can always be achieved through a redefinition of time.

2.2.2 The Quadratic Action

To obtain the quadratic action, that will yield the linear equations of motion, one expands Eq. (2.10) in terms of the perturbative quantities

$$\delta N \equiv N - 1, \quad \delta K_j^i \equiv K_j^i - H \delta_j^i, \quad R_j^i. \quad (2.27)$$

Then, the expansion of the Lagrangian L up to quadratic order yields

$$L(N, K_j^i, R_j^i, \dots) = \bar{L} + L_N \delta N + \frac{\partial L}{\partial K_j^i} \delta K_j^i + \frac{\partial L}{\partial R_j^i} \delta R_j^i + L^{(2)} + \dots, \quad (2.28)$$

with the quadratic part given by

$$\begin{aligned} L^{(2)} = & \frac{1}{2} L_{NN} \delta N^2 + \frac{1}{2} \frac{\partial^2 L}{\partial K_j^i \partial K_l^k} \delta K_j^i \delta K_l^k + \frac{1}{2} \frac{\partial^2 L}{\partial R_j^i \partial R_l^k} \delta R_j^i \delta R_l^k + \\ & + \frac{\partial^2 L}{\partial K_j^i \partial R_l^k} \delta K_j^i \delta R_l^k + \frac{\partial^2 L}{\partial N \partial K_j^i} \delta N \delta K_j^i + \frac{\partial^2 L}{\partial N \partial R_j^i} \delta N \delta R_j^i + \dots, \end{aligned} \quad (2.29)$$

where all the partial derivatives are evaluated on the FLRW background (without explicit notation, as will be the case in the rest of this Chapter). The coefficient L_{NN} denotes the second derivative of the Lagrangian with respect to N . The dots in the two above equations correspond to other possible terms which are not indicated explicitly to avoid too lengthy equations, but can be treated exactly in the same way.

The third term on the right hand side of (2.28) can be simplified as follows. Rewriting it as

$$\frac{\partial L}{\partial K_j^i} \delta K_j^i = \mathcal{F} \delta K = \mathcal{F}(K - 3H), \quad (2.30)$$

and noting that $K = \nabla_\mu n^\mu$, one can use the integration by parts

$$\int d^4x \sqrt{-g} \mathcal{F} K = - \int d^4x \sqrt{-g} n^\mu \nabla_\mu \mathcal{F} = - \int d^4x \sqrt{-g} \frac{\dot{\mathcal{F}}}{N}. \quad (2.31)$$

This implies that the Lagrangian (2.28) can be replaced by the equivalent Lagrangian

$$L^{\text{new}} = \bar{L} - 3H\mathcal{F} - \frac{\dot{\mathcal{F}}}{N} + L_N \delta N + L^{(2)}. \quad (2.32)$$

Let us now consider the quadratic part (2.29). Because of the symmetries of background, the coefficient of the second term is necessarily of the form²

$$\frac{\partial^2 L}{\partial K_i^j \partial K_k^l} = \hat{\mathcal{A}}_K \delta_j^i \delta_l^k + \mathcal{A}_K (\delta_l^i \delta_j^k + \delta^{ik} \delta_{jl}), \quad (2.33)$$

where we have introduced the (a priori time-dependent) coefficients $\hat{\mathcal{A}}_K$ and \mathcal{A}_K . Similarly, one can write

$$\frac{\partial^2 L}{\partial R_i^j \partial R_k^l} = \hat{\mathcal{A}}_R \delta_j^i \delta_l^k + \mathcal{A}_R (\delta_l^i \delta_j^k + \delta^{ik} \delta_{jl}), \quad (2.34)$$

and

$$\frac{\partial^2 L}{\partial K_i^j \partial R_k^l} = \hat{\mathcal{C}} \delta_j^i \delta_l^k + \mathcal{C} (\delta_l^i \delta_j^k + \delta^{ik} \delta_{jl}). \quad (2.35)$$

The mixed coefficients that appear on the second line are proportional to δ_j^i and can be written as

$$\frac{\partial^2 L}{\partial N \partial K_j^i} = \mathcal{B} \delta_i^j, \quad \frac{\partial^2 L}{\partial N \partial R_j^i} = \mathcal{B}_R \delta_i^j. \quad (2.36)$$

Taking into account the term $\sqrt{-g} = N\sqrt{h}$, it is straightforward to derive the quadratic part of the full Lagrangian $\mathcal{L} \equiv \sqrt{-g} L$, which is relevant to study linear perturbations. After some cancellations due to the background equations of motion,³ one finds

²This is equivalent to the definition below, expressed with covariant indices for the extrinsic curvature tensors, which makes the symmetry under exchange of the indices more manifest:

$$\frac{\partial^2 L}{\partial K_{ij} \partial K_{kl}} \equiv \hat{\mathcal{A}}_K \bar{g}^{ij} \bar{g}^{kl} + \mathcal{A}_K (\bar{g}^{ik} \bar{g}^{jl} + \bar{g}^{il} \bar{g}^{jk}).$$

³If matter is present, one must also include in the quadratic Lagrangian the terms from the expansion of the matter action with respect to the metric perturbations.

$$\begin{aligned}
\mathcal{L}_2 &= \bar{N} \mathcal{G} \delta_1 R \delta \sqrt{h} + a^3 \left(L_N + \frac{1}{2} \bar{N} L_{NN} \right) \delta N^2 \\
&+ \bar{N} a^3 \left[\mathcal{G} \delta_2 R + \frac{1}{2} \hat{\mathcal{A}}_K \delta K^2 + \mathcal{B} \delta K \delta N + \hat{\mathcal{C}} \delta K \delta R + \mathcal{C} \delta K_j^i \delta R_i^j \right. \\
&\left. + \mathcal{A}_K \delta K_j^i \delta K_i^j + \mathcal{A}_R \delta R_j^i \delta R_i^j + \frac{1}{2} \hat{\mathcal{A}}_R \delta R^2 + \left(\frac{\mathcal{G}}{\bar{N}} + \mathcal{B}_R \right) \delta N \delta R \right] + \dots,
\end{aligned} \tag{2.37}$$

where, in analogy with the definition (2.19) of \mathcal{F} , we have introduced the coefficient \mathcal{G} defined by

$$\frac{\partial L}{\partial R_j^i} = \mathcal{G} \delta_i^j. \tag{2.38}$$

We have also denoted as $\delta_1 R$ and $\delta_2 R$, respectively, the first and second order terms of the curvature R expressed in terms of the metric perturbations.

The above quadratic expression can be further simplified by reexpressing $\delta K_j^i \delta R_i^j$ in terms of the other terms, thanks to the identity

$$\int d^4 x \sqrt{-g} \lambda(t) R_{ij} K^{ij} = \int d^4 x \sqrt{-g} \left[\frac{\lambda(t)}{2} R K + \frac{\dot{\lambda}(t)}{2N} R \right]. \tag{2.39}$$

This implies the following replacement at quadratic order:

$$\bar{N} a^3 \mathcal{C} \delta K_j^i \delta R_i^j \rightarrow \frac{\bar{N} a^3}{2} \left[\left(\frac{\dot{\mathcal{C}}}{\bar{N}} + HC \right) \left(\delta_2 R + \frac{\delta \sqrt{h}}{a^3} \delta R \right) + \mathcal{C} \delta R \delta K + \frac{HC}{\bar{N}} \delta N \delta R \right]. \tag{2.40}$$

Consequently, the quadratic Lagrangian (2.37) is equivalent to the new one

$$\begin{aligned}
\mathcal{L}_2^{\text{new}} &= \bar{N} \mathcal{G}^* \delta_1 R \delta \sqrt{h} + a^3 \left(L_N + \frac{1}{2} \bar{N} L_{NN} \right) \delta N^2 \\
&+ \bar{N} a^3 \left[\mathcal{G}^* \delta_2 R + \frac{1}{2} \hat{\mathcal{A}}_K \delta K^2 + \mathcal{B} \delta K \delta N + \mathcal{C}^* \delta K \delta R \right. \\
&\left. + \mathcal{A}_K \delta K_j^i \delta K_i^j + \mathcal{A}_R \delta R_j^i \delta R_i^j + \frac{1}{2} \hat{\mathcal{A}}_R \delta R^2 + \left(\frac{\mathcal{G}^*}{\bar{N}} + \mathcal{B}_R^* \right) \delta N \delta R \right] + \dots,
\end{aligned} \tag{2.41}$$

with the ‘‘renormalized’’ coefficients

$$\begin{aligned}
\mathcal{G}^* &= \mathcal{G} + \frac{\dot{\mathcal{C}}}{2\bar{N}} + HC, \\
\mathcal{C}^* &= \hat{\mathcal{C}} + \frac{1}{2} \mathcal{C}, \\
\mathcal{B}_R^* &= \mathcal{B}_R - \frac{\dot{\mathcal{C}}}{2\bar{N}^2}.
\end{aligned} \tag{2.42}$$

Let me concentrate more particularly on the scalar sector, since this is where restrictions need to be imposed in order to keep second-order dynamics. I will use the further parametrization

$$N^i = \delta^{ij} \partial_j \psi, \quad (2.43)$$

for the scalar part of g^{0i} . Together with the form of the metric (2.7), the perturbations of the geometrical quantities read

$$\delta\sqrt{h} = 3a^3 \zeta, \quad \delta K^i_j = (\dot{\zeta} - H\delta N) \delta^i_j - \frac{1}{a^2} \delta^{ik} \partial_k \partial_j \psi, \quad (2.44)$$

and

$$\delta_1 R_{ij} = -\delta_{ij} \partial^2 \zeta - \partial_i \partial_j \zeta, \quad \delta_2 R = -\frac{2}{a^2} [(\partial\zeta)^2 - 4\zeta \partial^2 \zeta]. \quad (2.45)$$

I will restrict to the case where no time derivatives ∂^0 appear explicitly in the Lagrangian, since it leads in general to extra DOF (see [14] for a discussion on including such derivatives). In this case, the variation with respect to δN and ψ gives constraint equations. They allow to express δN and ψ in terms of ζ and its derivatives, yielding an action only for this variable. It is on this action that conditions need to be imposed to get second-order dynamics.⁴ They read

$$\hat{\mathcal{A}}_K + 2\mathcal{A}_K = 0, \quad C^* = 0, \quad 4\hat{\mathcal{A}}_R + 3\mathcal{A}_R = 0, \quad (2.46)$$

Then the most general action that abides by these criteria can be written as

$$\boxed{S_g = \int d^4x a^3 \frac{M^2}{2} \left[\delta K_{\mu\nu} \delta K^{\mu\nu} - \delta K^2 + (1 + \alpha_T) \left(\delta_{(2)} R + \frac{\delta\sqrt{h}}{a^3} R \right) + H^2 \alpha_K \delta N^2 \right.} \\ \left. + 4H\alpha_B \delta N \delta K + (1 + \alpha_H) R \delta N \right] + \dots}, \quad (2.47)$$

where $h = \det h_{ij}$ and the \dots denotes terms that vanish when the background equations are enforced. The functions M and α_i are all in principle dependent on time, which is allowed by the presence of the extra scalar field. Additionally, one can define

$$\alpha_M \equiv \frac{2\dot{M}}{HM}, \quad (2.48)$$

which parametrizes the potential time dependence of the Planck mass. These coefficients, originally introduced in [18], are defined so that the standard case of Λ CDM+GR would correspond to setting all of them to zero.

⁴It is too restrictive to impose no higher derivatives in all of the equations before the constraint are solved. Indeed, such constraints might remove these higher derivatives so that the actual propagating DOF still obeys a second-order EOM. See Sect. 3.2 for more details.

Table 2.1 In the first row, the parameters α_i in the Lagrangian of Eq. (2.47)

Equation (2.47)	M^2	α_M	α_K	α_B	α_T	α_H
Equation (2.41)	$2\mathcal{A}_K$	$\frac{1}{H} \frac{d}{dt} \ln \mathcal{A}_K$	$\frac{2L_N + L_{NN}}{2H^2 \mathcal{A}_K}$	$\frac{\mathcal{B}}{4H \mathcal{A}_K}$	$\frac{\mathcal{G}^*}{\mathcal{A}_K} - 1$	$\frac{\mathcal{G}^* + \mathcal{B}_K^*}{\mathcal{A}_K} - 1$
Parameters of [13]	$M_{\text{Pl}}^2 f + 2m_4^2$	$\frac{M_{\text{Pl}}^2 \dot{f} + 2(m_4^2)'}{M^2 H}$	$\frac{2c + 4M_2^4}{M^2 H^2}$	$\frac{M_{\text{Pl}}^2 \dot{f} - m_3^3}{2M^2 H}$	$-\frac{2m_4^2}{M^2}$	$\frac{2(\tilde{m}_4^2 - m_4^2)}{M^2}$

These parameters are written in terms of the Lagrangian coefficients of Eq. (2.41), defined in Eqs. (2.33)–(2.36) (second row), and in terms of the parameter of the EFT Lagrangian in [13] (third row). All these quantities are understood to be evaluated on the background, with $N = 1$

They can be related to the original Lagrangian (2.10) and its derivatives with respect to the various quantities N , K_{ij} , \dots . The starting point is to define the equivalent of the Planck mass, M , which is associated with the normalization of the tensor kinetic term, $\dot{\gamma}_{ij}^2$. Since $\dot{\gamma}_{ij}$ only appears in K_{ij} , the M is going to be given by the derivative of the Lagrangian with respect to the extrinsic curvature, Eq. (2.33). More precisely,

$$M^2 \equiv 2\mathcal{A}_K. \quad (2.49)$$

Then, all the coefficients α_i follow almost algorithmically (Table 2.1)

In the next section, for concreteness, I will give examples on how to get these parameters in the case of specific models.

2.3 Going from Models to the EFT of DE

Once a model is decomposed in 3+1 quantities, computing its parameters is completely automatic, making the link with possible constraints straightforward. Let me go through the functions α_a one at a time, increasing the complexity of the model needed to illustrate the parameter.

- α_K

Taking the simplest case of GR plus quintessence [19], i.e.

$$L = \frac{M_{\text{Pl}}^2}{2} [K_{\mu\nu}K^{\mu\nu} - K^2 + R] - \frac{1}{2}\nabla_\mu\phi\nabla^\mu\phi - V(\phi). \quad (2.50)$$

After going to unitary gauge, one finds

$$M = M_{\text{Pl}}, \quad \alpha_K = \frac{\dot{\phi}_0^2}{H^2 M_{\text{Pl}}^2}, \quad (2.51)$$

while all the others coefficients and $\dot{\phi}_0$ is the background value of the scalar field. One can indeed check that Λ CDM corresponds to all the α_i being zero: one recovers the cosmological constant for $\dot{\phi}_0 = 0$, which would set $\alpha_K = 0$.

As a side note, it might seem odd that the potential V does not appear in Eq. (2.51). The reason is that this parametrization is specifically designed to look at linear perturbations, while V is a background quantity in unitary gauge. More precisely, the Friedmann equations impose

$$V = \frac{M_{\text{Pl}}^2}{2} [2\dot{H} + 3H^2 (2 - \Omega_m)]. \quad (2.52)$$

Therefore, if the history of H and the matter content are known, V is fixed.

- α_B

This example requires a more complicated model: kinetic braiding [20]. This theory is characterized by a Lagrangian of the form

$$L_3 = L_{\text{GR}} + G_3(X) \square\phi = L_{\text{GR}} - \int G_{3X} \sqrt{-X} dX K. \quad (2.53)$$

Since the \square operator is made with covariant derivatives, $\square\phi$ contains derivative couplings $(\partial g)(\partial\phi)$ between gravity and the scalar, hence its name kinetic gravity braiding.

The last term is going to give a nonzero α_B in the EFT Lagrangian (2.47), and the whole set of coefficients is given by

$$M = M_{\text{Pl}} \quad \alpha_K = 12\dot{\phi}_0^3 \frac{G_{3X} - \dot{\phi}_0^2 G_{3XX}}{H M_{\text{Pl}}^2}, \quad \alpha_B = -\frac{G_{3X} \dot{\phi}_0^3}{H M_{\text{Pl}}^2}, \quad (2.54)$$

where I have used the fact that in unitary gauge $X = -\dot{\phi}_0^2/N^2$, so that a dependence on X can be seen as a dependence on N and vice versa.

- α_T

To get a non zero α_T , one needs a model that does not preserve the relation between the intrinsic and the extrinsic curvatures in Eq. (2.12). Since the extrinsic curvatures give terms in γ_{ij}^2 while the intrinsic one gives $(\partial_k \gamma_{ij})^2$, changing the relation between them brings a change in the speed of sound of tensors. This happens for example for what is known as the quartic galileon [21], whose Lagrangian is

$$L_4 = G_4(X) {}^{(4)}R - 2G_{4X}(X) [(\square\phi)^2 - (\nabla^\mu \nabla^\nu \phi)(\nabla_\mu \nabla_\nu \phi)]. \quad (2.55)$$

The covariant second derivatives of the scalar field introduce first derivatives for the metric through the Christoffel symbols, which modifies the kinetic terms for gravity and gives a non zero α_T . In unitary gauge this Lagrangian reads

$$L_4 = G_4 R + (2XG_{4X} - G_4)(K^2 - K^{ij} K_{ij}), \quad (2.56)$$

so that the EFT coefficients are

$$M^2 = 2(G_4 + G_{4X} \dot{\phi}_0^2), \quad \alpha_K = -12\dot{\phi}_0^2 \frac{G_{4X} - 8\dot{\phi}_0^2 G_{4XX} + 4\dot{\phi}_0^4 G_{4XXX}}{M^2}, \quad (2.57)$$

$$\alpha_B = 4\dot{\phi}_0^2 \frac{G_{4X} - 2\dot{\phi}_0^2 G_{4XX}}{M^2}, \quad \alpha_T = -4\dot{\phi}_0^2 \frac{G_{4X}}{M^2}, \quad (2.58)$$

I will not discuss here the case of α_H , which parametrizes deviations from Horndeski theories, since the next chapter is specifically focused on theories beyond Horndeski. In particular, the effect of α_H will be explored in Sect. 3.6.

The theoretical origin of the parameters α_a of Eq. (2.47) is summarized in Table 2.2.

Table 2.2 In the first row, the parameters α_i introduced in Eq. (2.47)

	M^2	α_M	α_K	α_B	α_T	α_H
Interpretation	Normalization of the tensor quadratic action \equiv Planck mass	Planck mass rate of change	Kinetic term for the scalar	Kinetic braiding between gravity and scalar	Modification of tensor sound speed	Theories beyond Horndeski
Example	GR (when constant)	$f(R)$ [22] Brans-Dicke [23]	k -essence [24]	Cubic Galileon [20]	Quartic Galileon [21]	G^3 theories (see Chap. 3)

2.4 Stability and Theoretical Consistency

Even if the terms in Eq. (2.47) passed the first condition of yielding second-order dynamics (which guarantees the absence of extra, ghost-like DOF), further restrictions need to be imposed on the EFT parameters. Indeed, before thinking about comparing the predictions of a theory to observations, stringent constraints must be imposed in order for the theory to be stable. This is where using a parametrization at the level of the action and not of the EOM has a clear advantage, since these stability conditions can in principle be read off directly from the action. The idea can be simplified thusly: in the case of two scalar fields⁵ $\psi_1(t, \vec{x})$, $\psi_2(t, \vec{x})$ their quadratic Lagrangian is generically of the form:

$$L = \xi \dot{\psi}_1^2 - c_1 \partial_i \psi_1^2 + \dot{\psi}_2^2 - c_2 \partial_i \psi_2^2 + V_{\text{int}}(\psi_1, \psi_2). \quad (2.59)$$

In this illustrative case, the stability of the theory requires the coefficient ξ to be positive. When this is not the case, the field ψ_1 is called a ghost and in general violent instabilities are present in the theory.

Let me give some intuition on why that is, by thinking of the Lagrangian as $L = T - V$, where T is the kinetic energy and V the potential one. If the two signs are not the same in T , kinetic energy can flow without limits from one field to the other without changing the total energy $E = T + V$, meaning that the ground state of the theory is not stable (see [25] for a discussion on classical and quantum ghosts).

On top of this, one needs to impose that the coefficients c_1 and c_2 (which represent the squared sound speeds) are positive, to avoid gradient instabilities. These instabilities can be understood very easily from the EOM: when varying (2.59) with respect to ψ_1 for example, one gets

$$\ddot{\psi}_1 - c_1 \Delta \psi_1 = \frac{1}{2} \frac{\partial V_{\text{int}}}{\partial \psi_1}. \quad (2.60)$$

If c_1 is negative, this equation admits in Fourier space a solution $\psi_{\vec{k}}$ proportional to $e^{\sqrt{|c_1|}kt}$, which is divergent.

The analysis in the case of the action (2.47) is more involved, since tensor modes are present on top of the scalar. Moreover, other non dynamical variables are present (scalar and vector), so that at first glance the form of the quadratic action is not as simple as (2.59). If we parametrize the unitary gauge metric as before

$$N = 1 + \delta N, \quad N^i = \partial_i \psi + N_V^i, \quad h_{ij} = a^2 e^{2\zeta} (\delta_{ij} + \gamma_{ij}), \quad (2.61)$$

⁵I will not treat the case of one field, as it present less interests. In particular, one cannot have a ghost field in this case: the sign of the kinetic term does not matter when there is nothing to compare it to. Moreover, in cosmology, the scalar field is always coupled to gravity.

with $\partial_i N_V^i = 0$ and $\gamma_{ii} = \partial_i \gamma_{ij} = 0$, only ζ and γ_{ij} are dynamical.⁶ Once the constraints are solved, the quadratic part of the action can be rewritten in terms of dynamical DOF only, in a manner very similar to Eq. (2.59):

$$S = \int d^4x \frac{M^2 a^3}{2} \left\{ \frac{\alpha}{(1 + \alpha_B)^2} \left[\dot{\zeta}^2 - c_s^2 \frac{\partial_i \zeta^2}{a^2} \right] + \frac{\dot{\gamma}_{ij}^2}{4} - (1 + \alpha_T) \frac{\partial_k \gamma_{ij}^2}{4a^2} + \frac{(\partial_i N_j^V + \partial_j N_i^V)^2}{4a^4} \right\}. \quad (2.62)$$

I have used the following definitions

$$\alpha \equiv \alpha_K + 6\alpha_B^2, \quad (2.63)$$

and

$$c_s^2 \equiv 2 \left\{ 1 + \alpha_T - \frac{1 + \alpha_H}{1 + \alpha_B} \left(1 + \alpha_M - \frac{\dot{H}}{H^2} \right) - \frac{1}{H} \frac{d}{dt} \left(\frac{1 + \alpha_H}{1 + \alpha_B} \right) \right\}, \quad (2.64)$$

the latter being valid only in the absence of matter. The stability conditions discussed above can be stated as

$$\begin{aligned} M^2 > 0, \quad \alpha_K + 6\alpha_B^2 > 0, \\ c_T^2 \equiv (1 + \alpha_T) > 0, \quad c_s^2 > 0, \end{aligned} \quad (2.65)$$

which defines the tensor sound speed.

The presence of matter, both at the background and perturbative levels, slightly complicates the situation. In the case $\alpha_H = 0$, one finds

$$c_s^2 = 2 \frac{(1 + \alpha_B)^2}{\alpha} \left\{ \frac{1}{1 + \alpha_B} \left(1 + \alpha_M - \frac{\dot{H}}{H^2} \right) - (1 + \alpha_T) - \frac{\alpha_B}{H(1 + \alpha_B)^2} \right\} - \frac{\rho_m + p_m}{\alpha M^2 H^2}, \quad (2.66)$$

while the speed of sound for matter and tensors are unchanged. In the case $\alpha_H \neq 0$, which will be treated in more details in Chap. 3, both the sound speed of matter and the extra scalar field are affected.

Of course, the conditions (2.65) can be translated into conditions on parameters of models, using for example Sect. 2.3. However, the advantage of the EFT of DE is that those conditions are really imposed on deviations from Λ CDM, not just on a specific model. It might well be that the regions of the parameter space they allow are not fully explored by any of the known theories (which led us to the theories beyond Horndeski of Chap. 3). As we will see, the same kind of reasoning applies to the comparison with observations.

⁶In general, the spatial metric contains also a (non-dynamical) vectorial part, which can be set to zero by using the spatial gauge freedom.

2.5 Evolution of Cosmological Perturbations

In this section I will discuss the effects of the deviations from Λ CDM on the evolution of perturbations, in the vector, tensor and scalar sectors, the latter being the richest—and most complicated—in term of phenomenology. The matter sector will be parametrized by its total stress energy tensor, decomposed at linear order as

$$T_0^0 \equiv -(\rho_m + \delta\rho_m), \quad (2.67)$$

$$T_i^0 \equiv \partial_i q_m + (T_i^0)^T \equiv (\rho_m + p_m)\partial_i v_m + (T_i^0)^V, \quad (2.68)$$

$$T_j^i \equiv (p_m + \delta p_m)\delta_j^i + \left(\partial^i \partial_j - \frac{1}{3}\delta_j^i \partial^2\right)\sigma_m + (\partial^i C_j + \partial_j C^i)^V + (T_{ij})^{TT}, \quad (2.69)$$

where $\delta\rho_m$ and δp_m are the energy density and pressure perturbations, q_m and v_m are respectively the 3-momentum and the 3-velocity potentials; σ_m is the anisotropic stress potential. $(T_i^0)^V$ is the transverse part of the matter energy flux, $(\partial^i C_j + \partial_j C^i)^V$ and $(T_{ij})^{TT}$ are respectively the transverse and the transverse-traceless parts of the spatial matter stress tensor.

2.5.1 Vector Sector

As we have seen from Eq. (2.62), the vector sector is the simplest one as it does not contain propagating DOF. However, the presence of a time varying Planck mass, characterized by $\alpha_M \neq 0$ still affects the perturbations. Indeed, when considering the full action supplemented by matter, the vector equation reads:

$$\frac{1}{2}\nabla^2 N_i^V = \frac{a^2}{M^2}(T_i^0)^V. \quad (2.70)$$

For a perfect fluid where $C_i^V = 0$, the conservation of the matter stress-energy tensor implies that $(T_i^0)^T \propto 1/a^3$ [26]. Thus, the metric vector perturbations scale as

$$N_V^i \propto \frac{1}{aM^2} = \frac{1}{a^{1+\alpha_M}}, \quad (2.71)$$

where the last equality holds for a constant α_M . It is therefore interesting to see that the evolution of the vector sector only depends on a single parameter.

Since they typically decay, vector modes are very difficult to observe. This very fact already signals that α_M cannot be too negative, i.e. the Planck mass cannot have been growing too strongly in time, otherwise they would not necessarily be negligible today. If vectors mode were to be detected, this would allow to constrain α_M without having to treat the other parameters.

2.5.2 Tensor Sector

The tensor sector, slightly more complicated, leads to the evolution equation

$$\ddot{\gamma}_{ij} + H(3 + \alpha_M)\dot{\gamma}_{ij} - (1 + \alpha_T)\frac{\nabla^2}{a^2}\gamma_{ij} = \frac{2}{M^2}(T_{ij})^{TT}. \quad (2.72)$$

Thus, even for a perfect fluid where the anisotropic stress is zero, the propagation of tensor modes is affected both by an additional friction term proportional to α_M , as well as a different speed of propagation. In principle, the combined observation of vector and tensor modes could therefore provide constraints on α_M and α_T independently of each other and of the other α_i .

2.5.3 Scalar Sector

2.5.3.1 Obtaining the Equations

In principle, five (non independent) scalar equations can be derived from the action (2.47). Four are the Einstein scalar equations (00, 0*i*, *ii* and *ij* traceless), where one needs to further introduce the scalar part of the traceless component of the spatial metric, χ

$$h_{ij} = a^2(1 + 2\zeta)\left[\delta_{ij} + \left(\partial_i\partial_j - \frac{\delta_{ij}}{3}\partial^2\right)\chi\right]. \quad (2.73)$$

Then, the action needs to be varied with respect to ζ , δN , ψ and χ , giving the four Einstein equations.

The fifth equation is the one for the scalar field ϕ . However, in unitary gauge this field is not explicit. One can still derive what would be the unitary gauge version of this equation (that will depend only on metric quantities) by imposing the invariance under time reparametrization of the action. Indeed, by definition of the unitary gauge,

$$\left.\frac{\delta S[\phi, g_{\mu\nu}]}{\delta\phi(x)}\right|_{\phi=t} = \frac{\delta S_{\text{u.g.}}[t, g_{\mu\nu}]}{\delta t}, \quad (2.74)$$

where the time derivative is understood as a partial one (that is to say, not taking into account the time dependence of the metric).

For a general infinitesimal diffeomorphism $x^\mu \rightarrow x^\mu + \xi^\mu$, the metric changes as $\delta g_{\mu\nu} = \nabla_\mu \xi_\nu + \nabla_\nu \xi_\mu$. Therefore,

$$\delta S_{\text{u.g.}} = \int d^4x \frac{\delta S_{\text{u.g.}}}{\delta g_{\mu\nu}(x)} (\nabla_\mu \xi_\nu(x) + \nabla_\nu \xi_\mu(x)) + \frac{\delta S_{\text{u.g.}}}{\delta t} \xi^0 = 0. \quad (2.75)$$

After integrating by parts and combining this with Eq. (2.74), one obtains that the equation of the scalar field in unitary gauge is simply the zero component of the divergence of Einstein's equations,⁷

$$\left. \frac{\delta S[\phi, g_{\mu\nu}]}{\delta\phi(x)} \right|_{\phi=t} = \frac{\delta S_{\text{u.g.}}}{\delta t} = 2g^{0\nu} \nabla_{\mu} \frac{\delta S_{\text{u.g.}}}{\delta g_{\mu\nu}} = 0, \quad (2.76)$$

where the last equality holds when Einstein's equations $\frac{\delta S_{\text{u.g.}}}{\delta g_{\mu\nu}} = 0$ are enforced. Hence, this yields the fifth scalar equation, which is not independent from the others.

These five equations are for the scalar variables of the metric, namely ζ , δN , ψ and χ . To describe scalar perturbations and their physics, the Newtonian gauge is more adapted than the unitary gauge. In order to go from one to the other, a time diffeomorphism is performed

$$t \rightarrow t + \pi(t, \vec{x}), \quad (2.77)$$

where π describes the fluctuations of the scalar field

$$\phi = t + \pi. \quad (2.78)$$

In Newtonian gauge the scalar part of the metric is parametrized as

$$ds^2 = -(1 + 2\Phi)dt^2 + a^2(t)(1 - 2\Psi)\delta_{ij}dx^i dx^j. \quad (2.79)$$

One can relate the metric perturbations in unitary gauge defined in Eq. (2.61) to the metric perturbations Φ and Ψ , as well as the scalar fluctuation π by⁸

$$\delta N = \Phi - \dot{\pi}, \quad \zeta = -\Psi + H\pi, \quad \psi = a^{-2}\pi, \quad \chi = 0. \quad (2.80)$$

Then, the five equations can be put in the following form (in Fourier space):

- The Hamiltonian constraint ((00) component of Einstein's equation) is

$$6(1 + \alpha_B)H\dot{\Psi} + (6 - \alpha_K + 12\alpha_B)H^2\Phi + 2(1 + \alpha_H)\frac{k^2}{a^2}\Psi + (\alpha_K - 6\alpha_B)H^2\dot{\pi} + 6\left[(1 + \alpha_B)\dot{H} + \frac{\rho_m + p_m}{2M^2} + \frac{1}{3}\frac{k^2}{a^2}(\alpha_H - \alpha_B) \right]H\pi = -\frac{\delta\rho_m}{M^2}, \quad (2.81)$$

⁷Since we assumed the presence of a Jordan frame, where matter is minimally coupled, its stress energy tensor is conserved independently.

⁸More precisely, to remove also the variable χ one needs a spatial diffeomorphism $x^i \rightarrow x^i + \partial_i\beta$.

- The momentum constraint ((0*i*) components of Einstein's equation) reads

$$2\dot{\Psi} + 2(1 + \alpha_B)H\Phi - 2H\alpha_B\dot{\pi} + \left(2\dot{H} + \frac{\rho_m + p_m}{M^2}\right)\pi = -\frac{(\rho_m + p_m)v_m}{M^2}. \quad (2.82)$$

- The traceless part of the *ij* components of Einstein's equation gives

$$(1 + \alpha_H)\Phi - (1 + \alpha_T)\Psi + (\alpha_M - \alpha_T)H\pi - \alpha_H\dot{\pi} = -\frac{\sigma_m}{M^2}, \quad (2.83)$$

- The trace of the same components gives, using the equation above,

$$\begin{aligned} & 2\ddot{\Psi} + 2(3 + \alpha_M)H\dot{\Psi} + 2(1 + \alpha_B)H\dot{\Phi} \\ & + 2\left[\dot{H} - \frac{\rho_m + p_m}{2M^2} + (\alpha_B H)^\cdot + (3 + \alpha_M)(1 + \alpha_B)H^2\right]\Phi \\ & - 2H\alpha_B\ddot{\pi} + 2\left[\dot{H} + \frac{\rho_m + p_m}{2M^2} - (\alpha_B H)^\cdot - (3 + \alpha_M)\alpha_B H^2\right]\dot{\pi} \\ & + 2\left[(3 + \alpha_m)H\dot{H} + \frac{\dot{p}_m}{2M^2} + \ddot{H}\right]\pi = \frac{1}{M^2}\left(\delta p_m - \frac{2}{3}\frac{k^2}{a^2}\sigma_m\right). \end{aligned} \quad (2.84)$$

- Finally, the evolution equation for π reads

$$\begin{aligned} & H^2\alpha_K\ddot{\pi} + \left\{[H^2(3 + \alpha_M) + \dot{H}]\alpha_K + (H\alpha_K)^\cdot\right\}H\dot{\pi} \\ & + 6\left\{\left(\dot{H} + \frac{\rho_m + p_m}{2M^2}\right)\dot{H} + \dot{H}\alpha_B[H^2(3 + \alpha_M) + \dot{H}] + H(\dot{H}\alpha_B)^\cdot\right\}\pi - 2\frac{k^2}{a^2}\dot{H}\pi \\ & - 2\frac{k^2}{a^2}\left\{\frac{\rho_m + p_m}{2M^2} + H^2[1 + \alpha_B(1 + \alpha_M) + \alpha_T - (1 + \alpha_H)(1 + \alpha_M)] + (H(\alpha_B - \alpha_H))^\cdot\right\}\pi \\ & + 6H\alpha_B\ddot{\Psi} + H^2(6\alpha_B - \alpha_K)\dot{\Phi} + 6\left[\dot{H} + \frac{\rho_m + p_m}{2M^2} + H^2\alpha_B(3 + \alpha_M) + (\alpha_B H)^\cdot\right]\dot{\Psi} \\ & + \left[6\left(\dot{H} + \frac{\rho_m + p_m}{2M^2}\right) + H^2(6\alpha_B - \alpha_K)(3 + \alpha_M) + 2(9\alpha_B - \alpha_K)\dot{H} + H(6\dot{\alpha}_B - \dot{\alpha}_K)\right]H\Phi \\ & + 2\frac{k^2}{a^2}\left\{\alpha_H\dot{\Psi} + [H(\alpha_M + \alpha_H(1 + \alpha_M) - \alpha_T) - \dot{\alpha}_H]\Psi + (\alpha_H - \alpha_B)H\Phi\right\} = 0. \end{aligned} \quad (2.85)$$

These equations are much more involved than in the two other sectors and as such are not readily useful. Nevertheless, one has to remember that there is only one propagating degree of freedom, which means that 4 of these equations are just constraints. Therefore, the five equations can be combined into a single equation for a single variable, e.g.

$$\boxed{\ddot{\Psi} + \frac{\beta_1\beta_2 + \beta_3\alpha_B^2\tilde{k}^2}{\beta_1 + \alpha_B^2\tilde{k}^2}H\dot{\Psi} + \frac{\beta_1\beta_4 + \beta_1\beta_5\tilde{k}^2 + c_s^2\alpha_B^2\tilde{k}^4}{\beta_1 + \alpha_B^2\tilde{k}^2}H^2\Psi = -\frac{1}{2M^2}\left[\frac{\beta_1\beta_6 + \beta_7\alpha_B^2\tilde{k}^2}{\beta_1 + \alpha_B^2\tilde{k}^2}\delta\rho_m + \frac{\beta_1\beta_8 + \beta_9\alpha_B^2\tilde{k}^2}{\beta_1 + \alpha_B^2\tilde{k}^2}H(\rho_m + p_m)v_m - \frac{\alpha_K}{\alpha}\delta p_m\right]}, \quad (2.86)$$

where $\tilde{k} \equiv k/(aH)$, α is defined in Eq. (2.63) and for simplicity, I have assumed that the anisotropic stress of matter is zero. The β_i are functions of the coefficients α_j , whose—rather cumbersome—expressions are given in the Appendix in the case $\alpha_H = 0$. Although this equation is enough to describe the dynamics of the scalar sector, it is useful to have the relation between the two metric potentials Φ and Ψ to connect with observations (in particular lensing, as explained in Sect. 1.2.3). This relation takes the form

$$\alpha_B^2\tilde{k}^2\left[\Phi - \Psi\left(1 + \alpha_T + \frac{\alpha_T - \alpha_M}{\alpha_B}\right)\right] + \beta_1\left[\Phi - \Psi(1 + \alpha_T)\left(1 + \alpha\frac{\alpha_T - \alpha_M}{2\beta_1}\right)\right] = \frac{\alpha_T - \alpha_M}{2H^2M^2}\left\{\alpha_B[\delta\rho_m - 3H(\rho_m + p_m)v_m] + HM^2\alpha\dot{\Psi} + H\frac{\alpha_K}{2}(\rho_m + p_m)v_m\right\}. \quad (2.87)$$

To complete the system of equations, one needs to provide the evolution equations for the matter sector. Since it is assumed to be minimally coupled, these equations come from the conservation of the stress energy tensor. At linear order in the perturbations, treating one species of matter only for simplicity, they read

$$\dot{\delta}_m - 3H(w_m\delta_m - \delta p_m) - (1 + w_m)\left(\frac{k^2}{a^2}v_m + 3\dot{\Psi}\right) = 0, \quad (2.88)$$

$$\dot{v}_m - \left[3Hw_m - \frac{\dot{w}_m}{1 + w_m}\right]v_m + \frac{\delta p_m}{1 + w_m} + \Phi = 0, \quad (2.89)$$

with the definitions

$$w_m \equiv \frac{p_m}{\rho_m}, \quad \delta_m \equiv \frac{\delta\rho_m}{\rho_m}, \quad (2.90)$$

where w_m is the usual equation of state parameter and δ_m the density contrast. Note that in general, when the fluid is not at rest, the relation between the pressure perturbation and the density contrast involves more than just the speed of sound (see for example [27]) which is why I kept explicitly δp_m in these equations.

2.5.3.2 Fluid Description

Similarly to the case of the cosmological constant Λ which can be seen either as a modification of gravity (belonging to the $G_{\mu\nu}$ side of Einstein's equation) or as a

new fluid with a density ρ_Λ (see Sect. 1.1.3), one can describe the dark energy, both in the background and perturbative equations, as an effective fluid. The idea is to regroup under a effective stress energy tensor $T_{\mu\nu}^\Lambda$ everything that is not either $G_{\mu\nu}$ nor $T_{\mu\nu}^{\text{matter}}$. At the background level this gives

$$\rho_D \equiv 3M^2 H^2 - \rho_m, \quad p_D \equiv -M^2(2\dot{H} + 3H^2) - p_m. \quad (2.91)$$

With these definitions, and using the conservation of the background matter stress-energy tensor,

$$\dot{\rho}_m + 3H(\rho_m + p_m) = 0, \quad (2.92)$$

the conservation of the background $T_{\mu\nu}^\Lambda$ reads

$$\dot{\rho}_D = -3H(\rho_D + p_D) + 3\alpha_M M^2 H^3 = 3H(\rho_m + p_m) + 6M^2 H(\dot{H} + \alpha_M H^2). \quad (2.93)$$

Another useful relation that one can use to express \dot{p}_D in terms of matter and geometry is

$$\dot{p}_D = -\dot{p}_m - M^2[2\ddot{H} + 2H\dot{H}(3 + \alpha_M) + 3\alpha_M H^3], \quad (2.94)$$

which can be derived from the equations above.

Equations (2.81)–(2.84) can be then rewritten in the usual form,

$$\frac{k^2}{a^2}\Psi + 3H(\dot{\Psi} + H\Phi) = -\frac{1}{2M^2} \sum_I \delta\rho_I, \quad (2.95)$$

$$\dot{\Psi} + H\Phi = -\frac{1}{2M^2} \sum_I q_I, \quad (2.96)$$

$$\Psi - \Phi = \frac{1}{M^2} \sum_I \sigma_I, \quad (2.97)$$

$$\ddot{\Psi} + H\dot{\Phi} + 2\dot{H}\Phi + 3H(\dot{\Psi} + H\Phi) = \frac{1}{2M^2} \sum_I \left(\delta p_I - \frac{2}{3} \frac{k^2}{a^2} \sigma_I \right), \quad (2.98)$$

where the sum is over the matter and the dark energy components. These equations implicitly define the quantities $\delta\rho_D$, q_D , δp_D and σ_D as the energy density perturbation, momentum, pressure perturbation and anisotropic stress of the dark energy fluid. An explicit definition is given in the Appendix.

With these definitions, one can verify that the evolution equation for π , Eq. (2.85), is equivalent to a conservation equation of the dark energy fluid quantities,

$$\delta\dot{\rho}_D + 3H(\delta\rho_D + \delta p_D) - 3(\rho_D + p_D)\dot{\Psi} - \frac{k^2}{a^2}q_D = \alpha_M H \sum_I \delta\rho_I. \quad (2.99)$$

The Euler equation,

$$\dot{q}_D + 3Hq_D + (\rho_D + p_D)\Phi + \delta p_D - \frac{2}{3}\frac{k^2}{a^2}\sigma_D = \alpha_M H \sum_I q_I, \quad (2.100)$$

is identically satisfied by the definitions of q_D , δp_D and σ_D .

To close the system, one needs to provide a relation between δp_D and σ_D in terms of $\delta\rho_D$, q_D and the other matter variables. In order to do so in the simpler case where $\alpha_H = 0$, we follow a procedure similar to the previous section. First, we solve Eqs. (2.81)–(2.83) for Ψ , $\tilde{\Psi}$ and $\tilde{\pi}$ and then we plug these solutions in Eqs. (2.95) and (2.96) to express π and Φ in terms of $\delta\rho_m$, q_m , σ_m , $\delta\rho_D$ and q_D . Φ is obtained from the first derivative of (2.83). To obtain $\tilde{\Psi}$ and $\tilde{\pi}$ we use Eqs. (2.84) and (2.85). Combining all these solutions we can finally express σ_D and δp_D in terms of the other fluid variables. We obtain

$$\begin{aligned} \delta p_D = & \frac{\gamma_1\gamma_2 + \gamma_3\alpha_B^2\tilde{k}^2}{\gamma_1 + \alpha_B^2\tilde{k}^2}(\delta\rho_D - 3Hq_D) + \frac{\gamma_1\gamma_4 + \gamma_5\alpha_B^2\tilde{k}^2}{\gamma_1 + \alpha_B^2\tilde{k}^2}Hq_D \\ & + \gamma_7(\delta\rho_m - 3Hq_m) + \frac{\gamma_1\gamma_6 + 3\gamma_7\alpha_B^2\tilde{k}^2}{\gamma_1 + \alpha_B^2\tilde{k}^2}Hq_m - \frac{6\alpha_B^2}{\alpha}\delta\rho_m, \end{aligned} \quad (2.101)$$

$$\begin{aligned} \sigma_D = & \frac{a^2}{2k^2} \left[\frac{\gamma_1\alpha_T + \gamma_8\alpha_B^2\tilde{k}^2}{\gamma_1 + \alpha_B^2\tilde{k}^2}(\delta\rho_D - 3Hq_D) + \frac{\gamma_9\tilde{k}^2}{\gamma_1 + \alpha_B^2\tilde{k}^2}Hq_D \right. \\ & \left. + \alpha_T(\delta\rho_m - 3Hq_m) + \frac{\gamma_{10}\tilde{k}^2}{\gamma_1 + \alpha_B^2\tilde{k}^2}Hq_m \right], \end{aligned} \quad (2.102)$$

where we use the notation $\tilde{k} \equiv k/(aH)$ and we have defined dimensionless coefficients γ_a , whose expressions are explicitly given in the Appendix. These relations for δp_D and σ_D are the equivalent of the Eqs. (2.86)–(2.87).

2.5.3.3 Interpretation

The system of Equations (2.86)–(2.89) is complete (provided δp_m and w_m are specified) and can in principle be solved to get the evolution of the matter perturbations and gravitational potentials. To do so without approximations would require a numerical implementation. However, the physics can be discussed analytically in specific cases, that give an idea of the effects expected. In particular, I will focus on the role played by kinetic braiding. Indeed, one can see appearing in Eq. (2.86) a new scale when $\alpha_B \neq 0$:

$$k_B = \frac{aH\beta_1^{1/2}}{\alpha_B}, \quad (2.103)$$

which has been called braiding scale [18]. We shall explore two examples that show it is associated with noticeable modifications of gravity.

- $\alpha_B = 0$:

It can be seen as the extreme limit where $k_B \rightarrow \infty$, meaning that all modes are outside of the braiding length, $k \ll k_B$. In this case most of the scale dependences go away. We are left with the simpler expression

$$\begin{aligned} \ddot{\Psi} + (4 + 2\alpha_M + 3\Upsilon) H \dot{\Psi} + \left(\beta_4 H^2 + c_s^2 \frac{k^2}{a^2} \right) \Psi = \\ - \frac{1}{2M^2} \left\{ c_s^2 [\delta\rho_m - 3H(\rho_m + p_m)v_m] + (\alpha_M - \alpha_T + 3\Upsilon)H(\rho_m + p_m)v_m - \delta p_m \right\}, \end{aligned} \quad (2.104)$$

where Υ is defined in the Appendix. Although both α_M and α_T can be nonzero here, the form of this equation is very similar to that obtained in the standard k -essence case [24]. One recovers in the quasistatic limit (i.e. by neglecting time derivatives and taking $k \gg aH/c_s$)

$$- \frac{k^2}{a^2} \Psi = \frac{1}{2M^2} \delta\rho_m, \quad \Phi = (1 + \alpha_T) \left[1 + \alpha_K \frac{\alpha_T - \alpha_M}{2\beta_1} \right] \Psi. \quad (2.105)$$

This means that no scale dependence is introduced in the effective Newton constant defined as

$$- \frac{k^2}{a^2} \Phi \equiv 4\pi G_{\text{eff}} \delta\rho_m. \quad (2.106)$$

As we will see, this no longer necessarily holds when $\alpha_B \neq 0$.

- $\alpha_B^2 \gg \alpha_K$:

This case corresponds to having most of the kinetic energy of the scalar field coming from kinetic braiding. Indeed, one can see in this case that the kinetic energy (the term in $\dot{\zeta}^2$ in Eq. (2.62)) is dominated by the contribution of α_B . For simplicity we consider only the case $\alpha_T = 0$. Moreover, to avoid gradient instabilities the following relation is required (see Eq. (2.66))

$$\alpha_B \lesssim \mathcal{O}(\alpha_M). \quad (2.107)$$

However, no restrictions are imposed on α_M , whose value can affect the braiding scale. Indeed, when $\alpha_B^2 \gg \alpha_K$, this is given by

$$\frac{k_B^2}{a^2} \simeq 3(H^2\alpha_M - \dot{H}), \quad (2.108)$$

which can be inside the Hubble horizon. In this case, considering modes with $k \gg k_B$, Eq. (2.86) simplifies to

$$\ddot{\Psi} + (3 + \alpha_M)H\dot{\Psi} + \left(\frac{k_B^2 \beta_5}{a^2} + c_s^2 \frac{k^2}{a^2} \right) \Psi \simeq -\frac{1}{2M^2} \left(\frac{k_B^2 \beta_6}{k^2} + c_s^2 + \frac{1}{3} - \frac{\alpha_M}{3\alpha_B} \right) \delta\rho_m, \quad (2.109)$$

where we have neglected relativistic terms on the right hand side of (2.86). If the ratio β_5/c_s^2 is larger than one, the scale dependence cannot be neglected even in the case $k \gg k_B$. Therefore, a non vanishing α_B , or the fact that $k_B < \infty$, brings a transition scale in the effective Newton constant,⁹ which is a strong signal that gravity is modified.

Another interpretation would be that dark energy clusters: one can write Einstein equations as

$$G^{\mu\nu} = \frac{T_m^{\mu\nu} + T_D^{\mu\nu}}{M^2}, \quad (2.110)$$

which defines effective fluid variables for dark energy/modified gravity. Thus, for subhorizon scales, the Poisson equation has the form

$$-\frac{k^2}{a^2} \Phi = \frac{1}{M^2} (\delta\rho_m + \delta\rho_D). \quad (2.111)$$

For a cosmological constant, there are no perturbation in the dark energy fluid, $\delta\rho_D = 0$, and the standard behavior is recovered. However, as soon as dark energy clusters, i.e. $\delta\rho_D \sim \mathcal{O}(\delta\rho_m)$, the relation between the gravitational potential and matter is no longer as simple, leading to a different (and potentially scale dependent) effective Newton constant.

The Eqs. (2.86) and (2.87) can be seen as the generalization to arbitrary scales of the usual parametrization in term of G_{eff} (defined in Eq. (2.106)) and the slip parameter

$$\gamma \equiv \frac{\Psi}{\Phi}, \quad (2.112)$$

that are employed in the quasistatic limit. However, if this limit is clearly defined in GR where it means focusing on subhorizon scales $k \gg aH$, its definition in the presence of an extra scalar field is more ambiguous. Indeed, in general, new scales (see [28] for a general discussion concerning new scales in modified gravity) and time dependences appear and it is not always clear how this limit would translate, although in general it is expected to hold well inside the sound horizon of the scalar perturbations, $kc_s \gg aH$.

⁹Although the standard relation defining G_{eff} involves Φ and not Ψ , it is easy to convince oneself that the relation between them set by Eq. (2.87) does not remove this transition.

To alleviate this uncertainty, one can look at what is called the extreme quasistatic limit [18] corresponding to wavenumber k much bigger than any scale in the problem, i.e. taking $k \rightarrow \infty$ in Eqs. (2.86)–(2.87). This yields the following expressions

$$8\pi G_{\text{eff}} = \frac{\alpha c_s^2(1 + \alpha_T) + 2[\alpha_B(1 + \alpha_T) + \alpha_T - \alpha_M]^2}{\alpha c_s^2} M^{-2}, \quad (2.113)$$

$$\gamma = \frac{\alpha c_s^2 + 2\alpha_B[\alpha_B(1 + \alpha_T) + \alpha_T - \alpha_M]}{\alpha c_s^2(1 + \alpha_T) + 2[\alpha_B(1 + \alpha_T) + \alpha_T - \alpha_M]^2}, \quad (2.114)$$

where I have expressed both quantities directly in terms of the functions α_a (recall that $\alpha = \alpha_K + 6\alpha_B^2$ and α_H is here set to zero). These two quantities are observable since the first affects directly the growth of structures and therefore affects the power spectrum of the large scale structure. The second is related to the gravitational potential felt by photon, $\Phi + \Psi$, and thus can be probed in weak lensing experiments (see for example [29]).

In this Section, I have shown that by looking at the evolution of cosmological perturbations, one can relate the parametrization of the action in Eq. (2.47) to observable quantities. The simplest cases from the theoretical side are the vector and tensor sectors. They only depend on the time variation of the Planck mass, α_M , and on the deviation from unity of the tensor sound speed, α_T . However, these sectors are precisely the fields of observations where the signals are the weakest.

The more experimentally accessible scalar sector corresponds to the most complicated domain, where all five functions α_i play a role. Although their effects are understood from a theoretical point of view (see Table 2.2), they appear in a non trivial way when going to observable quantities such as the growth of structures or weak lensing. This can be seen analytically in the quasistatic limit with the modifications of the way matter sources the gravitational potential (through G_{eff}) or the way the two potentials are related to each other (through γ). This is why, to break the degeneracies that remain, one may need to go beyond the quasistatic limit, starting for example from Eq. (2.86).

One idea would be to solve perturbatively Eqs. (2.86)–(2.89) around $k \rightarrow \infty$ without necessarily making assumptions on the time derivatives. This would be a way to see the range of validity of the quasistatic approximation (see also [30]). We have actually started looking into this, but taking care of the time dependence is rather subtle and requires more work.

2.6 Conclusions

In this chapter, I presented a method called the Effective Field Theory for Dark Energy, that allows to explore the vast landscape beyond the standard model of cosmology, Λ CDM. It is based on the parametrization of an action, describing

scalar-tensor theories in a very broad sense. I used the preferred time foliation that the scalar field offers, along with its 3+1 geometry, to construct a very generic Lagrangian that describes linear perturbations with second-order dynamics. This Lagrangian depends only on five functions of time, provided the expansion of the Universe and its matter content are known.

This has many advantages, both theoretically and observationally. The stability conditions that one needs to impose for a theory to be sensible can be easily read from this action. Moreover, this reduces to a single channel of analysis the comparison to experiments. The straightforward links that we developed between wide classes of models and the parameters make it particularly convenient to use, since constraints on the five parameters easily translate to constraints on models.

However, this point of view is somewhat limiting the potential of this approach. The action (2.47) explores domains beyond the models currently known, potentially leading to new models, as we shall see in the next chapter. Indeed, it is solely based on the fact that in general, the background solution of an additional field in a cosmological setting explicitly breaks time reparametrization invariance. This opens the possibility of new terms in the action beside the standard Ricci scalar. It really is deviations from Λ CDM +GR that are captured by this formalism.

Because of its minimal number of parameters, the EFT of DE has started to be used by the community. It first started with people developing codes, in particular [31], that is based on the popular CMB code CAMB [32] and others doing forecasts for galaxy surveys [33]. Now, the parametrization, conveniently optimized by [18], is being used in the analysis of the Planck collaboration [34]. Hopefully, future surveys such as EUCLID [35] and LSST [36] will also use it, and the constraints on the α_a will improve.

From a theoretical point of view, there is still work to be done. As I mentioned above, there is a yet untamed wealth of information contained in Eq. (2.86), which includes for example relativistic effects that become important when looking at increasingly large surveys. It would be interesting to see how much of this information can be extracted using numerical solutions, or analytical method generalizing the quasistatic limit.

Another point I have been working on recently consists of extending this formalism to the case where the Weak Equivalence Principle (WEP) is violated, i.e. species couple to different metrics. This has been studied for Λ CDM under the name of interacting dark energy (see for example [37–40]). The idea is to investigate the interplay between these two properties, namely modifications of gravity and violation of the WEP. In particular, we generalized the stability conditions (2.65) in [15] to include the different couplings of the matter fields. In a subsequent publication [16], we looked at the effect of deviation from Λ CDM and the WEP on various observables using Fisher matrices (in the quasistatic limit). The bottom line is that, even with future surveys, there is not enough information to disentangle the effects of the various α . It might be possible when looking beyond the quasistatic regime, where more scale and time dependence arise, that can potentially break degeneracies.

Looking back at the motivations presented in the Introduction, it will appear to the careful reader that the analysis presented here does not address what I referred

to as the old cosmological constant problem. This is a good remark. At the moment, there are no outstanding candidate theory that gives a hint at a resolution of this problem. The hope is that, by looking at the simplest deviation from Λ CDM, namely adding a scalar field, one might be then guided by the data towards the beginning of an answer. An extra scalar field might well be the manifestation of a more complex theory in certain limits (as it is for massive gravity for example [2]).

Appendix

In this Appendix, I compiled a few complicated expressions that were omitted from the main text of this chapter. The following shorthand notations for the variable Φ , Ψ and π

$$\mathcal{P} \equiv M^2(\dot{\pi} - \Phi), \quad \mathcal{Q} \equiv M^2(\dot{\Psi} + H\Phi + \dot{H}\pi), \quad \mathcal{R} \equiv M^2(\Psi + H\pi), \quad (2.115)$$

allow to express the fluid quantities of Sect. 2.5.3.2 in a compact manner

$$\delta\rho_D \equiv 2\frac{k^2}{a^2}(\alpha_H\mathcal{R} - \alpha_B M^2 H\pi) - 3H[(\rho_D + p_D)\pi - 2\alpha_B\mathcal{Q}] + H^2(\alpha_K - 6\alpha_B)\mathcal{P}, \quad (2.116)$$

$$q_D \equiv -2\alpha_B H\mathcal{P} - (\rho_D + p_D)\pi, \quad (2.117)$$

$$\sigma_D \equiv \alpha_M M^2 H\pi - \alpha_T \mathcal{R} - \alpha_H \mathcal{P}, \quad (2.118)$$

$$\begin{aligned} \delta p_D \equiv & [\dot{p}_D + \alpha_M H M^2 (2\dot{H} + 3H^2)]\pi - 2\alpha_M H\mathcal{Q} \\ & + \left(\frac{\rho_D + p_D}{M^2} + 6\alpha_B H^2 \right) \mathcal{P} + 2(\alpha_B H\mathcal{P})' + \frac{2}{3} \frac{k^2}{a^2} \sigma_D. \end{aligned} \quad (2.119)$$

Moreover, the parameters β in Eq. (2.86) can be related to the initial α parameters of the action (2.47) through (in the case $\alpha_H = 0$)

$$\beta_1 \equiv -\alpha_K \frac{\rho_m + p_m}{4H^2 M^2} - \frac{1}{2} \alpha \left(\frac{\dot{H}}{H^2} + \alpha_T - \alpha_M \right), \quad (2.120)$$

$$\beta_2 \equiv 2(2 + \alpha_M) + 3\Upsilon, \quad (2.121)$$

$$\beta_3 \equiv 3 + \alpha_M + \frac{\alpha_B^2}{H\alpha} \left(\frac{\alpha_K}{\alpha_B^2} \right)', \quad (2.122)$$

$$\beta_4 \equiv (1 + \alpha_T)[2\dot{H}/H^2 + 3(1 + \Upsilon) + \alpha_M] + \dot{\alpha}_T/H, \quad (2.123)$$

$$\beta_5 \equiv c_s^2 - \frac{2\alpha_B(\beta_3 - \beta_2)}{\alpha} + \frac{\alpha_B^2}{\beta_1}(1 + \alpha_T)(\beta_3 - \beta_2) + \frac{\alpha_B^2 \beta_4}{\beta_1}, \quad (2.124)$$

$$\beta_6 \equiv \beta_7 - 2\frac{\alpha_B(\beta_3 - \beta_2)}{\alpha}, \quad (2.125)$$

$$\beta_7 \equiv c_s^2 + 2 \frac{\alpha_B^2(1 + \alpha_T) + \alpha_B(\alpha_T - \alpha_M)}{\alpha}, \quad (2.126)$$

$$\beta_8 \equiv \beta_9 - \frac{(\alpha_K - 6\alpha_B)(\beta_3 - \beta_2)}{\alpha}, \quad (2.127)$$

$$\beta_9 \equiv -(1 + 3c_s^2 + \alpha_T) + \frac{\alpha_B^2}{H\alpha} \left(\frac{\alpha_K}{\alpha_B^2} \right), \quad (2.128)$$

$$\beta_{10} \equiv -6(1 + \Upsilon) - 4\dot{H}/H^2, \quad (2.129)$$

$$\beta_{11} \equiv \frac{2}{3} - 2 \frac{\alpha_B^2}{\beta_1} [(2 - \alpha_M) + 2\dot{H}/H^2] - 2 \frac{\alpha_B^4}{\beta_1 H\alpha} \left(\frac{\alpha_K}{\alpha_B^2} \right), \quad (2.130)$$

with

$$12\beta_1 H^3 M^2 \Upsilon \equiv 2\alpha M^2 \left\{ [\dot{H} + (\alpha_T - \alpha_M)H^2] + (3 + \alpha_M)H[\dot{H} + (\alpha_T - \alpha_M)H^2] \right\} \\ + \alpha_K \dot{p}_m - (\rho_m + p_m)H(\alpha_K - 6\alpha_B)(\alpha_T - \alpha_M) + 6(\rho_m + p_m) \frac{\alpha_B^4}{\alpha} \left(\frac{\alpha_K}{\alpha_B^2} \right). \quad (2.131)$$

On the other hand, the γ in Eq. (2.102) read

$$\gamma_1 \equiv \alpha_K \frac{\rho_D + p_D}{4H^2 M^2} - 3\alpha_B^2 \frac{\dot{H}}{H^2}, \quad (2.132)$$

$$\gamma_2 \equiv c_s^2 + \frac{\alpha_T}{3} - 2 \frac{\alpha_B(2 + \Gamma) + (1 + \alpha_B)(\alpha_M - \alpha_T)}{\alpha}, \quad (2.133)$$

$$\gamma_3 \equiv c_s^2 + \frac{\gamma_8}{3}, \quad (2.134)$$

$$\gamma_4 \equiv \frac{1}{\rho_D + p_D} \left\{ -\dot{p}_D/H + \alpha_M[\rho_D + p_D - 3H^2 M^2] \right. \\ \left. + 6 \frac{\alpha_B^2}{\alpha} [(3 + \alpha_M + \Gamma)(\rho_m + p_m) - \dot{p}_m/H] \right\}, \quad (2.135)$$

$$\gamma_5 \equiv -1 - \frac{(6\alpha_B - \alpha_K)(\alpha_T - \alpha_M)}{6\alpha_B^2} + \frac{\alpha_B^2}{H\alpha} \left(\frac{\alpha_K}{\alpha_B^2} \right), \quad (2.136)$$

$$\gamma_6 \equiv -6\alpha_B^2 \frac{2 + \Gamma}{\alpha} + \frac{\alpha_K \alpha_M - 6\alpha_B^2}{\alpha}, \quad (2.137)$$

$$\gamma_7 \equiv \frac{\alpha_K \alpha_M - 6\alpha_B^2}{3\alpha} - \frac{(6\alpha_B - \alpha_K)(\alpha_T - \alpha_M)}{3\alpha}, \quad (2.138)$$

$$\gamma_8 \equiv \alpha_T + \frac{\alpha_T - \alpha_M}{\alpha_B}, \quad (2.139)$$

$$\gamma_9 \equiv \alpha \frac{\alpha_T - \alpha_M}{2}, \quad (2.140)$$

$$\gamma_{10} \equiv 3\alpha_B^2(\alpha_T - \alpha_M), \quad (2.141)$$

where

$$\gamma_1 \Gamma \equiv \frac{\alpha_K}{4H^2 M^2} \left[(3 + \alpha_M)(\rho_m + p_m) - \dot{p}_m/H - \frac{\alpha_B^2(\rho_D + p_D)}{\alpha_K H} \left(\frac{\alpha_K}{\alpha_B^2} \right)' \right] - \alpha \frac{\ddot{H}}{2H^3}, \quad (2.142)$$

and

$$c_s^2 = - \frac{2(1 + \alpha_B) \left[\dot{H} - (\alpha_M - \alpha_T)H^2 + H^2 \alpha_B(1 + \alpha_T) \right] + 2H\dot{\alpha}_B + (\rho_m + p_m)/M^2}{H^2 \alpha}. \quad (2.143)$$

References

1. A. Joyce, B. Jain, J. Khoury, M. Trodden, Beyond the cosmological standard model. *Phys. Rept.* **568**, 1–98 (2015). 1407.0059
2. C. de Rham, Massive gravity. *Living Rev. Rel.* **17**, 7 (2014). 1401.4173
3. S. Hassan, R.A. Rosen, Bimetric gravity from ghost-free massive gravity. *JHEP* **1202**, 126 (2012). 1109.3515
4. **Supernova Search Team** Collaboration, A.G. Riess et al., Observational evidence from supernovae for an accelerating universe and a cosmological constant. *Astron. J.* **116**, 1009–1038 (1998). astro-ph/9805201
5. **Supernova Cosmology Project** Collaboration, S. Perlmutter et al., Measurements of Omega and Lambda from 42 high redshift supernovae. *Astrophys. J.* **517**, 565–586 (1999). astro-ph/9812133
6. N. Arkani-Hamed, H.-C. Cheng, M.A. Luty, S. Mukohyama, Ghost condensation and a consistent infrared modification of gravity. *JHEP* **0405**, 074 (2004). hep-th/0312099
7. C. Cheung, P. Creminelli, A.L. Fitzpatrick, J. Kaplan, L. Senatore, The effective field theory of inflation. *JHEP* **0803**, 014 (2008). 0709.0293
8. L. Senatore, K.M. Smith, M. Zaldarriaga, Non-Gaussianities in single field inflation and their optimal limits from the WMAP 5-year data. *JCAP* **1001**, 028 (2010). 0905.3746
9. P. Creminelli, G. D’Amico, M. Musso, J. Noreña, E. Trincherini, Galilean symmetry in the effective theory of inflation: new shapes of non-Gaussianity. *JCAP* **1102**, 006 (2011). 1011.3004
10. P. Creminelli, G. D’Amico, J. Noreña, F. Vernizzi, The effective theory of quintessence: the $w < -1$ side unveiled. *JCAP* **0902**, 018 (2009). 0811.0827
11. G. Gubitosi, F. Piazza, F. Vernizzi, The effective field theory of dark energy. *JCAP* **1302**, 032 (2013). 1210.0201
12. J.K. Bloomfield, E.E. Flanagan, M. Park, S. Watson, Dark energy or modified gravity? An effective field theory approach. *JCAP* **1308**, 010 (2013). 1211.7054
13. J. Gleyzes, D. Langlois, F. Piazza, F. Vernizzi, Essential building blocks of dark energy. *JCAP* **1308**, 025 (2013). 1304.4840
14. J. Gleyzes, D. Langlois, F. Vernizzi, A unifying description of dark energy. *Int. J. Mod. Phys. D* **23**, 3010 (2014). 1411.3712
15. J. Gleyzes, D. Langlois, M. Mancarella, F. Vernizzi, Effective theory of interacting dark energy. *JCAP* **1508(08)**, 054 (2015). 1504.05481
16. J. Gleyzes, D. Langlois, M. Mancarella, F. Vernizzi, Effective theory of dark energy at redshift survey scales. *JCAP* **1602(02)** 056 (2016). 1509.02191
17. R.L. Arnowitt, S. Deser, C.W. Misner, The dynamics of general relativity. *Gen.Rel.Grav.* **40**, 1997–2027 (2008). gr-qc/0405109

18. E. Bellini, I. Sawicki, Maximal freedom at minimum cost: linear large-scale structure in general modifications of gravity. *JCAP* **1407**, 050 (2014). 1404.3713
19. R. Caldwell, R. Dave, P.J. Steinhardt, Cosmological imprint of an energy component with general equation of state. *Phys. Rev. Lett.* **80**, 1582–1585 (1998). astro-ph/9708069
20. C. Deffayet, O. Pujolas, I. Sawicki, A. Vikman, Imperfect dark energy from kinetic gravity braiding. *JCAP* **1010**, 026 (2010). 1008.0048
21. C. Deffayet, X. Gao, D. Steer, G. Zahariade, From k-essence to generalised Galileons. *Phys. Rev. D* **84**, 064039 (2011). 1103.3260
22. H.A. Buchdahl, Non-linear Lagrangians and cosmological theory. *Mon. Not. R. Astron. Soc.* **150**, 1 (1970)
23. C. Brans, R. Dicke, Mach's principle and a relativistic theory of gravitation. *Phys. Rev.* **124**, 925–935 (1961)
24. C. Armendariz-Picon, V.F. Mukhanov, P.J. Steinhardt, A Dynamical solution to the problem of a small cosmological constant and late time cosmic acceleration. *Phys. Rev. Lett.* **85**, 4438–4441 (2000). astro-ph/0004134
25. F. Sbisà, Classical and quantum ghosts. *Eur. J. Phys.* **36**, 015009 (2015). 1406.4550
26. S. Weinberg, *Cosmology* (Oxford University Press, 2008)
27. R. Bean, O. Doré, Probing dark energy perturbations: the dark energy equation of state and speed of sound as measured by WMAP. *Phys. Rev. D* **69**, 083503 (2004). astro-ph/0307100
28. T. Baker, P.G. Ferreira, C.D. Leonard, M. Motta, New gravitational scales in cosmological surveys. *Phys. Rev. D* **90**(12), 124030, (2014). 1409.8284
29. G.-B. Zhao, L. Pogosian, A. Silvestri, J. Zylberberg, Searching for modified growth patterns with tomographic surveys. *Phys. Rev. D* **79**, 083513 (2009). 0809.3791
30. I. Sawicki, E. Bellini, Limits of quasistatic approximation in modified-gravity cosmologies. *Phys. Rev. D* **92**(8), 084061 (2015). 1503.06831
31. B. Hu, M. Raveri, N. Frusciante, A. Silvestri, Effective field theory of cosmic acceleration: an implementation in CAMB. *Phys. Rev. D* **89**(10) 103530 (2014). 1312.5742
32. A. Lewis, A. Challinor, A. Lasenby, Efficient computation of CMB anisotropies in closed FRW models. *Astrophys. J.* **538**, 473–476 (2000). astro-ph/9911177
33. F. Piazza, H. Steigerwald, C. Marinoni, Phenomenology of dark energy: exploring the space of theories with future redshift surveys. *JCAP* **1405**, 043 (2014). 1312.6111
34. **XXX Collaboration** Collaboration, P. Ade et. al., Planck 2015 results. XIV. Dark energy and modified gravity. 1502.01590
35. **EUCLID Collaboration** Collaboration, R. Laureijs et. al., Euclid Definition Study Report. 1110.3193
36. **LSST Science, LSST Project** Collaboration, P.A. Abell et. al., LSST Science Book, Version 2.0. 0912.0201
37. L. Amendola, Coupled quintessence. *Phys. Rev. D* **62**, 043511 (2000). astro-ph/9908023
38. J. Valiviita, R. Maartens, E. Majerotto, Observational constraints on an interacting dark energy model. *Mon. Not. R. Astron. Soc.* **402**, 2355–2368 (2010). 0907.4987
39. M. Baldi, V. Pettorino, G. Robbers, V. Springel, Hydrodynamical N-body simulations of coupled dark energy cosmologies. *Mon. Not. R. Astron. Soc.* **403** 1684–1702 (2010). 0812.3901
40. M. Zumalacárregui, T. Koivisto, D. Mota, P. Ruiz-Lapuente, Disformal scalar fields and the dark sector of the universe. *JCAP* **1005**, 038 (2010). 1004.2684

Chapter 3

Beyond Horndeski

Although using parametrizations such as the EFT of DE (for other examples, see [1, 2]) proves useful when testing our understanding of cosmology, finding a more complete description through a specific model provides advantages. For example, it allows to go beyond the linear approximation, which is necessary when looking at smaller scales, where it breaks down. A very important step in this endeavour was the work of Horndeski [3] and its rediscovery [4, 5]. What are now known as Horndeski theories, or generalized galileons, are the most general Lorentz invariant scalar-tensor theories leading to second-order equations of motion, both for the scalar and for the tensors. This property guarantees that they are well behaved and free of ghosts. The fondness for these theories comes from the standard lore that theories ruled by EOM with more than two derivatives should be automatically discarded because they suffer from instabilities, according to Ostrogradski's theorem. However, this reasoning is too hasty. Indeed, in order for this statement to be correct, the theory needs to be non degenerate, in a sense that I will make clear later.

In this chapter, I will describe scalar-tensor theories that are not contained in Horndeski's. As a consequence, their EOM contain terms with three derivatives, but I will show that the theories are still "healthy", meaning devoid of Ostrogradski's instability. First, I will spend some time on what Horndeski theories are, before moving to these new theories, that we dubbed G^3 for "Generalized Generalized Galileons". Finally, I will use the formalism of Chap. 2 to explore the novel phenomenology that appears when going beyond Horndeski.

3.1 Horndeski Theories

As I have said before, the easiest way to modify Λ CDM is to introduce a scalar field. The goal is therefore to write a Lagrangian for this scalar field

$$L(\phi, \phi_\alpha \equiv \nabla_\alpha \phi, \phi_{\beta\gamma} \equiv \nabla_\beta \nabla_\gamma \phi, \mathbf{g}_{\mu\nu}, \dots). \quad (3.1)$$

Usually, when writing such Lagrangians, only first derivatives of the scalar field are involved. However, one can be more general and include terms such as $\square\phi \equiv \mathbf{g}^{\mu\nu}\phi_{,\mu\nu}$. They are slightly more delicate, as they can lead to extra, unstable DOF. A sufficient condition to avoid this is to require that the EOM derived from the Lagrangian are at most second-order in derivative. Before turning to the case of a general metric $\mathbf{g}_{\mu\nu}$ it is instructive to focus on the Minkowski limit, where the only dynamical DOF is the scalar. The key ingredient are the so-called galileons Lagrangians of [6]:

$$L_2^{\text{gal},1} = X, \quad (3.2)$$

$$L_3^{\text{gal},1} = X\square\phi - \phi_{,\mu}\phi^{,\mu\nu}\phi_{,\nu}, \quad (3.3)$$

$$L_4^{\text{gal},1} = X[(\square\phi)^2 - \phi_{,\mu\nu}\phi^{,\mu\nu}] - 2(\phi^{,\mu}\phi^{,\nu}\phi_{,\mu\nu}\square\phi - \phi^{,\mu}\phi_{,\mu\nu}\phi_{,\lambda}\phi^{,\lambda\nu}), \quad (3.4)$$

$$L_5^{\text{gal},1} = X[(\square\phi)^3 - 3(\square\phi)\phi_{,\mu\nu}\phi^{,\mu\nu} + 2\phi_{,\mu\nu}\phi^{,\nu\rho}\phi_{,\rho}^{\mu}] - 3[(\square\phi)^2\phi_{,\mu}\phi^{,\mu\nu}\phi_{,\nu} - 2\square\phi\phi_{,\mu}\phi^{,\mu\nu}\phi_{,\nu\rho}\phi^{\rho} - \phi_{,\mu\nu}\phi^{,\mu\nu}\phi_{,\rho}\phi^{\rho\lambda}\phi_{,\lambda} + 2\phi_{,\mu}\phi^{,\mu\nu}\phi_{,\nu\rho}\phi^{\rho\lambda}\phi_{,\lambda}], \quad (3.5)$$

which are can be generalized to

$$L_2^{\text{Mink}} = A_2(\phi, X), \quad (3.6)$$

$$L_3^{\text{Mink}} = A_3(\phi, X)\square\phi, \quad (3.7)$$

$$L_4^{\text{Mink}} = A_4(\phi, X)[(\square\phi)^2 - \phi_{,\mu\nu}\phi^{,\mu\nu}], \quad (3.8)$$

$$L_5^{\text{Mink}} = A_5(\phi, X)[(\square\phi)^3 - 3(\square\phi)\phi_{,\mu\nu}\phi^{,\mu\nu} + 2\phi_{,\mu\nu}\phi^{,\nu\rho}\phi_{,\rho}^{\mu}], \quad (3.9)$$

where here $\phi_{,\mu\nu} = \partial_{\mu}\partial_{\nu}\phi$ since this is in flat space. For the choice of functions $A_a \propto X$ one recovers the previous expressions up to total derivatives.

The action $S = \int d^4x \sum_a L_a^{\text{Mink}}$ constitutes the most general action for a scalar in flat space that leads to second-order EOM. What is essential in order to avoid higher derivatives is the antisymmetric structure that appears, in particular in the quartic (3.8) and quintic (3.9) galileons. Note that the same sort of structure appears in ghost-free massive gravity [7, 8] when focusing on the scalar mode (taking the so-called decoupling limit).

If we now want to write a covariant version of the most general action leading to second-order EOM in curved spacetime, the allowed Lagrangians can be decomposed into four classes

$$L_2^H[G_2] \equiv G_2(\phi, X), \quad (3.10)$$

$$L_3^H[G_3] \equiv G_3(\phi, X)\square\phi, \quad (3.11)$$

$$L_4^H[G_4] \equiv G_4(\phi, X)({}^4R - 2G_{4X}(\phi, X)[(\square\phi)^2 - \phi^{,\mu\nu}\phi_{,\mu\nu}]), \quad (3.12)$$

$$L_5^H[G_5] \equiv G_5(\phi, X)({}^4G_{\mu\nu}\phi^{,\mu\nu} + \frac{1}{3}G_{5X}(\phi, X)[(\square\phi)^3 - 3\square\phi\phi^{,\mu\nu}\phi_{,\mu\nu} + 2\phi^{,\mu\nu}\phi_{,\nu\rho}\phi_{,\rho}^{\mu}]). \quad (3.13)$$

The first type (3.10) corresponds to quintessence and k -essence, while the second (3.11) corresponds to the kinetic gravity braiding Lagrangian (2.53).

The third Lagrangian (3.12) contains the Einstein Hilbert action (2.12), for $G_4 = M_{\text{Pl}}^2/2$. When $G_{4X} \neq 0$ the second piece has the structure inherited from the quartic galileon (3.8). However, when the metric is dynamical and the partial derivatives are replaced by covariant ones, a non minimal coupling term, $G_4(\phi, X)^{(4)}R$, is needed in order to keep the EOM second-order. Finally, the last type, Eq. (3.13), known as the quintic generalized galileon, is the extension of (3.12) to more fields ϕ . The list stops there because any Lagrangian with more fields satisfying Horndeski's conditions would be a total derivative.

In the following section, I am going to argue that one can in fact write a more general action that is still stable, even though it possesses terms with more than two derivatives in the EOM.

3.2 General Considerations on Higher Order Derivatives

The desire for second-order EOM stems from Ostrogradski's theorem, which can be stated as following: imagine the position $q(t)$ of a particle is described by a Lagrangian

$$L(q, \dot{q}, \ddot{q}). \quad (3.14)$$

Note that, usually, the Lagrangian does not depend on the second derivative of the position. In this peculiar case, one can define the conjugate momenta to these variable as

$$P_1 \equiv \frac{\partial L}{\partial \dot{q}} - \frac{d}{dt} \frac{\partial L}{\partial \ddot{q}}, \quad P_2 \equiv \frac{\partial L}{\partial \ddot{q}}. \quad (3.15)$$

Ostrogradski's theorem states (see for example [9]) that if the system is non-degenerate, i.e. if one can express the variable \dot{q} and \ddot{q} as functions of P_1 and P_2 , the system will suffer from ghost instabilities as discussed in Sect. 2.4. In this simple case, the non degeneracy conditions translates simply to the invertibility of the 2×2 matrix

$$\frac{\partial L}{\partial q^{(i)}} \frac{\partial L}{\partial q^{(j)}}, \quad (3.16)$$

where $q^{(j)}$ denotes the j th derivative of q w.r.t. time. It is easy to convince oneself that when this is the case, the EOM contains terms with more than two time derivatives.

Indeed, even though Ostrogradski's proof is formulated at the level of the action, its consequences can be directly seen in the EOM. Let's take the case of single DOF, $\psi(t)$, whose EOM contains three time derivatives.¹ This means that, in order to evolve ψ from an initial state, one needs three conditions: the usual "position" $\psi(t_0)$ and

¹Note that the case of three derivatives is somewhat particular, since only one additional initial condition is needed, instead of the two associated with a full DOF. Moreover, it is not possible to construct a Lagrangian for a single field ψ that gives odd number of time derivatives. However, it can happen when more than one field are present and constitutes thus a case worth mentioning.

“velocity” $\dot{\psi}(t_0)$ but also the “acceleration” $\ddot{\psi}(t_0)$. This goes against the idea that a DOF is given by the couple position-momentum. It signifies the presence of an extra DOF, which, according to Ostrogradski, is a ghost (in the sense of Eq. (2.59) with $\xi < 0$).

At the root of the proof is a notion of non degeneracy. This is not apparent in the case of one field since as soon as there is a higher derivative in the EOM, one must specify more initial conditions. However, when considering an action for more than one field, the non degeneracy conditions are not always this trivial: one can have the coefficient in front of higher derivative non zero but still have a degenerate system. A simple example is the following set of equations

$$\begin{aligned} \ddot{\psi} + \ddot{\phi} + H_1 \dot{\psi} + H_2^3 \phi &= 0, \\ \ddot{\psi} + \ddot{\phi} - H_3 \dot{\phi} &= 0, \end{aligned} \tag{3.17}$$

where the H_i are arbitrary constants. Naively, one could think this would require three initial conditions for ψ and ϕ , for a total of six, and the apparition of a third DOF. However, by plugging the second equation in the first, one can see the system is degenerate, since it is equivalent to

$$\begin{aligned} H_3 \ddot{\phi} + H_1 \dot{\psi} + H_2^3 \phi &= 0, \\ \ddot{\psi} + \ddot{\phi} - H_3 \dot{\phi} &= 0, \end{aligned} \tag{3.18}$$

which is a standard second-order system describing two DOF.

The case of Lorentz invariant scalar-tensor theories is even more involved. Indeed, because of the gauge freedom, the system is degenerate: we saw for example in Sect. 2.4 that the lapse N and the shift N_i yielded constraint equations. This explains the fact that even GR, which a priori has ten DOF (the ten components of the metric), propagates only two.

In the case of Eqs. (3.4) and (3.5) (as well as the other quartic (3.12) and quintic (3.13) Lagrangians), the degeneracy is increased by the specific antisymmetric structure of the Lagrangians: in particular, one can see that because of this structure, $\frac{\partial^2 L_a}{\partial \dot{\phi}^2} = 0$. Of course, as I said above, the degeneracy condition is really on the full matrix (3.16), but intuitively this is a sign that the theory is more degenerate.

It is exactly this degeneracy that would render the proof of Ostrogradski inapplicable in the Lagrangians of Horndeski, even before studying the EOM. Therefore, this realization gives hope that one can construct theories that are more general than Horndeski without introducing ghost DOF by considering Lagrangians that are degenerate enough. It should be noted that this is not a miracle recipe that would get rid of every ghost. The larger the number of derivatives, the more degenerate the theory needs to be, making it harder and harder to conceive one.

3.3 Generalized Generalized Galileons G^3

Before introducing G^3 theories, let me make a general remark here. When taking the flat space limit of any scalar-tensor theory, the possibility of non trivial degeneracy disappears since only the scalar remains. There, the number of possibilities is limited to the Lagrangians (3.6)–(3.9). This is why a necessary condition for any scalar-tensor theory to be ghost free is to reduce to these Lagrangians when $g_{\mu\nu} \rightarrow \eta_{\mu\nu}$.²

With this idea in mind, in [10, 11] we studied the following Lagrangians

$$L_4 = L_4^H[B_4(\phi, X)] + F_4(\phi, X)L_4^{\text{gal},1}, \quad (3.19)$$

$$L_5 = L_5^H[B_5(\phi, X)] + F_5(\phi, X)L_5^{\text{gal},1}, \quad (3.20)$$

where $L_4^{\text{gal},1}$ and $L_5^{\text{gal},1}$ the Lagrangians from Eqs. (3.4) and (3.5) with the replacement

$$\eta_{\mu\nu} \rightarrow g_{\mu\nu}, \quad \partial_\mu \rightarrow \nabla_\mu. \quad (3.21)$$

Under this form it is easy to see that the Horndeski case corresponds to $F_4 = F_5 = 0$. However, when these functions are not zero, the EOM contain terms with three derivatives. More precisely, the metric equations contain three derivatives of the scalar and the scalar field equation contains three derivative of the metric. This means that when going to flat space, the scalar field recovers its second-order EOM, which is expected since in flat space these Lagrangians reduce to Eqs. (3.8) and (3.9) (up to total derivatives, see [11]).

This is not how we first discovered these Lagrangians. The first hint we had was when looking at the EFT of DE and realizing that, at linear order, one could be more general than Horndeski theories: we had an additional parameter α_H in Eq. (2.47) that accounted for a deviation from Horndeski, while keeping the right number of DOF. We then built a non linear theory that respected this property. Therefore, when we first wrote it, it was in the context of the EFT of DE and as such it was in unitary gauge. Using Eqs. (2.4) and (2.13), the Lagrangians (3.19) and (3.20) can be recast into:

$$\boxed{\begin{aligned} L_4 &\equiv A_4(\phi, X) \left(K^2 - K_{\mu\nu} K^{\mu\nu} \right) + B_4(\phi, X) R, \\ L_5 &\equiv A_5(\phi, X) \left(K^3 - 3K K_{\mu\nu} K^{\mu\nu} + 2K_{\mu\nu} K^{\nu\rho} K^\mu{}_\rho \right) + B_5(\phi, X) K^{\mu\nu} \left(R_{\mu\nu} - \frac{1}{2} h_{\mu\nu} R \right), \end{aligned}} \quad (3.22)$$

where

$$\begin{aligned} A_4 &\equiv -B_4 + 2X B_{4X} - X^2 F_4, \\ A_5 &\equiv -\frac{X B_{5X}}{3} + (-X)^{5/2} F_5. \end{aligned} \quad (3.23)$$

²When this is not the case, the theory might be ghost free around specific background, but the property might not be Lorentz invariant.

This yields the expression of the Horndeski Lagrangians in terms of 3+1 quantities in the case $F_4 = F_5 = 0$, which was first derived in [12]. On top of making the connection with Chap. 2 easier, these expressions are going to allow us to prove that the theory has no extra DOF. In order to do so, we will specialize to the case where the scalar field is spacelike, so that we can go to unitary gauge.

One could rightfully argue that proving the soundness of the theory under this assumption does not guarantee it will hold on a different background. This is indeed true. However, it is a necessary condition and under this assumption one can actually say something quantitative about the number of DOF. Moreover, the fact that it also reduces to galileons in Minkowski is a strong signal that the theory is safe around any background. I will give a purely Lorentz invariant proof in a following section, which relies on knowing a priori a transformation of the metric that maps subsets of G^3 onto Horndeski. After this thesis was finished, various gauge-invariant studies of the G^3 Lagrangians appeared. [13] explicitly showed that the third derivatives can be eliminated (in a similar fashion as the reasoning of Eqs. (3.17) and (3.18)), while [14–16] used a clever and compact way of generalizing the variable of the unitary gauge to an arbitrary gauge, and then performed a Hamiltonian analysis (the reader unfamiliar with Hamiltonian analyses is encouraged to read Sect. 2 [14], which gives a very clear and detailed introduction). They confirm the results of the unitary gauge analysis below, with a few restrictions on what combinations of Lagrangians are allowed.

3.4 Hamiltonian Analysis

In unitary gauge, the proof is very general and is based on a Hamiltonian analysis. We are back to using the metric whose line element is

$$ds^2 = -N^2 dt^2 + h_{ij} (dx^i + N^i dt) (dx^j + N^j dt) . \quad (3.24)$$

Moreover, in this gauge, the extrinsic curvatures in Eq. (3.22) take their usual 3+1 expression

$$K_{ij} = \frac{1}{2N} [\dot{h}_{ij} - D_i N_j - D_j N_i] , \quad (3.25)$$

and again, the other components are not needed (see Eq. (2.9)).

To prove that there are no extra DOF, I will use a Hamiltonian analysis, that will allow me to count the number of DOF. The case is actually quite similar to the standard counting of DOF in GR, starting from Eq. (2.12).

The first step is to compute the conjugate momenta of the “position” variables (N, N_k, h_{ij}) in order to write the Hamiltonian as a function of the twenty canonical

variables (N, π_N) , (N_k, π_k) , (h_{ij}, π_{ij}) . Since the lapse and the shift do not appear with time derivatives, their conjugate momenta vanish

$$\pi_N = 0, \quad \pi_i = 0, \quad (3.26)$$

and their EOM will yield constraints.

The Hamiltonian is defined as

$$H \equiv \int d^3\vec{x} [\pi^{ij}\dot{h}_{ij} - \mathcal{L}]. \quad (3.27)$$

What is left to do is to invert the relation between \dot{h}_{ij} and π_{ij} . This can be done explicitly in the case of L_4 . However, in the case of L_5 the relation between these two quantities is not linear: expressing \dot{h}_{ij} as a function of π_{ij} requires taking the square root of a matrix. Therefore, even though the inversion is locally well defined, one cannot get an explicit expression (it was later shown in e.g. [14] that including L_5 in addition to L_4 and L_4^H leads to higher number of DOF).

After this inversion in the case of L_4 (3.19), the Hamiltonian can be put in the form

$$H = \int d^3\vec{x} [N\mathcal{H}_0(N) + N^i\mathcal{H}_i], \quad (3.28)$$

with

$$\mathcal{H}_i \equiv -2D_j\pi_i^j, \quad (3.29)$$

$$\begin{aligned} \mathcal{H}_0 &\equiv -\frac{1}{\sqrt{h}A_4} \left(\pi_{ij}\pi^{ij} - \frac{1}{2}\pi^2 \right) - \sqrt{h}B_4{}^{(4)}R, \\ A_4 &= -B_4 - NB_{4N} - F_4. \end{aligned} \quad (3.30)$$

The last equality stems from Eq. (3.23) in unitary gauge, where $X = -1/N^2$ (choosing $\phi_0(t) = t$). The Hamiltonian of GR has exactly the same form, with $B_4 = -A_4 = 1/(16\pi G)$, implying that \mathcal{H}_0 is independent of N , which is not the case in general.

To count the DOF in a constrained system such as the one described by Eq. (3.28), one has to sort the constraints according to their class in Dirac's terminology. A constraint can either be first-class, which implies that its Poisson bracket with all the other constraints vanish, or second class otherwise. Although these definitions are quite technical for the unfamiliar reader, let me distill their relevant properties. First class constraints are particular constraints that are in general associated with gauge freedom. This is why, on top of eliminating one variable, the freedom associated with the gauge removes an additional variable. The statement is thus that a first class constraint removes a full DOF (which corresponds to a couple of canonical variables). Second class constraints however do not stem from gauge freedom and as such remove only half a DOF (see for example [17] for a discussion on constrained Hamiltonian and number of DOF).

In the case of GR, all the constraints

$$\pi_N = 0, \quad \frac{\partial H}{\partial N} = \mathcal{H}_0 = 0, \quad \pi_i = 0, \quad \frac{\partial H}{\partial N_i} = \mathcal{H}_i = 0, \quad (3.31)$$

are first class (this is actually guaranteed by the fact that N and N_i only appear linearly in the action). This can be understood because, even though a specific foliation is chosen to decompose the Ricci scalar in 3+1 quantities, this foliation is completely arbitrary. Therefore, the time gauge freedom is still maintained in the action and N is the variable that enforces it. The same can be said about the spatial gauge freedom and N_i .

The counting can then be done as following: there are two constraints for (N, π_N) and six for (N_i, π_i) , each removing a full DOF. This leaves two DOF out of the naive ten, which are the two polarizations of gravity waves.

In the case of G^3 , the only difference is that the constraints associated with (N, π_N)

$$\pi_N = 0, \quad \frac{\partial H}{\partial N} = \mathcal{H}_0(N) + N\mathcal{H}'_0(N) = 0, \quad (3.32)$$

are in general second class and remove only half of DOF each. Technically, this is because in general \mathcal{H}_0 depends on N . More intuitively, this is just the expression that the time diffeomorphism invariance is broken by the choice of the unitary gauge, which represents a specific choice of time given by the scalar field.

However, as we discussed in Sect. 2.1, the action is still invariant under spatial diffs, so the six constraints for (N_i, π_i) remain first class. Actually, it is not exactly \mathcal{H}_i that is first class, but rather $\mathcal{H}_i + \pi_N \partial_i N$ (see for example [18]), which is actually the total momentum constraint that would appear for GR plus a scalar field.

The counting therefore yields three DOF, which are the expected tensor (two) and scalar (one) modes. Contrarily to what could have been thought naively, no extra DOF appears in the theory. Notice that imposing the Horndeski conditions (3.23) does not yield anything special in this formulation.

Nevertheless, the simplicity of the unitary gauge action hides the fact that the Lagrangians (3.19) and (3.20) are quite peculiar. Two things should be kept in mind.

- The counting of DOF could have yielded four. For example, if one were to simply detune the functions G_4 and G_{4X} in Eq. (3.19), when going to unitary gauge the action would contain terms in $\dot{N}K$. Indeed it can be checked using Eq. (2.4) that

$$(\square\phi)^2 - \phi_{\mu\nu}\phi^{\mu\nu} \supset -2\nabla_\mu X K n^\mu \propto \dot{N}K, \quad (3.33)$$

since $X \propto 1/N^2$ in unitary gauge. In this case, $\pi_N \neq 0$ and one can invert the momenta to write \dot{N} and \dot{h}_{ij} in terms of π_N and π_{ij} .³ Then the equations associated

³The last statement is essential. Indeed, there exist situations where $\pi_N \neq 0$ but the Lagrangian is too degenerate to allow the inversion of the momenta, so that there is actually no extra DOF. See [11, 19] for examples of such a case.

to N become dynamical: they are no longer constraints. The only constraints that remain are those for N_i , which remove six of the ten initial DOF: an extra mode appears, which is a ghost according to Ostrogradski's theorem.

- The proof in unitary gauge could be extended to any Lagrangians that depends on arbitrary combinations of the extrinsic curvature, see for example [20]. However, as soon as they do not appear in the specific forms of Eqs. (3.19) and (3.20), the theories do not reduce to galileons in flat space. As I mentioned above, this means that they potentially develop ghost like DOF when the unitary gauge is not defined, i.e. when the scalar field is not spacelike. As such, they might be Lorentz violating theories, which is what happens for Hořava-Lifshitz gravity [21, 22].

3.5 Field Redefinitions

A well known situation where Ostrogradski's theorem does not apply even though higher derivatives are present is when there exists an invertible mapping between a theory and one that is healthy (see e.g. [23]). The term invertible is here taken in its formal mathematical definition: the mapping must be a bijection between the two set of variables.

In particular, in the case of a single variable ψ mapped to $\tilde{\psi}$, the transformation cannot involve derivatives of the field: the “inversion” is always defined up to integration constants, implying the mapping is not injective. This means that one cannot remove the extra DOF associated to a term in $\psi^{(n>2)}$ by defining a new variable $\tilde{\psi} \equiv \psi^{(n-2)}$. The extra DOF are just hidden in the solution of the equation for $\tilde{\psi}$ in terms of ψ . This is yet another way of saying that when there is only one variable, there is no room to play with degeneracies: Ostrogradski's theorem always applies.

However, as soon as more variables are at play, the situation changes. For example, a transformation of the form

$$\begin{aligned}\psi_1 &\rightarrow \psi_2, \\ \phi_1 &\rightarrow \phi_2 + \ddot{\psi}_2,\end{aligned}\tag{3.34}$$

is invertible, since there are no differential equations to solve to express the new variables in terms of the old ones. Thus, the Lagrangian

$$L_2 = -\frac{\dot{\psi}_2^2}{2} - \frac{\dot{\phi}_2^2}{2} - \dot{\phi}_2 \psi_2^{(3)} - \frac{(\psi_2^{(3)})^2}{2}.\tag{3.35}$$

has the same number of DOF as the standard free field Lagrangian

$$L_1 = -\frac{\dot{\psi}_1^2}{2} - \frac{\dot{\phi}_1^2}{2},\tag{3.36}$$

since they are related by Eq. (3.34).

One can also see this in a way similar to Eq. (3.17) since the EOM derived from the Lagrangian (3.35) are

$$\ddot{\psi}_2 + \phi_2^{(4)} + \psi_2^{(6)} = 0, \quad (3.37)$$

$$\ddot{\phi}_2 + \psi_2^{(4)} = 0, \quad (3.38)$$

which are equivalent to

$$\ddot{\psi}_2 = 0, \quad \ddot{\phi}_2 = 0. \quad (3.39)$$

It turns out that in the case of G^3 , we found a way to write this mapping, when restricting to the case of either (3.19) or (3.20), but not when both are considered at the same time. The key is to use disformal transformations [24], such as

$$\begin{aligned} \bar{g}_{\mu\nu} &= \Omega(\phi, X)^2 g_{\mu\nu} + \Gamma(\phi, X) \phi_\mu \phi_\nu, \\ \bar{\phi} &= \phi. \end{aligned} \quad (3.40)$$

For most choices of Ω and Γ this transformation is invertible in the sense I defined above, since no differential equation needs to be solved to express the original quantities in terms of the tilde ones. It was shown [25] that when the functions Ω and Γ do not depend on $X = \phi_\mu \phi^\mu$, this transformation leaves the structure of Horndeski theories invariant. By this I mean that when performing such a transformation on the whole theory $L = \sum_{a=2}^5 L_a$, one gets a Lagrangian $\tilde{L} = \sum_{a=2}^5 \tilde{L}_a$, where L_a and \tilde{L}_a are of the forms (3.10)–(3.13), but with different functions G_b .

Once the functions Ω and Γ are allowed to depend on X , the Horndeski form is no longer preserved. In particular, when focusing on the case where only Γ depends on X , we showed in [11] that the transformation creates a bridge between Horndeski theories and G^3 . More precisely, when considering

$$g_{\mu\nu} \rightarrow \bar{g}_{\mu\nu} = \Omega^2(\phi) g_{\mu\nu} + \Gamma(\phi, X) \phi_\mu \phi_\nu, \quad (3.41)$$

the geometrical quantities above change as⁴

$$\bar{R} \rightarrow \Omega^{-2} R, \quad (3.42)$$

$$\bar{K}_{\mu\nu} \rightarrow \frac{K_{\mu\nu}}{\sqrt{\Omega^2 + \Gamma X}}. \quad (3.43)$$

Since the extrinsic and intrinsic curvatures transform differently, the function of (ϕ, X) in front of the two different parts of the Horndeski Lagrangians, e.g.

$$L_4 \equiv (B_4 - 2X B_{4X}) (K^2 - K_{\mu\nu} K^{\mu\nu}) + B_4(\phi, X) R, \quad (3.44)$$

⁴It is easier to see the effect of the transformation (3.41) on these quantities than directly on the scalar field and its derivatives. However this can be done, see for example [19].

will be modified differently. The freedom in $\Gamma(\phi, X)$ allows to detune these functions, leading to the case of Eq. (3.19) with arbitrary A_4 and B_4 . Conversely, if one starts from

$$L = A_4(\phi, \bar{X})(\bar{K}^2 - \bar{K}_{\mu\nu}\bar{K}^{\mu\nu}) + B_4(\phi, \bar{X})\bar{R}, \quad (3.45)$$

and performs a disformal transformation with Γ solution of

$$\Gamma_X = \frac{A_4 + B_4 - 2X B_{4X}}{X^2 A_4}, \quad (3.46)$$

the resulting Lagrangian belongs to the Horndeski class

$$\bar{L} = (\bar{B}_4 - 2\bar{X} B_{4\bar{X}})(\bar{K}^2 - \bar{K}_{\mu\nu}\bar{K}^{\mu\nu}) + \bar{B}_4(\phi, \bar{X})\bar{R}. \quad (3.47)$$

The same reasoning can be made for the case of L_5 alone. However, in general it is not possible to choose Γ to put both Lagrangians in the Horndeski form. Indeed, there is only a single free function of (ϕ, X) , which is not enough to eliminate the two functions A_4 and A_5 from Eqs. (3.19) and (3.20) simultaneously.

What about introducing a new function of (ϕ, X) by giving a X dependence to Ω ? By considering such a transformation, one not only goes out of Horndeski theories, but out of G^3 as well.

If one were to use a structure involving second derivatives of ϕ in Eq. (3.41), those would have to be covariant and introduce first derivatives of the metric through the Christoffel symbols. In principle, this means that the transformation for the metric becomes differential and would not conserve the number of DOF. We have not been able to find a field redefinition that brings the full action $L_4 + L_5$ to Horndeski.⁵ The very existence of such transformation is not guaranteed. This is where the strength of the Hamiltonian analysis is manifest: it is a standalone procedure and does not rely on exterior knowledge.

One could argue that since the theory can be mapped to Horndeski, the two theories are equivalent. However this is not the case, in particular in the context of late time acceleration. Indeed, the Universe is not just described by gravity plus a scalar field; the matter sector has to be accounted for. When changing the metric in a way similar to Eq. (3.41), the matter sector also changes: a coupling to the scalar field is introduced. This implies in particular that the stress energy tensor of matter is no longer conserved (this is similar to Brans-Dicke theory [26]) and has consequences already at the linear level.

⁵As it turns out, the combination $L_4 + L_5$ was shown to contain a ghost DOF [14].

3.6 Linear Analysis and Coupling to Matter

In order to study the stability conditions and to see how the presence of matter affects the theory, I now turn to the linear perturbations. For that, I will rely on the formalism of Chap. 2. Indeed, the Lagrangians (3.22) are particularly adapted since they already are in terms of geometrical quantities. The main difference with Horndeski will come from the presence of α_H in Eq. (2.47). I will show in this section how this brings a non standard derivative coupling between matter and the scalar field, which affects the propagation of matter perturbations. This also means that, contrarily to the standard idea of the Jeans phenomenon, gravity's effect will not be negligible at very small scales.

3.6.1 Stability and Ghosts

What I have proven with the Hamiltonian analysis in Sect. 3.4 is the absence of extra DOF. One might still be worried that some of those DOF are ghosts. In order to conduct an explicit analysis similar to the one of Sect. 2.4 in the presence of matter, I will describe the latter as a scalar field $\sigma(t, \vec{x}) \equiv \sigma_0(t) + \delta\sigma(t, \vec{x})$ with a non standard kinetic term, that is

$$S_m = \int d^4x \sqrt{-g} P(Y, \sigma), \quad Y \equiv g^{\mu\nu} \partial_\mu \sigma \partial_\nu \sigma. \quad (3.48)$$

This is enough to describe a perfect fluid, characterized by the stress energy tensor

$$T_{\mu\nu} = (\rho_m + p_m) u_\mu u_\nu - p_m g_{\mu\nu}, \quad (3.49)$$

$$p_m \equiv P, \quad \rho_m \equiv 2Y P_Y - P, \quad u_\nu \equiv \frac{\partial_\nu \sigma}{\sqrt{-X}}. \quad (3.50)$$

This choice allows to have a non trivial sound speed, given by $c_m^2 \equiv P_Y / (P_Y - 2\dot{\sigma}_0^2 P_{YY})$ [27].

What will interest us for stability is the kinetic mixing between the variable ζ in Eq. (2.61) and the gauge-invariant variable $Q_\sigma \equiv \delta\sigma - (\dot{\sigma}_0/H)\zeta$. The presence of $\alpha_H \neq 0$ or matter does not modify the quadratic action for tensors, so the conditions will be the same as in Sect. 2.4. Once the constraints are solved, the kinetic part of the quadratic Lagrangian (that is, the one where each field is derived once) is given in Fourier space by the matrix

$$\mathcal{M} = \frac{1}{2} \begin{pmatrix} \tilde{\mathcal{L}}_{\zeta\zeta} \omega^2 + \tilde{\mathcal{L}}_{\partial\zeta\partial\zeta} k^2 & A[\alpha_B \omega^2 - c_m^2 (\alpha_B - \alpha_H) k^2] \\ A[\alpha_B \omega^2 - c_m^2 (\alpha_B - \alpha_H) k^2] & -2P_Y c_m^{-2} (\omega^2 - c_m^2 k^2) \end{pmatrix}, \quad (3.51)$$

with

$$A = -\frac{2\dot{\sigma}_0 P_Y}{H c_m^2 (1 + \alpha_B)}. \quad (3.52)$$

$\tilde{\mathcal{L}}_{\zeta\dot{\zeta}}$ and $\tilde{\mathcal{L}}_{\partial\zeta\partial\dot{\zeta}}$ are functions of the parameters α_a , whose expressions are not very useful here, but can be found in Sect. 5.2 of [11]. In order to get the no ghost conditions, the positivity of the eigenvalues of the time kinetic matrix (i.e. the above matrix with $k = 0$) is required. This leads to the conditions

$$\alpha_K + 6\alpha_B^2 > 0, \quad P_Y c_m^{-2} = P_Y + 2Y P_{YY} < 0. \quad (3.53)$$

The first one is the same as in Sect. 2.4, while the second is the standard condition for k -essence. Once again, we can see here that the case of Horndeski is in no way special regarding ghosts, since α_H does not appear in the conditions. Nevertheless the sound speeds are modified, which changes the conditions to avoid gradient instabilities of Eq. (2.65). To see this, one first needs the dispersion relations. They can be obtained by requiring that the kinetic matrix is singular, implying that its determinant vanishes

$$(\omega^2 - c_m^2 k^2)(\omega^2 - \tilde{c}_s^2 k^2) = (c_s^2 - \tilde{c}_s^2) \left(\frac{\alpha_H}{1 + \alpha_H} \right)^2 \omega^2 k^2, \quad (3.54)$$

with

$$\tilde{c}_s^2 \equiv c_s^2 - \frac{\rho_m + P_m}{H^2 M^2} \frac{(1 + \alpha_H)^2}{\alpha_K + 6\alpha_B^2}. \quad (3.55)$$

This equation has two solutions, $\omega^2 = c_{\pm}^2$. To avoid gradient instabilities, we require that $c_{\pm}^2 > 0$.

One can see that when restricted to Horndeski, $\alpha_H = 0$, $\omega^2 = c_m^2 k^2$ is a solution of this equation and matter perturbations propagate at their usual sound speed. This is in itself not completely trivial, since the presence of α_B induces a kinetic braiding, which brings off-diagonal terms in (3.51).

When $\alpha_H \neq 0$, this mixing has a stronger effect: the presence of the scalar field ϕ modifies the sound speed of matter. Thinking back to the standard Newtonian picture of the pressure perturbation, $\delta p = c_m^2 \delta \rho$, this means that the scalar field act as additional pressure contribution. This will be clearer in Newtonian gauge, where the scalar field is explicit.

3.6.2 Newtonian Gauge and Einstein Frame

As I have said before, the Newtonian gauge is more appropriate to discuss the EOM, particularly in the Newtonian (small scales) limit. Therefore, I reintroduce again the scalar field thanks to the transformation

$$t \rightarrow t + \pi(t, \vec{x}), \quad (3.56)$$

and parametrize the scalar part of the metric as

$$ds^2 = -(1 + 2\Phi)dt^2 + a(t)^2(1 - 2\Psi)\delta_{ij}dx^i dx^j . \quad (3.57)$$

In the action in terms of π , Φ and Ψ , even the kinetic part alone is very involved. This makes the analysis of the propagating DOF rather complicated. However, very much alike the case of Brans-Dicke theory, one can do a field transformation at the level of the metric potentials that puts the gravitational part of the action in a simpler form. By extension of the Brans-Dicke case, where such transformation leaves only the Einstein Hilbert term for gravity, I will call this new frame the Einstein frame. The Einstein metric is related to the original Jordan metric (i.e. the metric to which matter is minimally coupled) through

$$\begin{aligned} \Phi_E &\equiv \frac{1 + \alpha_H}{1 + \alpha_T} \Phi + \left(\frac{1 + \alpha_m}{1 + \alpha_T} - \frac{1 + \alpha_B}{1 + \alpha_H} \right) H\pi - \frac{\alpha_H}{1 + \alpha_T} \dot{\pi} , \\ \Psi_E &\equiv \Psi + \frac{\alpha_H - \alpha_B}{1 + \alpha_H} H\pi . \end{aligned} \quad (3.58)$$

In terms of these variables the kinetic part of the EFT action reads

$$\begin{aligned} S = \int d^4x a^3 M^2 \left\{ \frac{\alpha}{2} \frac{H^2}{(1 + \alpha_H)^2} \left(\dot{\pi}^2 - \tilde{c}_s^2 \frac{(\nabla\pi)^2}{a^2} \right) \right. \\ \left. - 3\dot{\Psi}_E^2 + \frac{1 + \alpha_T}{a^2} [(\nabla\Psi_E)^2 - 2\nabla\Phi_E \nabla\Psi_E] \right\} . \end{aligned} \quad (3.59)$$

The new metric variables are not derivatively coupled to the scalar field, making transparent the kinetic structure of the theory. Notice that when $\alpha_H \neq 0$, Φ_E contains a derivative of π . This comes from the fact that in terms of the original variables Φ and Ψ , the quadratic action contains a term in $\nabla\Psi \nabla\dot{\pi}$, which is exactly the term leading to higher derivatives in the EOM. In this new frame however, the equations are explicitly second-order.

This is reminiscent of Sect. 3.5, where field redefinitions were used to map the theory with higher-order derivatives to one with only second-order EOM. And indeed, we proved in Appendix C of [11] that the term in $\dot{\pi}$ in Eq. (3.58) arises exactly because of the X dependence of Γ in Eq. (3.41).

This transformation also has an effect on the matter sector. In the Jordan frame, the matter action contains an interacting part

$$L_{\text{int}} \equiv \frac{1}{2} \delta g_{\mu\nu} \delta T^{\mu\nu} = -(\Phi \delta \rho_m + 3\Psi \delta p_m) , \quad (3.60)$$

which is the standard one for minimally coupled matter. However, when working with the Einstein frame metric, a coupling between the scalar field and the matter perturbations appears explicitly. If $\alpha_H = 0$, the coupling is of the form

$$L_{\text{int}} \supset C \pi \delta \rho_m , \quad (3.61)$$

where C is a function of time, not important for the present discussion. The stress energy of matter is not conserved and we have the schematic set of equations

$$\ddot{\delta \rho}_m - c_m^2 \frac{\nabla^2 \delta \rho_m}{a^2} + C_m \frac{\nabla^2 \pi}{a^2} \approx 0 , \quad (3.62)$$

$$\ddot{\pi} - \tilde{c}_s^2 \frac{\nabla^2 \pi}{a^2} - C_\phi \delta \rho_m \approx 0 , \quad (3.63)$$

where the symbol \approx stands for an equality in the limit $k \gg aH/c_m$. This means that, qualitatively, $\nabla^2 \pi \sim \delta \rho_m$ (very akin to the Poisson equation of GR), which translates into a non derived term in Eq. (3.62). This is negligible compared to the other terms at small scales, just as for the Jeans phenomenon in GR.

If now $\alpha_H \neq 0$, Eq. (3.58) implies the presence of a coupling

$$L_{\text{int}} \supset -\frac{\alpha_H}{1 + \alpha_H} \dot{\pi} \delta \rho_m . \quad (3.64)$$

The equation for matter contains new derivative terms which are relevant at small scales $k \gg aH/c_m$ since the system scalar plus matter then obeys

$$\boxed{\begin{aligned} \ddot{\delta \rho}_m - c_m^2 \frac{\nabla^2 \delta \rho_m}{a^2} - (\rho_m + p_m) \frac{\alpha_H}{1 + \alpha_H} \frac{\nabla^2 \dot{\pi}}{a^2} &\approx 0 , \\ \ddot{\pi} - \tilde{c}_s^2 \frac{\nabla^2 \pi}{a^2} - \frac{\alpha_H (1 + \alpha_H)}{\alpha H^2 M^2} \dot{\delta \rho}_m &\approx 0 . \end{aligned}} \quad (3.65)$$

The dispersion relations that one gets from this set of equations are exactly the same as in Eq. (3.54). One can see from the second line that now $\nabla^2 \pi \sim \dot{\delta \rho}_m$, which, when plugged back into the matter equation, adds a contribution to $\ddot{\delta \rho}_m$. This cannot be ignored when going to smaller and smaller scales, contrarily to the Horndeski case. Here is yet another proof that Horndeski and G^3 are not equivalent even though connections do exist between the two.

Let me end this section with a small comment on the notion of frames that I used here. The field redefinitions (3.58) are simply a convenient way of seeing the mixing of sound speeds. In a sense, it is a sort of diagonalization of the kinetic matrix. There is not more information in the Einstein frame than in the Jordan frame and if one were to get down to observable quantities, the results would be the same.

3.7 Conclusions

In this chapter, I introduced theories beyond Horndeski, that we dubbed G^3 . These theories can be seen as alternative covariantization of the flat space galileons [6]. As such, they are guaranteed to be ghost free in Minkowski space. When going to curved spacetime, the EOM get in general terms with three derivatives, which could be worrisome for stability. However, a careful Hamiltonian analysis shows that these theories are stable, since they exhibit only the three DOF contained from the beginning.

Links with Horndeski theories can be made for subclasses of G^3 via field redefinitions of the disformal nature (see Eq. (3.41)), but they cannot be used to map the full G^3 onto Horndeski. From a cosmological perspective, a new behavior is uncovered when matter is added to the picture, with novel features such as a mixing of sound speeds. Moreover, it was argued in [28] that, even with screening mechanisms, the time variation of the Planck mass coming from the non minimal coupling to the Ricci in Eq. (3.12) cannot be hidden. Since one can choose B_4 constant in Eq. (3.19) and still get a quartic galileon structure from the second piece, this might be a solution to alleviate this problem.

The community has started to turn its attention to these models. For example, the non gaussian features that arise from these new theories have been explored in [29] and the screening mechanism was studied in [30]. The latter is different from the one in Horndeski theories: the GR solution is recovered outside of massive objects, but it differs inside of these objects. This has an effect on the formation of stars, as shown in [31, 32]. This also affects others properties of stars, like the radius of brown dwarfs and minimum mass for hydrogen burning for red dwarfs [33], or the mass-radius relation in white dwarfs as well as their rotational frequency [34]. Those tests can be used to put constraints on the G^3 Lagrangians, that can be translated to constraints on α_H .

On a more general note, the considerations developed here shed light on the unwarranted theoretical prejudice on higher derivatives. The assumptions in Ostrogradski's proof are precise and they do not exclude completely their presence in the EOM. These sorts of theories need to be thoroughly analyzed before being discarded.

References

1. R.A. Battye, J.A. Pearson, Effective action approach to cosmological perturbations in dark energy and modified gravity. *JCAP* **1207**, 019 (2012). 1203.0398
2. T. Baker, P.G. Ferreira, C. Skordis, The parameterized post-Friedmann framework for theories of modified gravity: concepts, formalism and examples. *Phys. Rev. D* **87**(2) 024015 (2013), 1209.2117
3. G.W. Horndeski, Second-order scalar-tensor field equations in a four-dimensional space. *Int. J. Theor. Phys.* **10**, 363–384 (1974)
4. C. Deffayet, X. Gao, D. Steer, G. Zahariade, From k-essence to generalised Galileons. *Phys. Rev. D* **84** 064039 (2011). 1103.3260

5. T. Kobayashi, M. Yamaguchi, J. Yokoyama, Generalized G-inflation: inflation with the most general second-order field equations. *Prog. Theor. Phys.* **126**, 511–529 (2011). 1105.5723
6. A. Nicolis, R. Rattazzi, E. Trincherini, The Galileon as a local modification of gravity. *Phys. Rev. D* **79**, 064036 (2009). 0811.2197
7. C. de Rham, G. Gabadadze, Generalization of the Fierz-Pauli action. *Phys. Rev. D* **82**, 044020 (2010). 1007.0443
8. C. de Rham, G. Gabadadze, L. Heisenberg, D. Pirtskhalava, Cosmic acceleration and the Helicity-0 Graviton. *Phys. Rev. D* **83**, 103516 (2011). 1010.1780
9. R.P. Woodard, Avoiding dark energy with 1/R modifications of gravity. *Lecture Notes in Physics*, vol. 720 (2007), pp. 403–433. astro-ph/0601672
10. J. Gleyzes, D. Langlois, F. Piazza, F. Vernizzi, Healthy theories beyond Horndeski. *Phys. Rev. Lett.* **114**(21), 211101 (2015). 1404.6495
11. J. Gleyzes, D. Langlois, F. Piazza, F. Vernizzi, Exploring gravitational theories beyond Horndeski. *JCAP* **1502**(02), 018 (2015). 1408.1952
12. J. Gleyzes, D. Langlois, F. Piazza, F. Vernizzi, Essential building blocks of dark energy. *JCAP* **1308**, 025 (2013). 1304.4840
13. C. Deffayet, G. Esposito-Farese, D.A. Steer, Counting the degrees of freedom of generalized Galileons. *Phys. Rev. D* **92**, 084013 (2015). 1506.01974
14. D. Langlois, K. Noui, Degenerate higher derivative theories beyond Horndeski: evading the Ostrogradski instability. *JCAP* **1602**(02), 034 (2016). 1510.06930
15. D. Langlois, K. Noui, Hamiltonian analysis of higher derivative scalar-tensor theories. 1512.06820
16. J.B. Achour, D. Langlois, K. Noui, Degenerate higher order scalar-tensor theories beyond Horndeski and disformal transformations. 1602.08398
17. M. Henneaux, C. Teitelboim, *Quantization of Gauge Systems* (Princeton University Press, 1992)
18. C. Lin, S. Mukohyama, R. Namba, R. Saitou, Hamiltonian structure of scalar-tensor theories beyond Horndeski. *JCAP* **1410**(10), 071 (2014). 1408.0670
19. M. Zumalacárregui, J. García-Bellido, Transforming gravity: from derivative couplings to matter to second-order scalar-tensor theories beyond the Horndeski Lagrangian. *Phys. Rev. D* **89**(6), 064046 (2014). 1308.4685
20. X. Gao, Unifying framework for scalar-tensor theories of gravity. *Phys. Rev. D* **90**(8), 081501 (2014). 1406.0822
21. P. Hofava, Quantum gravity at a Lifshitz Point. *Phys. Rev. D* **79**, 084008 (2009). 0901.3775
22. D. Blas, O. Pujolas, S. Sibiryakov, Consistent extension of horava gravity. *Phys. Rev. Lett.* **104**, 181302 (2010). 0909.3525
23. C. de Rham, G. Gabadadze, A.J. Tolley, Helicity Decomposition of Ghost-free massive gravity. *JHEP* **1111**, 093 (2011). 1108.4521
24. J.D. Bekenstein, The relation between physical and gravitational geometry. *Phys. Rev. D* **48**, 3641–3647 (1993). gr-qc/9211017
25. D. Bettoni, S. Liberati, Disformal invariance of second order scalar-tensor theories: framing the Horndeski action. *Phys. Rev. D* **88**(8), 084020 (2013). 1306.6724
26. C. Brans, R. Dicke, Mach's principle and a relativistic theory of gravitation. *Phys. Rev.* **124**, 925–935 (1961)
27. J. Garriga, V.F. Mukhanov, Perturbations in k-inflation. *Phys. Lett. B* **458**, 219–225 (1999). hep-th/9904176
28. B. Li, A. Barreira, C.M. Baugh, W.A. Hellwing, K. Koyama, et al., Simulating the quartic Galileon gravity model on adaptively refined meshes. *JCAP* **1311**, 012 (2013). 1308.3491
29. M. Fasiello, S. Renaux-Petel, Non-Gaussian inflationary shapes in G^3 theories beyond Horndeski. *JCAP* **1410**(10), 037 (2014). 1407.7280
30. T. Kobayashi, Y. Watanabe, D. Yamauchi, Breaking of Vainshtein screening in scalar-tensor theories beyond Horndeski. *Phys. Rev. D* **91**(6), 064013 (2015). 1411.4130
31. K. Koyama, J. Sakstein, Astrophysical probes of the Vainshtein mechanism: stars and galaxies. *Phys. Rev. D* **91**, 124066 (2015). 1502.06872

32. R. Saito, D. Yamauchi, S. Mizuno, J. Gleyzes, D. Langlois, Modified gravity inside astrophysical bodies. *JCAP* **1506**, 008 (2015). 1503.01448
33. J. Sakstein, Testing gravity using Dwarf stars. *Phys. Rev. D* **92** (2015) 124045, 1511.01685
34. R.K. Jain, C. Kouvaris, N.G. Nielsen, White Dwarf critical tests for modified gravity. 1512.05946

Chapter 4

Predictions for Primordial Tensor Modes

Even though the detection turned out not to be of primordial origin [1], the BICEP2 results had the merit of putting the study of tensor modes in the spotlight by showing that the sensitivity for B -modes is reaching the levels of what is expected from theories. So far, most of the attention has been devoted to scalar perturbations, since those are the ones that give rise to the temperature anisotropies in the CMB. Although more easily connected to observations, the scalar sector is much more complex. The predictions for the power spectrum depends on many parameters, such as the speed of sound for the scalar, or the shape of the potential. This means that it is difficult to use temperature measurements to put robust constraints on models of inflation. The situation is even worse, since the almost scale invariant spectrum that Planck observed can be produced without having inflation [2].

Tensor modes on the other hand are much simpler from a theoretical point of view since their power spectrum depends only on the energy scale of inflation. After giving a brief introduction to the idea of inflation, I am going to show in this chapter that the tensor modes predictions are very robust, contrarily to the scalar case.

4.1 Introduction to Inflation

Inflation is a phase of accelerated expansion that is thought to have occurred at the very beginning of the Universe. The original motivation was to explain why the Universe was so uniform (recall that in Fig. 1.1, the fluctuations are less than 10^{-5}), what is known as the horizon problem [3]. Furthermore, it provides a (quantum) origin for the fluctuations that will later become galaxies. It is also one of the key ingredient behind the theoretical prediction in Fig. 1.3.

4.1.1 The Horizon Problem

The horizon problem has to do with causality. The Universe is very homogeneous on the whole sky (Fig. 1.1). The question is: where all the regions seen on the CMB map in casual contact at the time of emission? If there existed causally disconnected region at that time, there is no reason for their respective temperatures to agree up to one part 10^5 , since they had no way of communicating. In order to answer this question, we need to compute the size of the horizon at recombination. It is given by the distance a photon can travel between the initial time t_i and recombination t_{rec} . Its expression reads (cf. Sect. 1.1.2)

$$r_h = \int_{t_i}^{t_{\text{rec}}} \frac{dt}{a(t)} = \int_i^{\text{rec}} (aH)^{-1} d \ln a = \int_{z_{\text{rec}}}^{z_i} \frac{dz}{H(z)}, \quad (4.1)$$

where the integral has been expressed in terms of redshift using Eq. (1.5), and initial time is taken when $a(t_i) \rightarrow 0$ in the Big Bang scenario.

Let me clarify that there are two different horizons that we are dealing with. r_h is the comoving horizon: particles that are separated by a comoving distance greater than r_h have never been in contact throughout the history of the Universe. The second horizon is the Hubble horizon, $(aH)^{-1}$. At a given time t , if particles are separated by more than $(a(t)H(t))^{-1}$, they cannot communicate. However, that does not necessarily mean they could not communicate in the past if $r_h > (aH)^{-1}$ (the distance d can satisfy $r_h > d > (aH)^{-1}$).

Taking into account the presence of various fluids (radiation, matter, dark energy), the first Friedmann equation (1.8) together with the continuity equations (1.10) for each fluid, give

$$H(z) = H_0 \sqrt{\Omega_{r,0}(1+z)^4 + \Omega_{m,0}(1+z)^3 + \Omega_{\Lambda}}, \quad (4.2)$$

where the Ω parameters defined in Sect. 1.1.3 are evaluated at present time. Therefore, we can compute the angle that the horizon at recombination will represent on the sky, $\theta \equiv r_h/D_{\text{CMB}}$. D_{CMB} is the distance that photon have travelled since recombination and can be expressed as

$$D_{\text{CMB}} = \int_0^{z_{\text{rec}}} \frac{dz}{H(z)}, \quad (4.3)$$

Plugging the value of the Ω 's from Planck [4] and $z_{\text{rec}} \simeq 1100$, one gets

$$\theta \simeq 1^\circ. \quad (4.4)$$

Therefore, the CMB should not be homogeneous on angles larger than 2° , as illustrated in the Fig. 4.1.

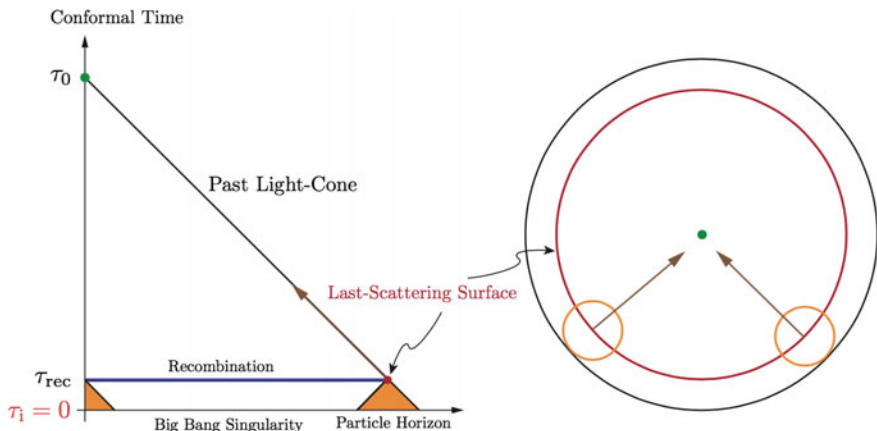


Fig. 4.1 Visualization of the horizon problem. *On the right*, the *black circle* corresponds to the Big Bang singularity, the *red one* to the time when CMB photons are emitted. The *orange circles* represent the horizon at that time, which is much smaller than the *red circle*. Courtesy of Daniel Baumann [5]

Inflation allows to overcome this problem, by making the horizon much larger. The idea is to have a sufficiently long phase where $(aH)^{-1}$ is decreasing with time. For example, if, from t_{infl} to t_i we had a fluid with density ρ and equation of state $w = p/\rho < -1/3$, the Friedmann equations would give us $\frac{d(aH)^{-1}}{dt} < 0$ and

$$r \propto \frac{1}{2(1+3w)} \left[a_{\text{infl}}^{\frac{1}{2(1+3w)}} - a_i^{\frac{1}{2(1+3w)}} \right], \quad (4.5)$$

which goes to $+\infty$ for $a_i \rightarrow 0$ since $1+3w < 0$. Therefore, if inflation lasts long enough, the regions of the CMB can be all in casual contact.

4.1.2 The Predictions of Inflation

We can rewrite the condition that $(aH)^{-1}$ is decreasing as

$$\epsilon \equiv -\frac{\dot{H}}{H^2} < 1. \quad (4.6)$$

We are going to concentrate on the case where $\epsilon \ll 1$, which is called slow-roll inflation. Since we want inflation to last a sufficiently long time, we are going to further require that ϵ is also slowly varying, which translates into

$$\eta \equiv \frac{\dot{\epsilon}}{H\epsilon} \ll 1. \quad (4.7)$$

The simplest way to have such a phase is to consider a canonical scalar field with a potential V , like in quintessence, whose Lagrangian reads

$$L = \frac{M_{\text{Pl}}^2}{2} {}^{(4)}R + \frac{(\partial_\mu \phi)^2}{2} + V(\phi). \quad (4.8)$$

Indeed, in this case we find that

$$H^2 = \frac{1}{3M_{\text{Pl}}^2} \left[\frac{1}{2} \dot{\phi}^2 + V \right], \quad \dot{H} = -\frac{\dot{\phi}^2}{2M_{\text{Pl}}^2}. \quad (4.9)$$

Therefore, if the kinetic energy of the scalar field is much smaller than its potential energy (a situation that is often called slowly rolling)

$$\epsilon = \frac{3(\rho + p)}{2\rho} \simeq \frac{3\dot{\phi}^2}{2V} \ll 1, \quad (4.10)$$

and we are indeed in slow-roll inflation. This simple model is therefore called single field slow-roll inflation.

The equation of motion for the scalar field on the background is

$$\ddot{\phi} + 3H\dot{\phi} + V_\phi = 0, \quad V_\phi \equiv \frac{\partial V}{\partial \phi}, \quad (4.11)$$

which reduces in the slow-roll limit to

$$3H\dot{\phi} + V_\phi = 0. \quad (4.12)$$

This means that we can relate the slow-roll parameter ϵ in Eq. (4.10) to the shape of the potential, i.e.

$$\epsilon = \frac{M_{\text{Pl}}^2}{2} \left(\frac{V_\phi}{V} \right)^2. \quad (4.13)$$

This is interesting since it limits the type of potentials that can cause inflation.

So far, we have only looked at the background, which has told us what type of potential is needed. Another great strength of inflation is that, from Eq. (4.8), one can study the perturbations around the homogeneous background, and make predictions for their distribution.

4.1.3 Characteristics of the Fluctuations

We can see that the Lagrangian (4.8) is very similar to that of Sect. 2.4. Using the same derivation as in that section, one can reduce Eq. (4.8) to a quadratic action for

the curvature perturbation ζ as well as for the tensors, γ_{ij} . In this simpler case, the quadratic action reads reads¹

$$S = \int dt d^3x a^3 \left\{ \frac{\dot{\phi}^2}{2H^2} \left[\dot{\zeta}^2 - \frac{(\partial_i \zeta)^2}{a^2} \right] + \frac{M_{\text{Pl}}^2}{8} \left[\dot{\gamma}_{ij}^2 - \frac{\partial_k \gamma_{ij}^2}{a^2} \right] \right\}. \quad (4.14)$$

In particular, this tells us that far outside the Hubble horizon, $k \ll aH$, ζ and γ_{ij} are constant ($\{\dot{\zeta}, \dot{\gamma}_{ij}\} = \mathcal{O}(k^2/a^2 H^2)$), which will be very important in the following.

Let us first focus on the scalar perturbations, which are the one responsible for the fluctuations in Fig. 1.1.

4.1.3.1 The Scalar Sector

In order to put the equation of motion in a more standard form, I will define a new time variable τ such that $d\tau = dt/a$. Note that with this definition, τ is equivalent to r in Eq. (4.1). As such, the initial time corresponds to $\tau \rightarrow -\infty$, and we can take $\tau = 0$ corresponding to the end of inflation. Moreover, I will use the shorthand notation $z^2 = a^2 \dot{\phi}^2 / H^2$ and work with the canonical variable $u = z\zeta$. In Fourier space, the equation of motion for a mode \mathbf{k} then reads

$$u_{\mathbf{k}}'' + \omega_k(\tau) u_{\mathbf{k}} = 0, \quad \omega_k \equiv k^2 - \frac{z''}{z}, \quad (4.15)$$

where a prime denotes a derivative w.r.t. τ . This is known as the Mukhanov-Sasaki equation. Just as in the standard example of quantum mechanics, one can quantize the harmonic oscillators, introducing the annihilation ($\hat{a}_{\mathbf{k}}$) and creation ($\hat{a}_{\mathbf{k}}^\dagger$) operators so that

$$u(\mathbf{x}, \tau) = \int \frac{d^3k}{(2\pi)^3} \left[u_{\mathbf{k}} \hat{a}_{\mathbf{k}} e^{i\mathbf{k}\mathbf{x}} + u_{\mathbf{k}}^* \hat{a}_{\mathbf{k}}^\dagger e^{-i\mathbf{k}\mathbf{x}} \right], \quad (4.16)$$

where a $*$ denotes complex conjugate and the functions $u_{\mathbf{k}}$ depend only on the norm of \mathbf{k} , because $\omega_k(\tau)$ depends only on the norm. In order for this expansion to make sense, we need to choose a vacuum $|0\rangle$ such that $a_{\mathbf{k}}|0\rangle = 0$. This is equivalent to giving the initial conditions necessary to solve Eq. (4.15). Bear in mind that even before choosing a vacuum, we have restrictions on $u_{\mathbf{k}}$. By imposing the standard canonical relation (in units where $\hbar = 1$)

$$[u(\tau, \mathbf{x}), \pi(\tau, \mathbf{x}')] = i \delta_D(\mathbf{x} - \mathbf{x}'), \quad \pi(\tau, \mathbf{x}) \equiv u'(\tau, \mathbf{x}'), \quad (4.17)$$

we get the relation

$$u_{\mathbf{k}}(u_{\mathbf{k}}^*)' - u_{\mathbf{k}}^* u_{\mathbf{k}}' = -i. \quad (4.18)$$

¹This action is the same as the one derived in the discussion on α_{K} for quintessence in Sect. 2.3, without matter.

Combining that with the fact that we want $|0\rangle$ to be the ground state of the Hamiltonian at initial time ($\tau \rightarrow -\infty$), one finds (see [5] for more details) that the functions u_k start in the Bunch-Davis vacuum, characterized by

$$u_k(\tau) \xrightarrow{\tau \rightarrow -\infty} \frac{e^{-ik\tau}}{\sqrt{2k}} \quad (4.19)$$

Now one can solve Eq. (4.15) to compute the power spectrum of u . In the de Sitter limit (i.e. in the limit $H = cst$ where $(aH)^{-1} = -\tau$), the time-dependent frequency reads

$$\omega_k(\tau) = k^2 - \frac{2}{\tau^2}, \quad (4.20)$$

and the equation has the solution

$$u_k = \alpha \frac{e^{-ik\tau}}{\sqrt{2k}} \left(1 - \frac{i}{k\tau}\right) + \beta \frac{e^{ik\tau}}{\sqrt{2k}} \left(1 + \frac{i}{k\tau}\right). \quad (4.21)$$

Imposing the Bunch-Davis vacuum sets $\alpha = 1$ and $\beta = 0$. From here one can evaluate the power spectrum of u in Fourier space defined as

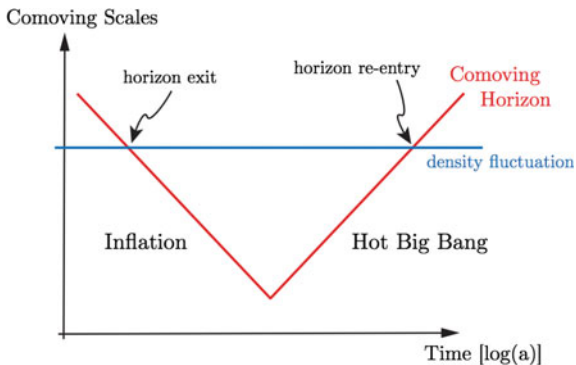
$$\langle \hat{u}_{\mathbf{k}} \hat{u}_{\mathbf{k}'} \rangle = P_u(k) \delta_D(\mathbf{k} + \mathbf{k}'), \quad \hat{u}_{\mathbf{k}} \equiv u_{\mathbf{k}} \hat{a}_{\mathbf{k}} + u_{\mathbf{k}}^* \hat{a}_{-\mathbf{k}}^\dagger. \quad (4.22)$$

In the superhorizon limit $k \ll aH = |\tau|^{-1}$, this power spectrum reduces to

$$P_u(k) = \frac{a^2 H^2}{2k^3}. \quad (4.23)$$

One of the key features of inflation is that $(aH)^{-1}$ is decreasing. This means that the Hubble horizon is shrinking, as illustrated in Fig. 4.2.

Fig. 4.2 Evolution of comoving scale as a function of time. The blue line is a fixed scale k^{-1} and the red in the comoving horizon aH^{-1} , which decreases during inflation. Then the mode re-enters the horizon and becomes observable. Courtesy of Daniel Baumann [5]



Therefore, if one waits long enough, a mode ζ_k with a fixed wavenumber k will exit the horizon, meaning that $k \ll aH$. As I pointed out after Eq. (4.14), once this happens, ζ is conserved. Thus, to compute the power spectrum of ζ_k at the end of inflation, it suffices to compute the power spectrum when the mode exits the horizon $aH = k$, and it will remain the same onwards, until after inflation, when the mode re-enters the horizon (see Fig. 4.2).²

Using the relation between ζ and the canonical variable u , we get that

$$P_\zeta = \frac{1}{4k^3} \frac{H^2}{\epsilon} \Big|_{k=aH}, \quad \Delta_\zeta^2 \equiv \frac{k^3}{2\pi^2} = \frac{H^2}{8\pi^2\epsilon} \Big|_{k=aH}. \quad (4.24)$$

Δ_ζ^2 is the dimensionless power spectrum of ζ . Since we are not exactly in de Sitter space, H and ϵ are not constant, but have a time dependence (that is slow-roll suppressed). The fact that the power spectrum is evaluated at $k = aH$ implies that any time dependence is translated into a scale dependence, that is often parametrized as

$$n_s - 1 \equiv \frac{d \ln \Delta_\zeta^2}{d \ln k} = -2\epsilon - \eta. \quad (4.25)$$

This is a very important result: it means that if the initial conditions are set during slow-roll inflation, we should observe a power spectrum of fluctuations that is nearly scale invariant (corresponding to $n_s = 1$) but not exactly. This is something that one can constrain using the power spectrum of the CMB (Fig. 1.3). The latest Planck results [6] are

$$n_s = 0.968 \pm 0.006 (68 \% \text{C.L.}), \quad (4.26)$$

excluding $n_s = 1$ at 5σ . Now, let me discuss the tensor perturbations in the slow-roll single field picture.

4.1.3.2 The Tensor Sector

The quadratic action for tensor modes (i.e. gravitational waves, which have finally been detected for two merging black holes by the LIGO collaboration [7]) has a form very similar to that of the scalar. This is even more apparent if one decomposes γ_{ij} into helicity modes

$$\gamma_{ij} = \int \frac{d^3k}{(2\pi)^3} \sum_s \gamma_{\mathbf{k}}^s \epsilon_{ij}^s e^{-i\mathbf{k}\cdot\mathbf{x}}, \quad (4.27)$$

²Then, the curvature starts evolving, which results in the transfer function $T(k)$ in Eq. (1.23).

with the polarization tensors ϵ_{ij}^s normalized as $\epsilon_{ij}^s \epsilon_{ij}^{s'} = 4\delta_{ss'}$ where s, s' denote the helicity states. Defining $v_{\mathbf{k}}^s \equiv \frac{M_{\text{Pl}} a}{2} \gamma_{\mathbf{k}}^s$,

$$(v_{\mathbf{k}}^s)'' + \left(k^2 - \frac{a''}{a}\right) v_{\mathbf{k}}^s = 0, \quad (4.28)$$

In the de Sitter limit, $a''/a = 2/\tau^2$, so that Eq. (4.28) has the same frequency as Eq. (4.15). From here, the calculation is therefore identical to the scalar case, so that $P_v = P_u$. Using the relation between v^s and γ^s , as well as the fact that γ_{ij} has two polarizations, one gets the power spectrum for primordial gravitational waves from inflation

$$P_\gamma = \frac{4}{k^3} \frac{H^2}{M_{\text{Pl}}^2} \Big|_{k=aH}, \quad \Delta_\gamma^2 = \frac{2}{\pi^2} \frac{H^2}{M_{\text{Pl}}^2} \Big|_{k=aH}. \quad (4.29)$$

Just like in the scalar case, one can compute the scale dependence of Δ_γ , parametrized by n_T

$$n_T \equiv \frac{d \ln \Delta_\gamma^2}{d \ln k} = -2\epsilon. \quad (4.30)$$

Note that, since ϵ is positive (see Eq. (4.10))³ and therefore, the power spectrum of gravitational waves is expected to be red (i.e. $n_T < 0$).

Another common parameter is the tensor to scalar ratio, r , defined as

$$r \equiv \frac{P_\gamma}{P_\zeta} = 16\epsilon, \quad (4.31)$$

There is only an upper bound on this quantity, $r < 0.12$ [1]. This is unfortunate, as this would directly measured the slow-roll parameter. Moreover, since the amplitude of P_ζ is measured in the CMB, knowing r gives access to the scale of inflation, H . The goal of this Chapter is to show that this is indeed a robust prediction of inflation.

In slow-roll single field, the two previous parameters are related by a consistency relation, $r = -8n_T$, which depends only on observable quantities. Thus, it is a excellent test of slow-roll single field inflation.

The fact that n_s is measured to be close to one, but not exactly one, is a strong argument in favor of inflation. However, I presented here the simplest model, slow-roll single field inflation. With more complicated model for the scalar field, one can reproduce those results without having a phase of inflation [2]. In the next section, I will explain how the tensor sector, contrarily to the scalar sector, could prove to be a more robust probe for inflation.

³Even in more general models, satisfying the cosmological Null Energy Condition $\rho + p > 0$ implies $\epsilon > 0$. Moreover, ϵ is usually what multiplies $\dot{\zeta}^2$ in the quadratic action, so that the stability conditions explained in Sect. 2.4 require that it is positive. This constraint can be circumvented when there is kinetic braiding [8], i.e. $\alpha_B \neq 0$ in the language of Chap. 2.

4.2 Tensor Sound Speed and Quadratic Action

The Effective Field Theory of Inflation (EFTI) framework [9], from which the EFT of DE in Chap. 2 is inspired, describes inflationary perturbations in unitary gauge. This specific time slicing breaks the explicit invariance under time diffs and velocities are no longer forced to be unity, as we have seen in Sect. 2.4. In particular, when the scalar sound speed is non trivial, the (dimensionless) power spectrum of the curvature perturbations ζ has an expression that depends both on $\epsilon = -\dot{H}/H^2$ and c_s . Since this expression is estimated at horizon crossing $c_s k = aH$, any time dependence can be related to a scale dependence. Therefore, in general, the scalar spectral tilt is

$$n_s - 1 = -2\epsilon - \eta - \frac{\alpha_s}{H}, \quad \eta = \frac{\dot{\epsilon}}{H\epsilon}, \quad \alpha_s \equiv \frac{\dot{c}_s}{c_s}. \quad (4.32)$$

It was argued for example in [2] that one could get nearly scale invariance, $n_s - 1 \ll 1$ without having slow-roll inflation, $\epsilon \ll 1$, by a proper choice of sound speed. Thus, measurements of the scalar tilt cannot distinguish between inflation and other scenarios.

For gravity waves, the situation is somewhat different. It is true that the tensor sound speed can be modified. When considering the EFTI action

$$S = \int d^4x \sqrt{-g} \frac{M_{\text{Pl}}^2}{2} \left[{}^{(4)}R - 2(\dot{H} + 3H^2) + 2\dot{H}g^{00} - (1 - c_T^{-2}(t))(\delta K_{\mu\nu}\delta K^{\mu\nu} - \delta K^2) \right], \quad (4.33)$$

and parametrizing the tensor perturbations γ as

$$h_{ij} = a^2 e^{2\zeta} (e^\gamma)_{ij}, \quad \gamma_{ii} = 0 = \partial_i \gamma_{ij}, \quad (4.34)$$

the quadratic action for tensors reads, using Eq. (2.9),

$$S_{\gamma\gamma} = \frac{M_{\text{Pl}}^2}{8} \int d^4x a^3 c_T^{-2} \left[\dot{\gamma}_{ij}^2 - c_T^2 \frac{(\partial_k \gamma_{ij})^2}{a^2} \right]. \quad (4.35)$$

The only other way to modify the tensor sound speed would be with a term in ${}^{(3)}R$ (that contains spatial derivatives of the metric), but this is equivalent to the case of (4.33) since the two are related by the Gauss-Codazzi relation Eq. (2.13). One can compute the tensor power spectrum associated with Eq. (4.35). For this, we do a change of variable $dy = c_T dt/a$

$$S_{\gamma\gamma} = \frac{M_{\text{Pl}}^2}{8} \int d^3x dy q^2 \left[(\gamma'_{ij})^2 - (\partial_k \gamma_{ij})^2 \right], \quad q \equiv a c_T^{-1/2}, \quad (4.36)$$

where a prime denote the derivative with respect to y . One can then decompose the helicity modes in Fourier space as in Eq. (4.27). Defining a new variable $v_{\mathbf{k}}^s \equiv q\gamma_{\mathbf{k}}^s$ we get the standard equation

$$(v_{\mathbf{k}}^s)'' + \left(k^2 - \frac{q''}{q}\right)v_{\mathbf{k}}^s = 0. \quad (4.37)$$

As I have said above, the idea is to see if one can get the same prediction as inflation, i.e. a nearly scale invariant power spectrum, without having inflation. To get a nearly scale invariant power spectrum one requires $q \sim y^{-1}$ (see e.g. [2]), and the power spectrum is given in the small k limit by

$$\langle \gamma_{\mathbf{k}}^s \gamma_{\mathbf{k}'}^{s'} \rangle = (2\pi)^3 \delta(\mathbf{k} + \mathbf{k}') \frac{1}{2k^3} \frac{1}{M_{\text{Pl}}^2 q^2 y^2} \delta_{ss'} = (2\pi)^3 \delta(\mathbf{k} + \mathbf{k}') \frac{1}{2k^3} \frac{(H - \alpha_t/2)^2}{M_{\text{Pl}}^2 c_T} \delta_{ss'}, \quad (4.38)$$

where $\alpha_t \equiv \dot{c}_T/c_T$ and I used the scale invariance condition $(qy)' = 0$ to express y in terms of H , α_t and c_T .

A priori one might be worried that the situation is the same as for the scalar. However, what we showed in [10] is that, through a disformal transformation plus a conformal one and a redefinition of time, one can always write the action in a form that is standard for the tensor modes, namely

$$\begin{aligned} S = & \int d\tilde{t} d^3x \sqrt{-\tilde{g}} \frac{M_{\text{Pl}}^2}{2} \left\{ {}^{(4)}\tilde{R} - 2(\dot{\tilde{H}} + 3\tilde{H}^2) + 2\dot{\tilde{H}}\tilde{g}^{00} \right. \\ & + \left[2(1 - c_T^2)\dot{\tilde{H}} - \frac{3}{2}\alpha_s^2 - c_T^2 \left(\dot{\alpha}_s + \tilde{H}\alpha_s + \frac{1}{2}\alpha_s^2 \right) \right] \times (1 - \sqrt{-\tilde{g}^{00}})^2 \\ & \left. + 2\alpha_s \delta\tilde{K} (1 - \sqrt{-\tilde{g}^{00}}) \right\}, \end{aligned} \quad (4.39)$$

where tildes are to distinguish the quantities from those in the original frame. In this action, only the Ricci scalar ${}^{(4)}\tilde{R}$ contributes to the quadratic action for γ , which is the same as in GR. The rest only modifies the scalar sector. Therefore, in this frame the tensor power spectrum is the standard one

$$\boxed{\langle \gamma_{\mathbf{k}}^s \gamma_{\mathbf{k}'}^{s'} \rangle = (2\pi)^3 \delta(\mathbf{k} + \mathbf{k}') \frac{1}{2k^3} \frac{\tilde{H}^2}{M_{\text{Pl}}^2} \delta_{ss'}}. \quad (4.40)$$

There is of course no contradiction with the result in the original frame, since when going through all the transformations, one can see that

$$\tilde{H} = c_T^{-1/2} (H - \alpha_t/2). \quad (4.41)$$

The tilde frame has the advantage of having a constant Planck mass (i.e. the normalization of the quadratic action), making the connection to the present Planck mass (and therefore present observations) clearer. Contrarily to the case of Chap. 3, there is no matter during inflation that would couple differently after disformal and conformal transformations.

From Eq. (4.40), one can compute the tensor tilt n_T , which has its usual form in the tilde frame

$$n_T = 2 \frac{\dot{\tilde{H}}}{\tilde{H}^2}, \quad (4.42)$$

but has a more complicated relation to the H because of Eq. (4.41).

In particular, one can choose the variation of the tensor sound speed such that the tilt is blue, $n_T > 0$, without violating the Null Energy Condition (NEC) for a FLRW universe, which is $\dot{H} < 0$. Violating this condition usually leads to instabilities [11].⁴ Therefore, in the original frame, one can have $n_T > 0$ without instabilities.

In the tilde frame, having $n_T > 0$ really implies $\dot{\tilde{H}} > 0$, i.e. violation of the NEC. However, the system is still devoid of instabilities, because the terms in the last two lines of Eq. (4.39), in particular the one in $\delta K \delta g^{00}$, are going to contribute to the kinetic energy of the scalar field. Indeed, this term gives a non zero α_B in the language of the EFT of DE, which means the no-ghost condition is modified by its presence (see Eq. (2.65) and also [8])

Thus, one can without loss of generality assume that the tensor quadratic action comes only from the usual 4D Ricci scalar. We went further in the comparison between the two frames and proved also that the non-Gaussianity was the same in both. This means that it cannot be enhanced by a non trivial speed of sound, which is the case for scalars [5] and was claimed for tensors in the literature.

4.3 Other Operators

In the previous section, I explained that the quadratic action for tensors can always be cast in the standard form, i.e.

$$S_{\gamma\gamma} = \frac{M_{\text{Pl}}^2}{8} \int d^4x a^3 \left[\dot{\gamma}_{ij}^2 - \frac{(\partial_k \gamma_{ij})^2}{a^2} \right]. \quad (4.43)$$

This statement holds as long as one does not consider higher derivatives terms.⁵ In an effective field theory approach, which is assumed to be the low energy limit of a more complex theory, one expects generally higher derivatives terms to be

⁴The idea is that if $\dot{H} > 0$, the kinetic term for the scalar field in Eq. (4.33), which is $-g^{00}$ has the wrong sign (in the sense of Sect. 2.4).

⁵With two derivatives, only the terms in Eq. (4.43) can appear, the other possibilities being total derivatives.

suppressed. Therefore, they can be treated as small corrections to the power spectrum (4.40). Only two terms are possible (they need to respect the spatial diffeomorphism invariance, just like for the EFT of DE), both of them violating parity

$$\varepsilon^{ijk} \partial_i \dot{\gamma}_{jl} \dot{\gamma}'_{lk} , \quad \varepsilon^{ijk} \partial_i \partial_m \gamma_{jl} \partial_m \gamma_{lk} . \quad (4.44)$$

The contribution of an arbitrary combination of the two to the quadratic action is

$$- \frac{M_{\text{Pl}}^2}{8} \int d^4x \frac{1}{H\eta} \left[\frac{\alpha}{\Lambda} \varepsilon^{ijk} \partial_i \gamma'_{jl} \gamma'_{lk} + \frac{\beta}{\Lambda} \varepsilon^{ijk} \partial_i \partial_m \gamma_{jl} \partial_m \gamma_{lk} \right] , \quad (4.45)$$

where a prime denotes here the derivative with respect to the conformal time $\tau \equiv \int dt/a$, α and β are dimensionless coefficients and Λ is the scale that suppresses these higher dimension operators. In order to get an idea of the corrections that this brings to the power spectrum, I will take the simplest case, where α and β are constant. In addition, I will assume that they are indeed corrections, namely that the scale Λ is much higher than the energy scale of the problem, H . Then, to compute the power spectrum, we can treat (4.45) as an interaction term and use the in-in formalism [12]. In the late-time limit, $\tau \rightarrow 0$, the result does not depend on α and the power spectrum is modified to

$$\langle \gamma_{\mathbf{k}}^{\pm} \gamma_{\mathbf{k}'}^{\pm} \rangle = (2\pi)^3 \delta(\mathbf{k} + \mathbf{k}') \frac{H^2}{2M_{\text{Pl}}^2 k^3} \left(1 \pm \beta \frac{\pi H}{2 \Lambda} \right) . \quad (4.46)$$

Such a parity violating power spectrum would yield non zero TB and EB power spectra in the CMB polarization. The authors of [13] quote the detectability of parity violations of order one in the power spectrum with future experiments, which is probably far from what is expected here.

Finally, another way to modify the standard predictions for tensor modes is to change the non-Gaussianity by introducing cubic terms in the EFTI Lagrangian. Since we cannot construct operators with explicit underived γ that respect the 3-D symmetry, the lowest order in derivatives is two. The only two operators that one can then construct are $\delta K_{ij} \delta K^{ij}$ and ${}^{(3)}R$. We have seen in the previous section that they can always be reabsorbed in the Ricci scalar by suitable transformations. The only other way is to pay the price of an additional derivative and consider operators such as $\delta K_{ij} \delta K^{ik} \delta K_k^j$. However, they should be suppressed with respect to lower derivatives terms and only bring small corrections to the correlator $\langle \gamma \gamma \gamma \rangle$. The same sort of reasoning can be made for the correlator $\langle \gamma \zeta \zeta \rangle$ which, at lowest order in derivatives, can only come from the term g^{00} . On the other hand, it is hard to say anything definite for $\langle \gamma \gamma \zeta \rangle$ which can be enhanced by operators such as $\delta K_{ij} \delta K^{ij} \delta N$.

4.4 Conclusions

By means of field redefinitions, I have shown that one can always put the quadratic action for tensor in the standard form during inflation. In particular, the sound speed of tensor can always be set to unity. Physically, this makes sense, since during inflation where there is no matter, the benchmark for velocities is the one of gravitons. It means that the power spectrum for gravity waves is always given by the simple form of Eq. (4.40). This is heavy with consequences. First, it means that the amplitude of the power spectrum directly gives the energy scale of inflation. There is no degeneracy with the shape of the potential or the sound speed as for scalars. Second, this implies that measuring a scale invariant power spectrum can only mean that H is almost constant, i.e. that there was a period of inflation.

References

1. **BICEP2, Planck** Collaboration, P. Ade et al., Joint analysis of BICEP2/*Keck Array* and *Planck* data. *Phys. Rev. Lett.* **114**, 101301 (2015). 1502.00612
2. J. Khoury, F. Piazza, Rapidly-varying speed of sound, scale invariance and non-Gaussian signatures. *JCAP* **0907**, 026 (2009). 0811.3633
3. A.H. Guth, Inflationary universe: a possible solution to the horizon and flatness problems. *Phys. Rev. D* **23**, 347–356 (1981)
4. **Planck Collaboration** Collaboration, P. Ade et al., Planck 2015 results. XIII. Cosmological parameters. 1502.01589
5. D. Baumann, TASI lectures on inflation. 0907.5424
6. **Planck** Collaboration, P.A.R. Ade et al., Planck 2015 results. XX. Constraints on inflation. 1502.02114
7. **Virgo, LIGO Scientific** Collaboration, B.P. Abbott et al., Observation of gravitational waves from a binary black hole merger. *Phys. Rev. Lett.* **116**(6), 061102 (2016). 1602.03837
8. P. Creminelli, M.A. Luty, A. Nicolis, L. Senatore, Starting the universe: stable violation of the null energy condition and non-standard cosmologies. *JHEP* **0612**, 080 (2006). hep-th/0606090
9. C. Cheung, P. Creminelli, A.L. Fitzpatrick, J. Kaplan, L. Senatore, The effective field theory of inflation. *JHEP* **0803**, 014 (2008). 0709.0293
10. P. Creminelli, J. Gleyzes, J. Noreña, F. Vernizzi, Resilience of the standard predictions for primordial tensor modes. *Phys. Rev. Lett.* **113**(23), 231301 (2014). 1407.8439
11. S. Dubovsky, T. Gregoire, A. Nicolis, R. Rattazzi, Null energy condition and superluminal propagation. *JHEP* **0603**, 025 (2006). hep-th/0512260
12. J.M. Maldacena, Non-Gaussian features of primordial fluctuations in single field inflationary models. *JHEP* **0305**, 013 (2003). astro-ph/0210603
13. A. Ferté, J. Grain, Detecting chiral gravity with the pure pseudospectrum reconstruction of the cosmic microwave background polarized anisotropies. *Phys. Rev. D* **89**(10), 103516 (2014). 1404.6660

Chapter 5

Consistency Relations of the Large Scale Structure

The CMB is great source of observational knowledge in cosmology and it has been extensively used, in particular by Planck [1]. To obtain even more information on cosmology, the next step is to rely on the large scale structure, via galaxy surveys for example. This has two main advantages. First, contrarily to the CMB which is a 2-D surface, galaxy surveys span the full 3-D space, which greatly increases their statistical power. Second, they probe the late time universe, where the effects of dark energy are expected to be the strongest, which means more constraining power. However, even within Λ CDM+GR, it is still hard to make accurate late-time predictions at small scales. Indeed, if for the CMB the physics is well described by the linear regime, at late-time the structure has grown into the non linear regime, which means a breakdown of the usual perturbative tools. Moreover, if the dark matter distribution can be predicted through N-body simulations for example, this cannot be said for galaxies. The problem is that galaxies are what we observe when doing those experiments, so that one needs models to relate their distribution to that of dark matter. This limits the theoretical control we have on predicting the galaxies' distribution.

Fortunately, there exist testable relations that do not rely on a specific description of the small scale physics. One such example are consistency relations of the large scale structure [2–4] (see also [5] for inflationary consistency relations). They allow to make a bridge between $(n + 1)$ -point and n -point correlation functions in the limit where one of the fields, called the long mode, varies much less than the others. Their strength resides in the fact that very little information on the physics of the short modes is needed, which can in principle be in the non linear regime. Moreover, these relations are very robust since they are based only on two assumptions: the Gaussianity of initial conditions and the validity of the Equivalence Principle (EP). The later is particularly interesting for the late-time universe, as some models for dark energy involve a fifth force that may break the EP.

In the first part [6] of a series of three papers, these relations were derived for the large scale structure including relativistic corrections. This is necessary if one wants to follow the evolution of the modes from inflation to now. In the second part [7],

that I will present in this chapter, we focused on the non relativistic case to include a resummation of infrared effects, as well as a generalization to redshift space, where observations are made. Then, I will discuss the last part [8] where we proposed to use these relations to test the Equivalence Principle.

5.1 Deriving Consistency Relations

When the EP is satisfied, i.e. objects respond identically to gravity, only second derivatives of the gravitational field are important. Let me work in conformal time and decompose a gravitational field Φ_L as

$$\Phi_L(\eta, \vec{x}) = \Phi_L|_0 + \partial_i \Phi_L|_0 x^i + \frac{1}{2} \partial_i \partial_j \Phi_L|_0 x^i x^j + \dots \quad (5.1)$$

The first two terms of the r.h.s. can be removed by an appropriate change of coordinates which corresponds to going to the accelerated frame in the elevator argument of Einstein.

The last term, however, is physical, since it is related to tidal forces. In the non relativistic limit, a constant gravitational field has no effect, so that I will focus on the constant gradient term $\partial_i \Phi_L|_0$. In Fourier space, this can be thought of as $\Phi_L(\vec{q})$ with $\vec{q} \rightarrow 0$. To remove this constant gradient, the following change of coordinates is performed

$$\vec{\tilde{x}} = \vec{x} + \delta\vec{x}(\eta), \quad \delta\vec{x}(\eta) \equiv - \int \vec{v}_L(\tilde{\eta}) d\tilde{\eta}, \quad (5.2)$$

while the conformal time η is left untouched. The velocity \vec{v}_L satisfies the Euler equation in the presence of the homogeneous force, whose solution is

$$\vec{v}_L(\eta) = -\frac{1}{a(\eta)} \int a(\tilde{\eta}) \vec{\nabla} \Phi_L(\tilde{\eta}) d\tilde{\eta}. \quad (5.3)$$

If we denote by $\delta^{(g)}(\vec{x}, \eta)$ the overdensity in the galaxy distribution,¹ the EP guarantees then that

$$\begin{aligned} \langle \delta^{(g)}(\vec{x}_1, \eta_1) \dots \delta^{(g)}(\vec{x}_n, \eta_n) | \Phi_L(\vec{y}) \rangle &\approx \langle \delta^{(g)}(\vec{x}_1, \eta_1) \dots \delta^{(g)}(\vec{x}_n, \eta_n) \rangle_0 \\ &= \int \frac{d^3 k_1}{(2\pi)^3} \dots \frac{d^3 k_n}{(2\pi)^3} \langle \delta_{k_1}^{(g)}(\eta_1) \dots \delta_{k_n}^{(g)}(\eta_n) \rangle_0 e^{i \sum_a \vec{k}_a \cdot (\vec{x}_a + \delta\vec{x}(\vec{y}, \eta_a))}. \end{aligned} \quad (5.4)$$

\vec{y} is an arbitrary point—e.g., the midpoint between $\vec{x}_1, \dots, \vec{x}_n$ —whose choice is irrelevant at order q/k . The notation on the l.h.s. means that the correlation function is evaluated in the presence of a constant gradient of Φ_L , while the subscript 0 on the r.h.s. signifies that it is evaluated with $\Phi_L = 0$. Note that in order for this relation to

¹Note that this is for concreteness; the argument would hold for any type of overdensity.

hold, the fact that short and long mode are not correlated is essential. This is where the assumption of Gaussianity plays a role.

The next step is to express the displacement $\delta\vec{x}(\eta)$ on the r.h.s. as a function of an overdensity. For this, one combines Eqs. (5.2) and (5.3) with the continuity equation $\delta' + \nabla \cdot \vec{v} = 0$ to obtain in, Fourier space

$$\delta\vec{x}(\vec{q}, \eta) = -i \frac{\vec{q}}{q^2} \delta(\vec{q}, \eta) \equiv -i \frac{\vec{q}}{q^2} D(\eta) \delta_0(\vec{q}), \quad (5.5)$$

where in the second equality we have defined $D(\eta)$, the linear growth factor of density fluctuations. $\delta_0(\vec{q})$ is a Gaussian random field with power spectrum $P_0(p)$ which represents the initial condition of the density fluctuations of the long mode [9]. Finally, one multiplies each side by δ_L , and takes the average over the long mode. Since the only dependence on Φ_L in Eq. (5.4) is in the exponential of $i \sum_a \vec{k}_a \cdot \delta\vec{x}(\eta_a)$, we obtain

$$\begin{aligned} \langle \delta_L(\vec{x}, \eta) \langle \delta_1^{(g)} \dots \delta_n^{(g)} | \Phi_L \rangle \rangle_{\Phi_L} &\approx \int \frac{d^3 k_1}{(2\pi)^3} \dots \frac{d^3 k_n}{(2\pi)^3} \langle \delta_{k_1}^{(g)}(\eta_1) \dots \delta_{k_n}^{(g)}(\eta_n) \rangle_0 e^{i \sum_a \vec{k}_a \cdot \vec{x}_a} \\ &\times \int \frac{d^3 q}{(2\pi)^3} e^{i \vec{q} \cdot \vec{x}} \langle \delta_{\vec{q}}(\eta) e^{i \sum_a \vec{k}_a \cdot \delta\vec{x}(\vec{y}, \eta_a)} \rangle_{\Phi_L}, \end{aligned} \quad (5.6)$$

where on the l.h.s. $\delta_i^{(g)} \equiv \delta^{(g)}(\vec{x}_i, \eta_i)$. It is then convenient to rewrite this exponential as

$$\exp \left[i \sum_a \vec{k}_a \cdot \delta\vec{x}(\vec{y}, \eta_a) \right] = \exp \left[\int^\Lambda \frac{d^3 p}{(2\pi)^3} J(\vec{p}) \delta_0(\vec{p}) \right], \quad (5.7)$$

where

$$J(\vec{p}) \equiv \sum_a D(\eta_a) \frac{\vec{k}_a \cdot \vec{p}}{p^2} e^{i \vec{p} \cdot \vec{y}}. \quad (5.8)$$

The integral is restricted to soft momenta, smaller than a UV cut-off Λ , which must be much smaller than the hard modes of momentum k . Averaging the right-hand side of Eq. (5.7) over the long wavelength Gaussian random initial condition $\delta_0(\vec{p})$ yields

$$\left\langle \exp \left[\int^\Lambda \frac{d^3 p}{(2\pi)^3} J(\vec{p}) \delta_0(\vec{p}) \right] \right\rangle_{\Phi_L} = \exp \left[\frac{1}{2} \int^\Lambda \frac{d^3 p}{(2\pi)^3} J(\vec{p}) J(-\vec{p}) P_0(p) \right]. \quad (5.9)$$

We can use this relation to compute the expectation value of δ_L with the exponential,

$$\begin{aligned} \left\langle \delta_{\vec{q}}(\eta) \exp \left(i \sum_a \vec{k}_a \cdot \delta\vec{x}(\vec{y}, \eta_a) \right) \right\rangle_{\Phi_L} &= (2\pi)^3 D(\eta) \frac{\delta}{\delta J(\vec{q})} \left\langle \exp \left[\int^\Lambda \frac{d^3 p}{(2\pi)^3} J(\vec{p}) \delta_0(\vec{p}) \right] \right\rangle_{\Phi_L} \\ &= P(q, \eta) \frac{J(-\vec{q})}{D(\eta)} \exp \left[\frac{1}{2} \int^\Lambda \frac{d^3 p}{(2\pi)^3} J(\vec{p}) J(-\vec{p}) P_0(p) \right], \end{aligned} \quad (5.10)$$

where we have defined the power spectrum at time η : $P(q, \eta) \equiv D^2(\eta)P_0(q)$. Finally, rewriting Eq. (5.6) in Fourier space using the above relation and the definition of J , Eq. (5.8), we obtain the resummed consistency relations in the squeezed limit,

$$\begin{aligned} \langle \delta_{\vec{q}}(\eta) \delta_{\vec{k}_1}^{(g)}(\eta_1) \cdots \delta_{\vec{k}_n}^{(g)}(\eta_n) \rangle' &\approx -P(q, \eta) \sum_a \frac{D(\eta_a)}{D(\eta)} \frac{\vec{k}_a \cdot \vec{q}}{q^2} \langle \delta_{\vec{k}_1}^{(g)}(\eta_1) \cdots \delta_{\vec{k}_n}^{(g)}(\eta_n) \rangle'_0 \\ &\times \exp \left[-\frac{1}{2} \int^\Lambda \frac{d^3 p}{(2\pi)^3} J(p)^2 P_0(p) \right], \end{aligned} \quad (5.11)$$

where, here and in the following, primes on correlation functions indicate that the momentum conserving delta functions have been removed. However, what one observes in practice is not the expectation value $\langle \dots \rangle_0$ with the long modes set artificially to zero: one wants to average over the long modes and this gives

$$\langle \langle \delta_{\vec{k}_1}^{(g)}(\eta_1) \cdots \delta_{\vec{k}_n}^{(g)}(\eta_n) | \Phi_L \rangle \rangle_{\Phi_L} \approx \exp \left[-\frac{1}{2} \int \frac{d^3 p}{(2\pi)^3} J(p)^2 P_0(p) \right] \langle \delta_{\vec{k}_1}^{(g)}(\eta_1) \cdots \delta_{\vec{k}_n}^{(g)}(\eta_n) \rangle. \quad (5.12)$$

Once written in terms of the observable quantity the consistency relation comes back to the simple form:

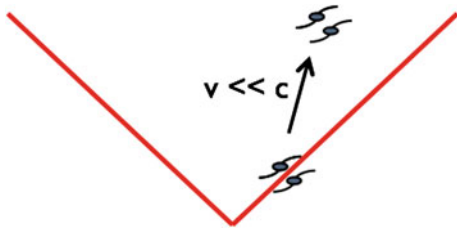
$$\boxed{\langle \delta_{\vec{q}}(\eta) \delta_{\vec{k}_1}^{(g)}(\eta_1) \cdots \delta_{\vec{k}_n}^{(g)}(\eta_n) \rangle' \approx -P(q, \eta) \sum_a \frac{D(\eta_a)}{D(\eta)} \frac{\vec{k}_a \cdot \vec{q}}{q^2} \times \langle \delta_{\vec{k}_1}^{(g)}(\eta_1) \cdots \delta_{\vec{k}_n}^{(g)}(\eta_n) \rangle'.} \quad (5.13)$$

Moreover the \approx signifies that this equality is valid in the limit $q \rightarrow 0$. Note that, to derive this relation, $\delta_{\vec{q}}$ is assumed to be small and obey linear theory, but no assumption is made on the size of the displacement (5.5), allowing for

$$\frac{|\delta_{\vec{x}}|}{|\vec{x}|} \sim \frac{k}{q} \delta_{\vec{q}} \sim 1. \quad (5.14)$$

This result is very robust: nowhere in the derivation does one need to specify anything on the short modes except Gaussianity and EP. In particular, the divergence in $\frac{k_a}{q}$ in the r.h.s. disappears at equal time $\eta_a = \eta$ because $\sum_a \vec{k}_a = \vec{q}$. This can be understood more physically as the following: when looking at correlations between a long and several short modes, what we are really doing is measuring how much objects have fallen in a constant gravitational gradient. The correlation at equal time corresponds exactly to the case where we have waited for the same amount of time for each objects. Since they all feel the same field, the displacement they made is

Fig. 5.1 Galaxies getting out of the light cone for unequal time correlators



the same and translational invariance guarantees that the effect on the correlation is zero.² Only in the unequal time case does one get a divergent contribution.

However, this case seems less reachable from an observational point of view. Indeed, for the equal time correlators, we are basically comparing the positions at the moment we see the objects with the positions we know they had in the beginning, since in cosmology we know the initial conditions. For unequal time, we would have to observe the positions at a given time and then wait different amounts of time for different objects. But since they fall at velocities much smaller than the speed of light, they would not remain on the lightcone and therefore become unobservable as schematically shown in Fig. 5.1. Nevertheless, this is a good test for N-body simulations, where one is not restricted to measurements on the lightcone.

Let me reiterate that the equalities that I have just shown do not rely on any assumptions except the EP and the Gaussianity of the initial conditions. The long modes are however supposed to obey linear perturbation theory, which is the case provided they are sufficiently long ($q_a \lesssim 0.1 h \text{ Mpc}^{-1}$ at redshift $z = 0$).

As shown below, one can straightforwardly extend this procedure and derive consistency relations involving an arbitrary number of soft legs in the correlation functions or use it to study the effect of soft loops and internal lines.

5.1.1 Several Soft Legs

The generalization of the consistency relations above to multiple soft legs relies on taking successive functional derivatives with respect to $J(\vec{q}_i)$ of Eq. (5.9). As an example, we can explicitly compute the consistency relations with two soft modes. In this case the $(n + 2)$ -point function reads

$$\begin{aligned} \langle \delta_L(\vec{y}_1, \tau_1) \delta_L(\vec{y}_2, \tau_2) \delta_1^{(g)} \dots \delta_n^{(g)} \rangle &\approx \int \frac{d^3 k_1}{(2\pi)^3} \dots \frac{d^3 k_n}{(2\pi)^3} \langle \delta_{\vec{k}_1}^{(g)}(\eta_1) \dots \delta_{\vec{k}_n}^{(g)}(\eta_n) \rangle_0 e^{i \sum_a \vec{k}_a \cdot \vec{x}_a} \\ &\times \int \frac{d^3 q_1}{(2\pi)^3} \frac{d^3 q_2}{(2\pi)^3} e^{i(\vec{q}_1 \cdot \vec{y}_1 + \vec{q}_2 \cdot \vec{y}_2)} \left\langle \delta_{\vec{q}_1}(\tau_1) \delta_{\vec{q}_2}(\tau_2) e^{\int^\Lambda \frac{d^3 p}{(2\pi)^3} J(\vec{p}) \delta_0(\vec{p})} \right\rangle. \end{aligned} \quad (5.15)$$

²The consistency relation does not give exactly zero, because a long mode is not exactly a constant gradient, but only an approximation.

To compute the average over the long modes in the last line, it is enough to take two functional derivatives of Eq. (5.9),

$$\begin{aligned} \left\langle \delta_{\vec{q}_1}(\tau_1) \delta_{\vec{q}_2}(\tau_2) e^{\int^\Lambda \frac{d^3 p}{(2\pi)^3} J(\vec{p}) \delta_0(\vec{p})} \right\rangle &= (2\pi)^6 D(\tau_1) D(\tau_2) \frac{\delta}{\delta J(\vec{q}_1)} \frac{\delta}{\delta J(\vec{q}_2)} \left\langle e^{\int^\Lambda \frac{d^3 p}{(2\pi)^3} J(\vec{p}) \delta_0(\vec{p})} \right\rangle \\ &= \frac{J(-\vec{q}_1)}{D(\tau_1)} \frac{J(-\vec{q}_2)}{D(\tau_2)} P(q_1, \tau_1) P(q_2, \tau_2) e^{\frac{1}{2} \int^\Lambda \frac{d^3 p}{(2\pi)^3} J(\vec{p}) J(-\vec{p}) P_0(p)}, \end{aligned} \quad (5.16)$$

where we have assumed $\vec{q}_1 + \vec{q}_2 \neq 0$ to get rid of unconnected contributions. In Fourier space, this yields

$$\begin{aligned} \langle \delta_{\vec{q}_1}(\tau_1) \delta_{\vec{q}_2}(\tau_2) \delta_{\vec{k}_1}^{(g)}(\eta_1) \cdots \delta_{\vec{k}_n}^{(g)}(\eta_n) \rangle' &\approx P(q_1, \tau_1) P(q_2, \tau_2) \\ &\times \sum_a \frac{D(\eta_a)}{D(\tau_1)} \frac{\vec{k}_a \cdot \vec{q}_1}{q_1^2} \sum_b \frac{D(\eta_b)}{D(\tau_2)} \frac{\vec{k}_b \cdot \vec{q}_2}{q_2^2} \langle \delta_{\vec{k}_1}^{(g)}(\eta_1) \cdots \delta_{\vec{k}_n}^{(g)}(\eta_n) \rangle', \end{aligned} \quad (5.17)$$

where again we have used Eq. (5.12) to write the result in terms of correlation functions averaged over the long modes.

As a simple example, let us consider Eq. (5.17) in the case where $n = 2$ and $\delta^{(g)}$ describes dark matter perturbations, i.e. $\delta^{(g)} \equiv \delta$. In this case, at lowest order in $\frac{k}{q} \delta(\vec{q}, \eta)$ —i.e. setting the exponential in the third line to unity—the above relation reduces to

$$\begin{aligned} \langle \delta_{\vec{q}_1}(\tau_1) \delta_{\vec{q}_2}(\tau_2) \delta_{\vec{k}_1}(\eta_1) \delta_{\vec{k}_2}(\eta_2) \rangle' &\approx \frac{(D(\eta_1) - D(\eta_2))^2}{D(\tau_1) D(\tau_2)} \frac{\vec{q}_1 \cdot \vec{k}_1}{q_1^2} \frac{\vec{q}_2 \cdot \vec{k}_1}{q_2^2} P(q_1, \tau_1) P(q_2, \tau_2) \\ &\times \langle \delta_{\vec{k}_1}(\eta_1) \delta_{\vec{k}_2}(\eta_2) \rangle'. \end{aligned} \quad (5.18)$$

We can check that this expression correctly reproduces the tree-level trispectrum computed in perturbation theory in the double-squeezed limit. This can be easily computed by summing the two types of diagrams displayed in Fig. 5.2. The diagram on the left-hand side represents the case where the density perturbations of the short modes are both taken at second order, yielding

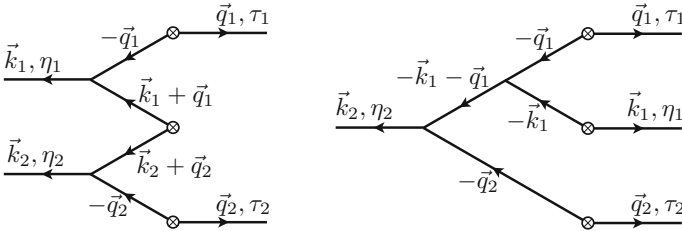


Fig. 5.2 Two diagrams that contribute to the tree-level trispectrum. *Left* T_{1122} . *Right* T_{1113} . The crossed circles denote power spectra

$$\begin{aligned}
T_{1122} &= D(\tau_1)D(\tau_2)D(\eta_1)D(\eta_2)P_0(q_1)P_0(q_2)F_2(-\vec{q}_1, \vec{k}_1 + \vec{q}_1) \\
&\quad \times F_2(-\vec{q}_2, \vec{k}_2 + \vec{q}_2)\langle\delta_{\vec{k}_1}(\eta_1)\delta_{\vec{k}_2}(\eta_2)\rangle' + \text{perms} \\
&\approx -8\frac{\vec{q}_1 \cdot \vec{k}_1}{2q_1^2}\frac{\vec{q}_2 \cdot \vec{k}_1}{2q_2^2}\frac{D(\eta_1)D(\eta_2)}{D(\tau_1)D(\tau_2)}P(q_1, \tau_1)P(q_2, \tau_2)\langle\delta_{\vec{k}_1}(\eta_1)\delta_{\vec{k}_2}(\eta_2)\rangle',
\end{aligned} \tag{5.19}$$

where, on the right-hand side of the first line, $F_2(\vec{p}_1, \vec{p}_2)$ is the usual kernel of perturbation theory, which in the limit where $p_1 \ll p_2$ simply reduces to $\vec{p}_1 \cdot \vec{p}_2 / (2p_1^2)$ [9]. The second type of diagram, displayed on the right-hand side of Fig. 5.2, is obtained when one of the short density perturbations is taken at third order; it gives

$$\begin{aligned}
T_{1113} &= D(\eta_2)^2 D(\tau_1)D(\tau_2)P_0(q_1)P_0(q_2)F_3(-\vec{q}_1, -\vec{q}_2, -\vec{k}_1)\langle\delta_{\vec{k}_1}(\eta_1)\delta_{\vec{k}_2}(\eta_2)\rangle' + \text{perms} \\
&\approx 4\frac{\vec{q}_1 \cdot \vec{k}_1}{2q_1^2}\frac{\vec{q}_2 \cdot \vec{k}_1}{2q_2^2}\frac{D(\eta_2)^2}{D(\tau_1)D(\tau_2)}P(q_1, \tau_1)P(q_2, \tau_2)\langle\delta_{\vec{k}_1}(\eta_1)\delta_{\vec{k}_2}(\eta_2)\rangle',
\end{aligned} \tag{5.20}$$

where, on the right-hand side of the first line, $F_3(\vec{p}_1, \vec{p}_2, \vec{p}_3)$ is the third-order perturbation theory kernel, which in the limit where $p_1, p_2 \ll p_3$ reduces to $(\vec{p}_1 \cdot \vec{p}_3)(\vec{p}_2 \cdot \vec{p}_3) / (4p_1^2 p_2^2)$ [9]. As expected, summing up all the contributions to the connected part of the trispectrum, i.e. $T_{1122} + T_{1131} + T_{1113}$, using Eqs. (5.19) and (5.20) and $k_2 \approx -k_1$ one obtains Eq. (5.18).

5.1.2 Soft Loops

So far we have derived consistency relations where the long modes appear explicitly as external legs. We now show that our arguments can also capture the effect on short-scale correlation functions of soft modes running in loop diagrams. We already did this in Eq. (5.12)

$$\langle\langle\delta_{\vec{k}_1}^{(g)}(\eta_1) \cdots \delta_{\vec{k}_n}^{(g)}(\eta_n)|\Phi_L\rangle\rangle_{\Phi_L} \approx \exp\left[-\frac{1}{2}\int\frac{d^3p}{(2\pi)^3}J(p)^2P_0(p)\right]\langle\delta_{\vec{k}_1}^{(g)}(\eta_1) \cdots \delta_{\vec{k}_n}^{(g)}(\eta_n)\rangle_0. \tag{5.21}$$

The exponential in this expression can be expanded at a given order, corresponding to the number of soft loops dressing the n -point correlation function. Each loop carries a contribution $\propto k^2 \int dp P_0(p)$ to the correlation function. However, this expression makes it very explicit that at all loop order these contributions have no effect on equal-time correlators, because in this case the exponential on the right-hand side is identically unity. This confirms previous analysis on this subject [10–15]. It is important to notice again, however, that in our derivation this cancellation is more general and robust than in those references, as it takes place independently of the equations of motion for the short modes and is completely agnostic about the short-scale physics. It simply derives from the equivalence principle.

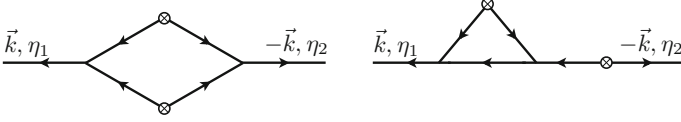


Fig. 5.3 Two diagrams that contribute to the 1-loop power spectrum. *Left* P_{22} . *Right* P_{31}

Nevertheless, soft loops contribute to unequal-time correlators. As a check of the expression above, one can compute the contribution of soft modes to the 1-loop unequal-time matter power spectrum, $\langle \delta_{\vec{k}_1}^{(g)}(\eta_1) \delta_{\vec{k}_2}^{(g)}(\eta_2) \rangle'$, and verify that this reproduces the standard perturbation theory result. Expanding at order $(\frac{k}{p}\delta)^2$ the exponential in Eq. (5.12) for $n = 2$, one obtains the 1-loop contribution to the power spectrum,

$$\begin{aligned} \langle \delta_{\vec{k}}^{(g)}(\eta_1) \delta_{-\vec{k}}^{(g)}(\eta_2) \rangle'_{1\text{-soft loop}} &\approx -\frac{1}{2} (D(\eta_1) - D(\eta_2))^2 \\ &\times \int^\Lambda \frac{d^3 p}{(2\pi)^3} \left(\frac{\vec{p} \cdot \vec{k}}{p^2} \right)^2 P_0(p) \langle \delta_{\vec{k}}^{(g)}(\eta_1) \delta_{-\vec{k}}^{(g)}(\eta_2) \rangle'_0. \end{aligned} \quad (5.22)$$

Let us now compute the analogous contribution in perturbation theory. Two types of diagrams are going to be relevant; these are shown in Fig. 5.3. The one on the left, usually called P_{22} , yields

$$P_{22} \approx 4D(\eta_1)D(\eta_2) \int^\Lambda \frac{d^3 p}{(2\pi)^3} \left(\frac{\vec{p} \cdot \vec{k}}{2p^2} \right)^2 P_0(p) \langle \delta_{\vec{k}}^{(g)}(\eta_1) \delta_{-\vec{k}}^{(g)}(\eta_2) \rangle'_0, \quad (5.23)$$

while the diagram on the right, P_{31} , gives

$$P_{31} \approx -2D(\eta_1)^2 \int^\Lambda \frac{d^3 p}{(2\pi)^3} \left(\frac{\vec{p} \cdot \vec{k}}{2p^2} \right)^2 P_0(p) \langle \delta_{\vec{k}}^{(g)}(\eta_1) \delta_{-\vec{k}}^{(g)}(\eta_2) \rangle'_0. \quad (5.24)$$

Summing up all the different contributions, $P_{22} + P_{31} + P_{13}$, one obtains Eq. (5.22).

5.1.3 Soft Internal Lines

Another kinematical regime in which the consistency relations can be applied is the limit in which the sum of some of the external momenta becomes very small, for instance $|\vec{k}_1 + \dots + \vec{k}_m| \ll k_1, \dots, k_m$. In this limit, the dominant contribution to the n -point function comes from the diagram where m external legs of momenta $\vec{k}_1, \dots, \vec{k}_m$ exchange soft modes with momentum $\vec{q} = \vec{k}_1 + \dots + \vec{k}_m$ with $n - m$ external legs with momenta $\vec{k}_{m+1}, \dots, \vec{k}_n$ (for an analogous case in inflation see [16, 17]). In the language of our approach, this contribution comes from averaging a product of m -point and $(n - m)$ -point functions under the effect of long modes.

In this case, the n -point function in real space can be written as

$$\begin{aligned} \langle \delta(\vec{x}_1, \eta_1) \cdots \delta(\vec{x}_m, \eta_m) \delta(\vec{x}_{m+1}, \eta_{m+1}) \cdots \delta(\vec{x}_n, \eta_n) \rangle &\approx \left\langle \delta(\vec{x}_1, \eta_1) \cdots \delta(\vec{x}_m, \eta_m) | \Phi_L \right\rangle \\ &\times \left\langle \delta(\vec{x}_{m+1}, \eta_{m+1}) \cdots \delta(\vec{x}_n, \eta_n) | \Phi_L \right\rangle \end{aligned} \quad (5.25)$$

where here and in the rest of the section we drop the superscript (g) on the galaxy density contrast to lighten the notation. Now we can straightforwardly apply the equations from the previous sections. As before, the long mode can be traded for the change of coordinates. Rewriting the right-hand side in Fourier space we get

$$\begin{aligned} &\langle \delta(\vec{x}_1, \eta_1) \cdots \delta(\vec{x}_m, \eta_m) \delta(\vec{x}_{m+1}, \eta_{m+1}) \cdots \delta(\vec{x}_n, \eta_n) \rangle \\ &\approx \int \frac{d^3 k_1}{(2\pi)^3} \cdots \frac{d^3 k_n}{(2\pi)^3} \langle \delta_{\vec{k}_1}(\eta_1) \cdots \delta_{\vec{k}_m}(\eta_m) \rangle_0 \langle \delta_{\vec{k}_{m+1}}(\eta_{m+1}) \cdots \delta_{\vec{k}_n}(\eta_n) \rangle_0 e^{i \sum_a \vec{k}_a \cdot \vec{x}_a} \\ &\times \left\langle \exp \left[i \sum_{a=1}^m \vec{k}_a \cdot \delta \vec{x}(\vec{y}_1, \eta_a) \right] \cdot \exp \left[i \sum_{a=m+1}^n \vec{k}_a \cdot \delta \vec{x}(\vec{y}_2, \eta_a) \right] \right\rangle_{\Phi_L}, \end{aligned} \quad (5.26)$$

where \vec{y}_1 and \vec{y}_2 are two different points respectively close to $(\vec{x}_1, \vec{x}_2, \dots, \vec{x}_m)$ and $(\vec{x}_{m+1}, \vec{x}_{m+2}, \dots, \vec{x}_n)$. The average over the long mode can be rewritten as

$$\left\langle \exp \left[\int^\Lambda \frac{d^3 \vec{p}}{(2\pi)^3} (J_1(\vec{p}) + J_2(\vec{p})) \delta_0(\vec{p}) \right] \right\rangle_{\Phi_L} \quad (5.27)$$

with

$$J_1(\vec{p}) = \sum_{a=1}^m D(\eta_a) \frac{\vec{k}_a \cdot \vec{p}}{p^2} e^{i \vec{p} \cdot \vec{y}_1}, \quad J_2(\vec{p}) = \sum_{a=m+1}^n D(\eta_a) \frac{\vec{k}_a \cdot \vec{p}}{p^2} e^{i \vec{p} \cdot \vec{y}_2}. \quad (5.28)$$

Taking the expectation value over the long mode using the expression for averaging the exponential of a Gaussian variable, i.e. Eqs. (5.9), and (5.26) can be written as

$$\begin{aligned} &\langle \delta(\vec{x}_1, \eta_1) \cdots \delta(\vec{x}_m, \eta_m) \delta(\vec{x}_{m+1}, \eta_{m+1}) \cdots \delta(\vec{x}_n, \eta_n) \rangle \\ &\approx \int \frac{d^3 k_1}{(2\pi)^3} \cdots \frac{d^3 k_n}{(2\pi)^3} \langle \delta_{\vec{k}_1}(\eta_1) \cdots \delta_{\vec{k}_m}(\eta_m) \rangle' \langle \delta_{\vec{k}_{m+1}}(\eta_{m+1}) \cdots \delta_{\vec{k}_n}(\eta_n) \rangle' e^{i \sum_a \vec{k}_a \cdot \vec{x}_a} \\ &\times \exp \left[- \int^\Lambda \frac{d^3 p}{(2\pi)^3} J_1(\vec{p}) J_2(\vec{p}) P_0(\vec{p}) \right]. \end{aligned} \quad (5.29)$$

We are interested in the soft internal lines, that come from the cross term, i.e. the last line of Eq. (5.29). Notice that $J_1(\vec{p})$ and $J_2(\vec{p})$ are evaluated at different points \vec{y}_1 and \vec{y}_2 separated by a distance \vec{x} .³ It is lengthy but straightforward to take the Fourier transform of this equation, which yields

$$\begin{aligned}
& \langle \delta_{\vec{k}_1}^-(\eta_1) \cdots \delta_{\vec{k}_m}^-(\eta_m) \delta_{\vec{k}_{m+1}}^-(\eta_{m+1}) \cdots \delta_{\vec{k}_n}^-(\eta_n) \rangle' \\
& \approx \langle \delta_{\vec{k}_1}^-(\eta_1) \cdots \delta_{\vec{k}_m}^-(\eta_m) \rangle' \langle \delta_{\vec{k}_{m+1}}^-(\eta_{m+1}) \cdots \delta_{\vec{k}_n}^-(\eta_n) \rangle' \\
& \times \int d^3x e^{-i \sum_{i=1}^m \vec{k}_i \cdot \vec{x}} \exp \left[- \int^\Lambda \frac{d^3p}{(2\pi)^3} e^{i \vec{p} \cdot \vec{x}} \sum_{a=1}^m D(\eta_a) \frac{\vec{k}_a \cdot \vec{p}}{p^2} \sum_{a=m+1}^n D(\eta_a) \frac{\vec{k}_a \cdot \vec{p}}{p^2} P_0(p) \right].
\end{aligned} \tag{5.30}$$

The last line encodes the effect of soft modes with total momentum $\vec{q} = \vec{k}_1 + \cdots + \vec{k}_m$ exchanged between m external legs of momenta $\vec{k}_1, \dots, \vec{k}_m$ and $n - m$ external legs with momenta $\vec{k}_{m+1}, \dots, \vec{k}_n$, in the limit $q/k_i \rightarrow 0$. Expanding the exponential at a given order in $P_0(p)$ yields the number of soft lines exchanged. The integral in d^3x ensures that the sum of the internal momenta is \vec{q} .

Equation (5.30) can be easily generalized to consider the case where more than two sums of momenta become small, i.e. when soft internal lines are exchanged between more than two hard-modes diagrams. The conclusion is always the same: soft internal lines do not contribute to equal time correlators at order $\propto k^2 \int dp P_0(p)$. Again, this statement is very general irrespectively of the assumption about the short scales.

As a concrete example, let us consider the case $m = 2, n = 4$, i.e. a 4-point function in the collapsed limit $|\vec{k}_1 + \vec{k}_2| \ll k_1, k_2$, and the exchange of a single soft line. In this case, expanding the exponential at first order in $P_0(p)$, the above equation yields

$$\begin{aligned}
& \langle \delta_{\vec{k}_1}^-(\eta_1) \delta_{\vec{k}_2}^-(\eta_2) \delta_{\vec{k}_3}^-(\eta_3) \delta_{\vec{k}_4}^-(\eta_4) \rangle'_c \approx - \langle \delta_{\vec{k}_1}^-(\eta_1) \delta_{\vec{k}_2}^-(\eta_2) \rangle' \langle \delta_{\vec{k}_3}^-(\eta_3) \delta_{\vec{k}_4}^-(\eta_4) \rangle' \\
& \times \int^\Lambda d^3p (D(\eta_1) - D(\eta_2)) \frac{\vec{k}_1 \cdot \vec{p}}{p^2} (D(\eta_3) - D(\eta_4)) \frac{\vec{k}_3 \cdot \vec{p}}{p^2} P_0(p) \delta_D(\vec{p} - \vec{k}_1 - \vec{k}_2),
\end{aligned} \tag{5.31}$$

where we have considered only the connected diagram and, for simplicity, we are neglecting soft loops attached to each lines. To compare with perturbation theory, we need to compute the tree-level exchange diagram. The contribution from taking \vec{k}_1 and \vec{k}_3 at second order yields

$$\begin{aligned}
T_{121} & \approx -4D(\eta_1)D(\eta_3)P_0(|\vec{k}_1 + \vec{k}_2|) \frac{\vec{k}_1 \cdot (\vec{k}_1 + \vec{k}_2)}{2|\vec{k}_1 + \vec{k}_2|^2} \frac{\vec{k}_3 \cdot (\vec{k}_1 + \vec{k}_2)}{2|\vec{k}_1 + \vec{k}_2|^2} \\
& \times \langle \delta_{\vec{k}_1}^-(\eta_1) \delta_{\vec{k}_2}^-(\eta_2) \rangle' \langle \delta_{\vec{k}_3}^-(\eta_3) \delta_{\vec{k}_4}^-(\eta_4) \rangle',
\end{aligned} \tag{5.32}$$

³For definiteness, we can choose $\vec{y}_1 = \frac{1}{m} \sum_{a=1}^m \vec{x}_a$ and $\vec{y}_2 = \frac{1}{n-m} \sum_{a=m+1}^n \vec{x}_a$.

and summing up the other permutations lead to

$$\begin{aligned} \langle \delta_{\vec{k}_1}(\eta_1) \delta_{\vec{k}_2}(\eta_2) \delta_{\vec{k}_3}(\eta_3) \delta_{\vec{k}_4}(\eta_4) \rangle'_c &\approx -(D(\eta_1) - D(\eta_2))(D(\eta_3) - D(\eta_4)) P_0(|\vec{k}_1 + \vec{k}_2|) \\ &\times \frac{\vec{k}_1 \cdot (\vec{k}_1 + \vec{k}_2)}{|\vec{k}_1 + \vec{k}_2|^2} \frac{\vec{k}_3 \cdot (\vec{k}_1 + \vec{k}_2)}{|\vec{k}_1 + \vec{k}_2|^2} \langle \delta_{\vec{k}_1}(\eta_1) \delta_{\vec{k}_2}(\eta_2) \rangle' \langle \delta_{\vec{k}_3}(\eta_3) \delta_{\vec{k}_4}(\eta_4) \rangle', \end{aligned} \quad (5.33)$$

which confirms Eq. (5.31). One can easily extend this check to the case of several soft-lines.

5.2 Going to Redshift Space

The relation derived in the previous section were set in real space, or the Fourier space associated with it. However, observations for galaxies are made in redshift space. In the plane parallel approximation, the mapping between the two spaces is given by

$$\vec{s} = \vec{x} + \frac{v_z}{\mathcal{H}} \hat{z}, \quad \mathcal{H} \equiv \frac{d \ln a}{d\eta}, \quad (5.34)$$

where \hat{z} is the direction of the line of sight, $v_z \equiv \vec{v} \cdot \hat{z}$ and \vec{v} is the peculiar velocity. Therefore, one could worry that the consistency relations do not translate nicely in redshift space, since one has to deal with peculiar velocities. As I will show, this is not the case. The ingredient needed is to see how velocities are affected by the presence of a constant gradient. This is straightforward, since we already used the Euler equation to get that

$$\vec{v} \rightarrow \vec{v} - \vec{v}_L(\eta), \quad \vec{v}_L(\eta) = -(\delta \vec{x})', \quad (5.35)$$

with v_L given by Eq. (5.3) and $\delta \vec{x}$ by Eq. (5.2). Thus, one can see how the redshift coordinates change when removing a constant gradient of the gravitational field,

$$\vec{s} \rightarrow \vec{s} + \delta \vec{x} + \frac{(\delta x_z)'}{\mathcal{H}} \hat{z}. \quad (5.36)$$

Using the form of the time dependence of $\delta \vec{x}$ in Eq. (5.5), this can be cast into

$$\vec{s} \rightarrow \vec{s} + \delta \vec{x} + f \delta x_z \hat{z}, \quad f \equiv \frac{d \ln D}{d \ln a}. \quad (5.37)$$

Then, to see how the density changes in redshift space, let me write its expression as

$$\rho(\vec{s}) = m a^{-3} \int d^3 p \mathcal{F} \left(\vec{s} - \frac{v_z}{\mathcal{H}} \hat{z}, \vec{p} \right). \quad (5.38)$$

where $\mathcal{F}(\vec{x}, \vec{p})$ is the real space distribution function. Therefore, the statistical properties of $\rho(\vec{s})$ are inherited from real space. In the presence of the long mode

$$\begin{aligned} \rho_s(\vec{s})_{\Phi_L} &= \frac{m}{a^3} \int d^3 p \mathcal{F} \left(\vec{s} - \frac{v_z}{\mathcal{H}} \hat{z} + \delta \vec{x}, \vec{p} + am \delta \vec{v} \right) \\ &= \frac{m}{a^3} \int d^3 p' \mathcal{F} \left(\vec{s} - \frac{v_z - \delta v_z}{\mathcal{H}} \hat{z} + \delta \vec{x}, \vec{p}' \right) = \rho_s(\vec{s} + \delta \vec{s}), \end{aligned} \quad (5.39)$$

and this relation does not depend on a fluid description, implying it is valid even at small scales where shell-crossings occur. Using this, we can write

$$\langle \delta^{(g,s)}(\vec{s}_1, \eta_1) \cdots \delta^{(g,s)}(\vec{s}_n, \eta_n) | \Phi_L \rangle \approx \langle \delta^{(g,s)}(\vec{s}_1, \eta_1) \cdots \delta^{(g,s)}(\vec{s}_n, \eta_n) \rangle, \quad (5.40)$$

which is the redshift space equivalent of Eq. (5.4), since I used the redshift space density contrast $\delta^{(g,s)}$. The last step is very similar to the real space case, except for one thing. To express everything in term of the redshift space quantities, one needs to relate δ_0 contained in $\delta \vec{x}$ (see Eq. (5.5)) to $\delta^{(g,s)}$. Since this is for the long mode, one can use linear perturbation theory to get [9]

$$\delta^{(g,s)}(\vec{q}, \eta) = \left(b_1 + f \mu_{\vec{q}}^2 \right) D(\eta) \delta_0(q), \quad \mu_{\vec{q}} \equiv \vec{q} \cdot \hat{z} / q, \quad (5.41)$$

where b_1 is the linear galaxy bias. Combining all of this, one obtains the consistency relation in redshift space

$$\boxed{\langle \delta_{\vec{q}}^{(g,s)}(\eta) \delta_{\vec{k}_1}^{(g,s)}(\eta_1) \cdots \delta_{\vec{k}_n}^{(g,s)}(\eta_n) \rangle \approx - \frac{P_{g,s}(q, \eta)}{b_1 + f \mu_{\vec{q}}^2} \sum_a \frac{D(\eta_a) k_a}{D(\eta) q} [\hat{q} \cdot \hat{k}_a + f(\eta_a) \mu_{\vec{q}} \mu_{\vec{k}_a}] \times \langle \delta_{\vec{k}_1}^{(g,s)}(\eta_1) \cdots \delta_{\vec{k}_n}^{(g,s)}(\eta_n) \rangle,} \quad (5.42)$$

with $\hat{p} \equiv \vec{p}/p$. Notice that, just as in the real space case, the divergence in the consistency relation vanishes at equal times. This adds to the robustness of the results: any deviation, even in redshift space, would be a sign of violation of the EP and/or non-Gaussianity in the initial conditions [3]. In the next section, I will focus on the constraints one can put on EP violations using these relations [8].

5.3 Violation of the Equivalence Principle

When the Equivalence Principle is not satisfied, one cannot remove the effect of a constant gravitational field with a common change of coordinates. Indeed, in principle, different objects feel differently the effect of a long mode, which is nothing more

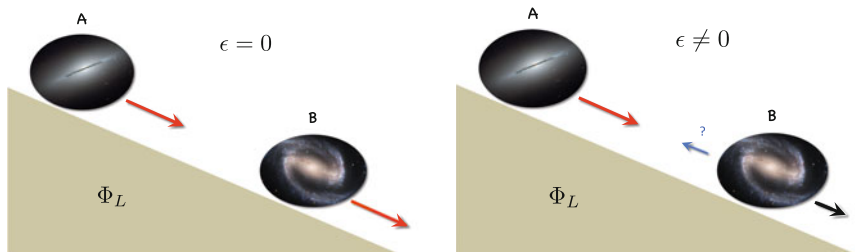


Fig. 5.4 Two types of objects in a constant gradient of Φ_L . ϵ characterizes deviations from EP, so that on the *left*, it is valid, while it is violated on the *right*. The galaxies are from STScI–Hubble Space Telescope

than saying that objects fall at different rates in the same potential and in general, one expects the bispectrum to be of the form

$$\lim_{q \rightarrow 0} \langle \delta_{\vec{q}}(\eta) \delta_{\vec{k}_1}^{(A)}(\eta) \delta_{\vec{k}_2}^{(B)}(\eta) \rangle' = \left(\epsilon \frac{\vec{k} \cdot \vec{q}}{q^2} + \mathcal{O}[(q/k)^0] \right) P(q, \eta) P_{AB}(k, \eta), \quad (5.43)$$

where ϵ is a (model dependent) parameter that characterizes the violation of the EP and $\vec{k} \equiv (\vec{k}_1 - \vec{k}_2)/2$.

The situation is actually much more complicated than when the EP is satisfied, as can be see in Fig. 5.4. On the right panel, the EP is violated, and objects do not fall by the same amount (represented by the red and black arrows) in a constant gravitational field, contrarily to the left panel. Therefore, the distance between them changes in time and the force that each object has on the other (gravitational and/or electromagnetic if they are charged, represented by the blue arrow) changes as well. In general, this greatly complicates the dynamics and no definite answer can be found for the form of ϵ in Eq. (5.43).

This is why in [8], we chose a specific model, to serve as a benchmark for EP violations.

5.3.1 A Toy Model

The idea is to consider the case of two species A and B , in the presence of an extra scalar field φ that couples only to species B , for example through a conformal coupling [18–20]. The setup is then

$$\delta'_X + \vec{\nabla} \cdot [(1 + \delta_X) \vec{v}_X] = 0, \quad X = A, B, \quad (5.44)$$

for the continuity equations (the time evolution of φ is neglected). The Euler equation for B contains the fifth force, whose coupling is parameterized by α ,

$$\vec{v}'_A + \mathcal{H}\vec{v}_A + (\vec{v}_A \cdot \vec{\nabla}) \vec{v}_A = -\vec{\nabla}\Phi, \quad (5.45)$$

$$\vec{v}'_B + \mathcal{H}\vec{v}_B + (\vec{v}_B \cdot \vec{\nabla}) \vec{v}_B = -\vec{\nabla}\Phi - \alpha \vec{\nabla}\varphi. \quad (5.46)$$

Assuming that the stress energy tensor of the scalar field is negligible, Φ is related to matter densities through the standard Poisson equation

$$\nabla^2\Phi = 4\pi G \rho_m \delta \equiv 4\pi G \rho_m (w_A \delta_A + w_B \delta_B), \quad (5.47)$$

where ρ_m is the total matter density and $w_X \equiv \rho_X/\rho_m$. The final ingredient is a relation between φ and the matter density. In the quasistatic limit, the equation for the scalar field reduces to [20]

$$\nabla^2\varphi = \alpha \cdot 8\pi G \rho_m w_B \delta_B. \quad (5.48)$$

Let us start with the linear theory and, following [20], look for two of the four independent solutions of the system in which the density and the velocity of the species B differ from those of the species A by a (possibly time-dependent) bias factor b ,

$$\delta_k^{(A)}(\eta) = D(\eta) \delta_0(\vec{k}), \quad (5.49)$$

$$\theta_k^{(A)}(\eta) = -\mathcal{H}(\eta) f(\eta) \delta_k^{(A)}(\eta), \quad (5.50)$$

$$\delta_k^{(B)}(\eta) = b(\eta) \delta_k^{(A)}(\eta), \quad (5.51)$$

$$\theta_k^{(B)}(\eta) = -\mathcal{H}(\eta) f(\eta) \delta_k^{(B)}(\eta), \quad (5.52)$$

where we have defined $\theta^{(X)} \equiv \vec{\nabla} \cdot \vec{v}_X$ and $\delta_0(\vec{k})$ is a Gaussian random variable. Plugging this ansatz in Eqs. (5.44)–(5.48) and using the background Friedmann equations for a flat universe, we find, at linear order,

$$f = \frac{d \ln D}{d \ln a}, \quad (5.53)$$

$$\frac{df}{d \ln a} + f^2 + \left(2 - \frac{3}{2}\Omega_m\right) f - \frac{3}{2}\Omega_m(w_A + w_B b) = 0, \quad (5.54)$$

$$\frac{db}{d \ln a} = 0, \quad (5.55)$$

$$w_B b + w_A \left(1 - \frac{1}{b}\right) - w_B(1 + 2\alpha^2) = 0. \quad (5.56)$$

Using Eqs. (5.53) and (5.54), the linear growth factor D satisfies a second-order equation,

$$\frac{d^2 D}{d \ln a^2} + \left(2 - \frac{3}{2}\Omega_m\right) \frac{dD}{d \ln a} - \frac{3}{2}\Omega_m(w_A + w_B b)D = 0, \quad (5.57)$$

whose growing and decaying solutions are D_+ and D_- . Note that Eq. (5.55) implies that the bias b is time independent. In the absence of EP violation ($\alpha = 0$) we get $b = 1$ (using $w_A + w_B = 1$) and we recover from Eq. (5.57) the usual evolution of the growth of matter perturbations.

Following [21, 22], we introduce $y \equiv \ln D_+$ as the time variable. Defining the field multiplet

$$\Psi_a \equiv \begin{pmatrix} \delta^{(A)} \\ -\theta^{(A)}/\mathcal{H}f_+ \\ \delta^{(B)} \\ -\theta^{(B)}/\mathcal{H}f_+ \end{pmatrix}, \quad (5.58)$$

the equations of motion of the two fluids can be then written in a very compact form as

$$\partial_y \Psi_a(\vec{k}) + \Omega_{ab} \Psi_b(\vec{k}) = \gamma_{abc} \Psi_b(\vec{k}_1) \Psi_c(\vec{k}_2), \quad (5.59)$$

where integration over \vec{k}_1 and \vec{k}_2 is implied on the right-hand side. The entries of γ_{abc} vanish except for

$$\begin{aligned} \gamma_{121} = \gamma_{343} &= (2\pi)^3 \delta_D(\vec{k} - \vec{k}_1 - \vec{k}_2) \frac{\vec{k}_1 \cdot (\vec{k}_1 + \vec{k}_2)}{k_1^2}, \\ \gamma_{222} = \gamma_{444} &= (2\pi)^3 \delta_D(\vec{k} - \vec{k}_1 - \vec{k}_2) \frac{\vec{k}_1 \cdot \vec{k}_2 (\vec{k}_1 + \vec{k}_2)^2}{2k_1^2 k_2^2}, \end{aligned} \quad (5.60)$$

the matrix Ω_{ab} reads

$$\Omega_{ab} = \begin{pmatrix} 0 & -1 & 0 & 0 \\ -\frac{3}{2} \frac{\Omega_m}{f_+^2} w_A & \frac{3}{2} \frac{\Omega_m}{f_+^2} (w_A + b w_B) - 1 & -\frac{3}{2} \frac{\Omega_m}{f_+^2} w_B & 0 \\ 0 & 0 & 0 & -1 \\ -\frac{3}{2} \frac{\Omega_m}{f_+^2} w_A & 0 & -\frac{3}{2} \frac{\Omega_m}{f_+^2} (w_B b + w_A (1 - \frac{1}{b})) & \frac{3}{2} \frac{\Omega_m}{f_+^2} (w_A + b w_B) - 1 \end{pmatrix}, \quad (5.61)$$

and we have employed Eq. (5.56) to replace the dependence on α^2 by a dependence on the bias b . The solution of Eq. (5.59) can be formally written as

$$\Psi_a(y) = g_{ab}(y) \phi_b + \int_0^y dy' g_{ab}(y - y') \gamma_{bcd} \Psi_c(y') \Psi_d(y'), \quad (5.62)$$

where ϕ_b is the initial condition, $\phi_b = \Psi_b(y = 0)$, and $g_{ab}(y)$ is the linear propagator which is given by [21]

$$g_{ab}(y) = \frac{1}{2\pi i} \int_{\xi - i\infty}^{\xi + i\infty} d\omega (\omega I + \Omega)_{ab}^{-1} e^{\omega y}, \quad (5.63)$$

where ξ is a real number larger than the real parts of the poles of $(\omega I + \Omega)^{-1}$.

In the following we consider small couplings to the fifth force, $\alpha^2 \ll 1$, which by virtue of Eq. (5.56) implies $b \simeq 1$. In this case, it is reasonable to use the approximation $f_+^2 \simeq \Omega_m$, which for $b = 1$ is very good throughout the whole evolution [23]. We choose to use this approximation because it considerably simplifies the presentation but one can easily drop it and make an exact computation. The linear evolution is characterized by four modes. Expanding for small $b - 1$, apart from the ‘‘adiabatic’’ growing and decaying modes already introduced above, respectively going as $D_+ = e^y$ and $D_- = e^{-\frac{3}{2}[1+w_B(b-1)]y}$, one finds two ‘‘isodensity’’ modes, one decaying as $D_i = e^{-\frac{1}{2}[1+3(1+w_A)(b-1)]y}$ and an almost constant one going as $D_c = e^{3w_A(b-1)\alpha^2 y}$.⁴

We are interested in the equal-time 3-point function involving the two species. In particular, we compute

$$\langle \delta_{\vec{k}_3}^-(\eta) \delta_{\vec{k}_1}^{(A)}(\eta) \delta_{\vec{k}_2}^{(B)}(\eta) \rangle = w_A \langle \Psi_1(k_3, \eta) \Psi_1(k_1, \eta) \Psi_3(k_2, \eta) \rangle + w_B \langle \Psi_3(k_3, \eta) \Psi_1(k_1, \eta) \Psi_3(k_2, \eta) \rangle, \quad (5.64)$$

where $\delta \equiv w_A \delta^{(A)} + w_B \delta^{(B)}$. The calculation can be straightforwardly done at tree level by perturbatively expanding the solution (5.62) as $\Psi_a = \Psi_a^{(1)} + \Psi_a^{(2)} + \dots$, which up to second order in δ_0 yields

$$\begin{aligned} \Psi_a^{(1)}(y) &= \mathbf{g}_{ab}(y) \phi_b, \\ \Psi_a^{(2)}(y) &= \int_0^y dy' \mathbf{g}_{ab}(y-y') \gamma_{bcd} \Psi_c^{(1)}(y') \Psi_d^{(1)}(y'), \end{aligned} \quad (5.65)$$

and by applying Wick’s theorem over the Gaussian initial conditions. In the squeezed limit, the expression for (5.64) simplifies considerably. Assuming that the initial conditions are in the most growing mode, i.e. they are given by $\phi_a(\vec{k}) = u_a \delta_0(\vec{k})$ with $u_a = (1, 1, b, b)$, at leading order in $b - 1$ one finds

$$\begin{aligned} \lim_{q \rightarrow 0} \langle \delta_{\vec{q}}(\eta) \delta_{\vec{k}_1}^{(A)}(\eta) \delta_{\vec{k}_2}^{(B)}(\eta) \rangle &\simeq -(b-1) P(q, \eta) P(k, 0) \frac{\vec{k} \cdot \vec{q}}{q^2} \\ &\times \int_0^y dy' e^{2y'} [\mathbf{g}_{11} + \mathbf{g}_{12} - \mathbf{g}_{31} - \mathbf{g}_{32}](y-y'), \end{aligned} \quad (5.66)$$

which shows that the long wavelength adiabatic evolution has no effect on the 3-point function⁵ [12, 13]. Retaining the most growing contribution and using $b \simeq 1 + 2w_B \alpha^2$ one finally finds

⁴With an abuse of language, we denote the modes (+) and (−) as adiabatic and (i) and (c) as isodensity even though, strictly speaking, they do not correspond to the usual notion of adiabatic and isocurvature. Indeed, (+) and (−) correspond to $\delta_A = \delta_B/b$ and not to $\delta_A = \delta_B$ as in the standard adiabatic case, while (i) and (c) yield $w_A \delta^{(A)} + b w_B \delta^{(B)} = 0$ instead of $w_A \delta^{(A)} + w_B \delta^{(B)} = 0$ which one finds in the standard isodensity case (see [12] for a discussion of adiabatic and isodensity modes in the standard case $b = 1$).

⁵For $b = 1$ one finds $\mathbf{g}_{11}^{(+)} = \mathbf{g}_{31}^{(+)}$, $\mathbf{g}_{12}^{(+)} = \mathbf{g}_{32}^{(+)}$, $\mathbf{g}_{11}^{(-)} = \mathbf{g}_{31}^{(-)}$ and $\mathbf{g}_{12}^{(-)} = \mathbf{g}_{32}^{(-)}$.

$$\boxed{\lim_{q \rightarrow 0} \langle \delta_{\vec{q}}(\eta) \delta_{\vec{k}_1}^{(A)}(\eta) \delta_{\vec{k}_2}^{(B)}(\eta) \rangle' \simeq \frac{7}{5} w_B \alpha^2 \frac{\vec{k} \cdot \vec{q}}{q^2} P(q, \eta) P^{(AB)}(k, \eta)}, \quad (5.67)$$

with δ defined in Eq. (5.47) and

$$\langle \delta_{\vec{k}}(\eta) \delta_{\vec{k}'}(\eta) \rangle = (2\pi)^3 \delta_D(\vec{k} + \vec{k}') P(k), \quad \langle \delta_{\vec{k}}^{(X)}(\eta) \delta_{\vec{k}'}^{(Y)}(\eta) \rangle = (2\pi)^3 \delta_D(\vec{k} + \vec{k}') P^{(XY)}(k). \quad (5.68)$$

This corresponds to having $\epsilon = \frac{7}{5} w_B \alpha^2$ in Eq. (5.43). Now that we have an explicit form for the bispectrum $B^{(AB)}(k_1, k_2, k_3)$, defined by

$$\langle \delta_{\vec{k}_1}(\eta) \delta_{\vec{k}_2}^{(A)}(\eta) \delta_{\vec{k}_3}^{(B)}(\eta) \rangle = (2\pi)^3 \delta_D(\vec{k}_1 + \vec{k}_2 + \vec{k}_3) B^{(AB)}(k_1, k_2, k_3). \quad (5.69)$$

I will show in the next part how one can use future galaxy surveys to constrain α .

5.3.2 Estimate of the Signal to Noise

To see how well this effect can be measured, I will present an estimate of the signal to noise. Physically, this quantity measure how far the new bispectrum is from the standard prediction, in unit of the expected variance. The signal to noise calculation closely follows the standard calculation for the case of primordial non-Gaussianities (see for example [24]). We will assume a survey of a given comoving volume V which defines the fundamental scale in momentum space, $k_f = 2\pi/V^{1/3}$. In this setup, the bispectrum estimator is given by

$$B(k_1, k_2, k_3) = \frac{V_f}{V_{123}} \int_{k_1} d^3 q_1 \int_{k_2} d^3 q_2 \int_{k_3} d^3 q_3 \delta(\vec{q}_1 + \vec{q}_2 + \vec{q}_3) \cdot \delta_{\vec{q}_1} \delta_{\vec{q}_2} \delta_{\vec{q}_3}, \quad (5.70)$$

where $V_f = (2\pi)^3/V$ is the volume of the fundamental cell, the integration is done over the spherical shells with bins defined by $q_i \in (k_i - \delta k/2, k_i + \delta k/2)$ and

$$V_{123} \equiv \int_{k_1} d^3 q_1 \int_{k_2} d^3 q_2 \int_{k_3} d^3 q_3 \delta(\vec{q}_1 + \vec{q}_2 + \vec{q}_3) \approx 8\pi^2 k_1 k_2 k_3 \delta k^3. \quad (5.71)$$

We will assume no significant correlation among different triangular configurations or, in other words, that the bispectrum covariance matrix is diagonal and given by a Gaussian statistics. It can be shown that in this case the variance is given by (see for example [24])

$$\Delta B^2(k_1, k_2, k_3) = k_f^3 \frac{S_{123}}{V_{123}} P_{\text{tot}}(k_1) P_{\text{tot}}(k_2) P_{\text{tot}}(k_3), \quad (5.72)$$

where $s_{123} = 6, 2, 1$ for equilateral, isosceles and general triangles, respectively. The power spectrum $P_{\text{tot}}(k)$ is given by

$$P_{\text{tot}}(k) = P(k) + \frac{1}{(2\pi)^3} \frac{1}{\bar{n}}, \quad (5.73)$$

where the last term on the right hand side accounts for the shot noise and \bar{n} is the number density of galaxies in the survey. In what follows we will neglect the shot noise contribution because we want to estimate the total amount of signal in principle available for a survey of a given volume, without restricting our analysis specifically to galaxy surveys. Moreover, for our estimates we will use only modes that are in the linear regime where the shot noise is expected to be negligible.

Given these definitions, the signal-to-noise ratio is calculated as

$$\left(\frac{S}{N}\right)^2 = \sum_T \frac{(B_{\text{new physics}}(k_1, k_2, k_3) - B_{\text{standard}}(k_1, k_2, k_3))^2}{\Delta B^2(k_1, k_2, k_3)}, \quad (5.74)$$

where the sum runs over all possible triangles formed by \vec{k}_1 , \vec{k}_2 and \vec{k}_3 given k_{\min} and k_{\max} . Typically, the sum is written down such that the same triangles are not counted twice and the symmetry factor s_{123} takes care of special configurations. In our case, with two different species of particles, the bispectrum is not symmetric when momenta are exchanged and the previous equations have to be modified accordingly. We will impose $s_{123} = 1$ for all configurations and the sum over triangles will be

$$\sum_T \equiv \sum_{k_1=k_{\min}}^{k_{\max}} \sum_{k_2=k_{\min}}^{k_{\max}} \sum_{k_3=k_{\min}^*}^{k_{\max}^*}, \quad (5.75)$$

where $k_{\min}^* \equiv \max(k_{\min}, |\vec{k}_1 - \vec{k}_2|)$, $k_{\max}^* \equiv \min(|\vec{k}_1 + \vec{k}_2|, k_{\max})$ and the discrete sum is done with $|\vec{k}_{\max} - \vec{k}_{\min}|/\delta k$ steps where δk is a multiple of k_f . In the following we fix $\delta k = k_f$.

Now that we have defined the estimator, we apply it to the case of violation of the EP. We will not restrict ourselves to squeezed triangle configurations but we exploit all possible triangular configurations of Eq. (5.64).

In the case at hand, the signal to noise takes the form

$$\left(\frac{S}{N}\right)^2 = \sum_T \frac{[B_{\alpha^2}^{(AB)}(k_1, k_2, k_3) - B_{\alpha^2=0}^{(AB)}(k_1, k_2, k_3)]^2}{\Delta[B^{(AB)}]^2(k_1, k_2, k_3)}, \quad (5.76)$$

the sum T is described in Eq. (5.75). k_{\min} given by the size of the survey $k_{\min} = 2\pi/V^{1/3}$ and k_{\max} signals when linear theory breaks down. I will take $k_{\max} = \pi/(2R)$ where R is chosen in such a way that linear density fluctuations of the matter field in a sphere of radius R have a root mean squared σ_R (defined in Eq. (1.27)) equal to 0.5.

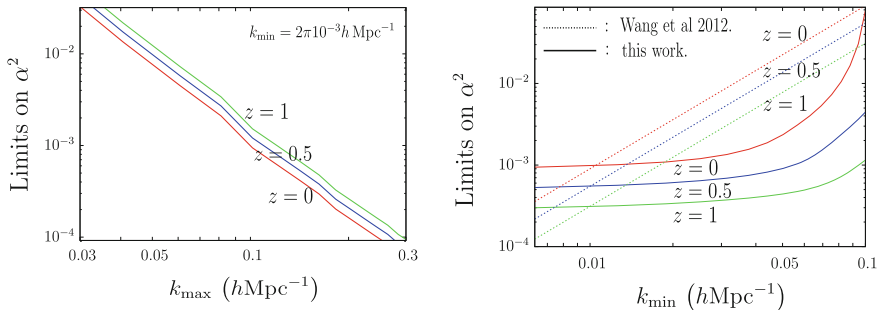


Fig. 5.5 Limits on α^2 for a survey with volume $V = 1(\text{Gpc}/h)^3$ at three different redshifts, $z = 0$, $z = 0.5$ and $z = 1$. *Left* Expected bound on α^2 as a function of k_{\max} . We have chosen $k_{\min} = 2\pi/V^{1/3}$ so that the violation of the EP extends to the whole survey. *Right* Expected bound on α^2 as a function of k_{\min} . k_{\max} is given by 0.10, 0.14, 0.19 $h \text{Mpc}^{-1}$ for $z = 0, 0.5, 1$ respectively. The *dotted lines* represent $\alpha^2 \lesssim 10^{-6} (\text{m}/\text{H})^2$, i.e. the bound on α^2 from screening the Milky Way [25]

Moreover, the bispectra are computed using perturbation theory in the full case (not only in the squeezed limit $q \ll k$) to gain access to more modes. To get the limit on the detectability of EP violations in our model, one requires that the signal to noise (5.76) is of order one. The constraints are shown in Fig. 5.5.

The variance of the mixed bispectrum is given by

$$\Delta[B^{(AB)}]^2(k_1, k_2, k_3) = k_f^3 \frac{S_{123}}{V_{123}} P(k_1) P^{(A)}(k_2) P^{(B)}(k_3), \quad (5.77)$$

On the left panel, the constraints are compared with that for chameleon models derived in Ref. [25] from requiring that the Milky Way must be screened. This yields

$$\alpha^2 \lesssim 10^{-6} (\text{m}/\text{H})^2. \quad (5.78)$$

On the left panel one sees a improvement of the bound when increasing the redshift. This comes from the fact that, when going back in time, structures are less formed and the linear regime extends to larger k . This is why the choice of k_{\max} increases with z .

Let me comment now on the applicability of such results.

First, it should be kept in mind that this is only a toy model, to get an estimate. The form of ϵ in (5.43) is model dependent and in general is different from the value obtained in Eq. (5.67). The robustness is really that ϵ vanishes when there are no violation of EP. However, the simple model gives an order of magnitude of what can be expected.

The next to leading order $\mathcal{O}[(q/k)^0]$ is also very model dependent. If one wants to use as much modes as possible and not restrict to $q/k \ll 1$, this form has to be specified. For example, a scale dependent bias gives in general contributions and one should marginalize over it, which would deteriorate the constraints. Nevertheless,

the peculiar scale and angular dependences of the signal we want to probe give hope that this effect should not be large.

There are two main scenarios for A and B where our model with a fifth force could apply.

- Species A are baryons and B dark matter. While the absence of fifth force is well tested on Earth for baryons [26], the dark matter sector is less constrained, even though Planck already constrains $\alpha^2 \lesssim 10^{-4}$ [27]. However, this situation is not ideal from an observational point of view: it is hard to separate galaxies into baryons and dark matter, since they all have fairly similar baryon to dark matter ratio.
- The second scenario would be when A represents screened objects and B unscreened. This is also challenging. Indeed, for chameleon theories, the requirement that the Milky way is screened implies [25]

$$\alpha^2 \lesssim 10^{-6} (m/H)^2, \quad (5.79)$$

where m is the Compton mass of the chameleon. In this case k_{\min} can be identified with m , the inverse of the Compton wavelength of the chameleon. Figure 5.5 shows that the condition (5.79) is already pretty restrictive, though for $m \gtrsim 0.01 h \text{ Mpc}^{-1}$, our constraints are better.

Another difficulty is that for galaxies to be unscreened, they need to have a smaller gravitational potential than the Milky Way, while it is typically the opposite in galaxy surveys.

5.4 Conclusions

On cosmological scales, there are few tests as robust and simple as consistency relations. Using the Equivalence Principle as well as the Gaussianity of the initial conditions, one can derive relations between the $(n+1)$ -point and n -point correlation functions, when one of the mode is much longer than the others. This long mode is the only one that needs to be dealt with explicitly (using linear perturbation theory), while no additional information on the short modes is necessary. This means one does not have to worry about baryons, bias, shell-crossing, etc., when using these relations, which makes them very robust. In this chapter, I proved that this robustness extends further. Indeed, they hold regardless of the size of the displacement caused by the long mode. Moreover, they translate very easily in redshift space, where observations are made. Therefore, by looking for potential violations of these relations, one can put constraints on non-Gaussianity⁶ [24] that will in the future surpass those from Planck [30].

⁶Another promising mean of probing non-Gaussianity in the large scale structure is through scale-dependent bias [28, 29].

For the late universe, they allow to test deviations from the Equivalence Principle, which is a central property of Λ CDM+GR. Once the accelerated expansion is assumed to come from a scalar field, this opens the gate to new couplings that may not obey this principle.

By means of a simple toy model, I have given the bounds on EP violations one can expect from testing consistency relations in large scale structure. Although the bounds are not competitive with local tests, I want to emphasize that this is a unique test that probes the EP on cosmological scales. It is precisely at this scales that the laws of gravity need to be modified to account for the acceleration and we do not have yet a definite idea on how to do it. Thus, the model independence of this test makes it essential to better understand our Universe.

References

1. **Planck Collaboration** Collaboration, R. Adam, et al., Planck 2015 results. I. Overview of products and scientific results. 1502.01582
2. A. Kehagias, A. Riotto, Symmetries and consistency relations in the large scale structure of the universe, Nucl. Phys. **B873**, 514–529 (2013). 1302.0130
3. M. Peloso, M. Pietroni, Galilean invariance and the consistency relation for the nonlinear squeezed bispectrum of large scale structure, JCAP **1305**, 031 (2013). 1302.0223
4. P. Creminelli, M. Zaldarriaga, Single field consistency relation for the 3-point function. JCAP **0410**, 006 (2004). astro-ph/0407059
5. J.M. Maldacena, Non-Gaussian features of primordial fluctuations in single field inflationary models. JHEP **0305**, 013 (2003). astro-ph/0210603
6. P. Creminelli, J. Noreña, M. Simonović, F. Vernizzi, Single-field consistency relations of large scale structure. JCAP **1312**, 025 (2013). 1309.3557
7. P. Creminelli, J. Gleyzes, M. Simonović, F. Vernizzi, Single-field consistency relations of large scale structure. Part II: Resummation and redshift space. JCAP **1402** 051 (2014). 1311.0290
8. P. Creminelli, J. Gleyzes, L. Hui, M. Simonović, F. Vernizzi, Single-field consistency relations of large scale structure. Part III: Test of the equivalence principle. JCAP **1406**, 009 (2014). 1312.6074
9. F. Bernardeau, S. Colombi, E. Gaztanaga, R. Scoccimarro, Large scale structure of the universe and cosmological perturbation theory. Phys. Rep. **367**, 1–248 (2002). astro-ph/0112551
10. B. Jain, E. Bertschinger, Selfsimilar evolution of cosmological density fluctuations. Astrophys. J. **456**, 43 (1996). astro-ph/9503025
11. R. Scoccimarro, J. Frieman, Loop corrections in nonlinear cosmological perturbation theory. Astrophys. J. Suppl. **105**, 37 (1996). astro-ph/9509047
12. F. Bernardeau, N. Van de Rijt, F. Vernizzi, Resummed propagators in multi-component cosmic fluids with the eikonal approximation. Phys. Rev. **D85**, 063509 (2012). 1109.3400
13. F. Bernardeau, N. Van de Rijt, F. Vernizzi, Power spectra in the eikonal approximation with adiabatic and nonadiabatic modes. Phys. Rev. **D87**(4), 043530 (2013). 1209.3662
14. D. Blas, M. Garny, T. Konstandin, On the non-linear scale of cosmological perturbation theory. JCAP **1309**, 024 (2013). 1304.1546
15. J.J.M. Carrasco, S. Foreman, D. Green, L. Senatore, The 2-loop matter power spectrum and the IR-safe integrand. JCAP **1407**, 056 (2014). 1304.4946
16. D. Seery, M.S. Sloth, F. Vernizzi, Inflationary trispectrum from graviton exchange. JCAP **0903**, 018 (2009). 0811.3934
17. L. Leblond, E. Pajer, Resonant trispectrum and a dozen more primordial N-point functions. JCAP **1101**, 035 (2011). 1010.4565

18. L. Amendola, Coupled quintessence. *Phys. Rev. D* **62**, 043511 (2000). astro-ph/9908023
19. L. Hui, A. Nicolis, C. Stubbs, Equivalence principle implications of modified gravity models. *Phys. Rev. D* **80**, 104002 (2009). 0905.2966
20. F. Saracco, M. Pietroni, N. Tetradis, V. Pettorino, G. Robbers, Non-linear matter spectra in coupled quintessence. *Phys. Rev. D* **82**, 023528 (2010). 0911.5396
21. M. Crocce, R. Scoccimarro, Renormalized cosmological perturbation theory. *Phys. Rev. D* **73**, 063519 (2006). astro-ph/0509418
22. G. Somogyi, R.E. Smith, Cosmological perturbation theory for baryons and dark matter I: one-loop corrections in the RPT framework. *Phys. Rev. D* **81**, 023524 (2010). 0910.5220
23. R. Scoccimarro, S. Colombi, J.N. Fry, J.A. Frieman, E. Hivon, A. Melott, Nonlinear evolution of the bispectrum of cosmological perturbations. *Astrophys. J.* **496**, 586 (1998). astro-ph/9704075
24. R. Scoccimarro, E. Sefusatti, M. Zaldarriaga, Probing primordial non-Gaussianity with large-scale structure. *Phys. Rev. D* **69**, 103513 (2004). astro-ph/0312286
25. J. Wang, L. Hui, J. Khoury, No-go theorems for generalized Chameleon field theories. *Phys. Rev. Lett.* **109**, 241301 (2012). 1208.4612
26. S. Schlamminger, K.-Y. Choi, T. Wagner, J. Gundlach, E. Adelberger, Test of the equivalence principle using a rotating torsion balance. *Phys. Rev. Lett.* **100**, 041101 (2008). 0712.0607
27. V. Pettorino, Testing modified gravity with Planck: the case of coupled dark energy. *Phys. Rev. D* **88**(6), 063519 (2013). 1305.7457
28. N. Dalal, O. Doré, D. Huterer, A. Shirokov, The imprints of primordial non-gaussianities on large-scale structure: scale dependent bias and abundance of virialized objects. *Phys. Rev. D* **77**, 123514 (2008). 0710.4560
29. M. Alvarez, T. Baldauf, J.R. Bond, N. Dalal, R. de Putter, et al., *Testing Inflation with Large Scale Structure: Connecting Hopes with Reality*. 1412.4671
30. **Planck Collaboration** Collaboration, P. Ade, et al., Planck 2015 results. XVII. Constraints on primordial non-Gaussianity. 1502.01592

Chapter 6

Conclusion

6.1 Summary

In this thesis, I have condensed what I thought were the most interesting results that I obtained during my Ph.D. I have voluntarily left out parts of the technical details and focused on the physical origin of these results, as well as their impact.

In Chap. 2, I explained how we developed a very general parametrization for linear perturbations, called the Effective Field Theory of Dark Energy (EFT of DE). It is largely model independent since it is based mainly on symmetry considerations inherited from the spatially homogeneous structure of our Universe. In this approach, the deviations from Λ CDM are given in terms of a minimal set of five functions of time. These functions can be related to virtually every model of modified cosmology, but the real strength of this approach is that it is not necessary to do so. Theoretical, as well as observational [1] constraints can be put directly on these parameters, shaping our understanding of linear cosmology without having to rely on a specific model.

By extending the stability conditions found in this chapter to the non linear case, we devised a set of Lagrangians that go beyond what was believed to be the most general stable scalar-tensor theories. I gave an overview of these new theories, called G^3 , and their genesis in Chap. 3, along with a very general procedure that allows to identify well posed theories. The main goal behind this work was to convince the community not to discard every theory with higher order derivatives in their equations of motion. In the case of G^3 , I have presented the unusual mixing that occurs between matter and scalar perturbations already at the linear level, using the EFT of DE.

Turning now specifically to tensor modes, in Chap. 4 I have shown that their standard predictions from single field inflation are very robust. In principle, the action for tensors can be non standard because of the presence of an extra scalar. However, using field redefinitions, I have shown that one can always return to the usual case at the linear level. Even at the next order in perturbations, the choice of modifications is rather limited. This means that the power spectrum is always given solely in term

of the Hubble parameter H , which represents the energy scale of inflation and that non-Gaussianity cannot be enhanced. As a corollary, this proves that a scale invariant power spectrum for gravity waves constitutes very strong evidence for inflation.

Section 5.11 was dedicated to an approach somewhat different from the others. It was not focused on scalar-tensor theories *per se*, but rather on very robust tests called consistency relations. They are relations between correlation functions of the density contrast δ in the limit where one (or several) of the momenta becomes much smaller than the others. To use them does not require any knowledge of the short scale behavior, where non linearities and baryonic physics play an important role. They are very useful to probe the non-Gaussianity in the initial conditions and/or the Equivalence Principle, that can be violated in theories alternative to Λ CDM.

6.2 Outlook

While writing the thesis, I have also been working on extending the formalism of the EFT of DE to the case where dark matter is non minimally coupled to the scalar field, whereas baryons are only coupled to gravity (a sort of generalization of Sect. 5.3.1). This scenario has been well studied in the literature, beginning with conformal couplings of the form ϕT_{μ}^{μ} [2] and more recently disformal ones $\phi_{\mu}\phi_{\nu}T^{\mu\nu}$ in [3] for example. What is usually done in these studies is to assume that gravity is described by GR, on top of which one adds a quintessence scalar field. The idea we had was to consider a general conformal plus disformal coupling for dark matter (that is, $\tilde{g}_{\mu\nu}T^{\mu\nu}$, with $\tilde{g}_{\mu\nu}$ given by Eq. (3.41)) combined with modifications of gravity as in Chap. 2. In particular, this brings two additional functions of time to the analysis, which are going to change the stability conditions of Sect. 2.4 and the phenomenology discussed in Sect. 2.5.3.3. The results can be found in two publications, [4, 5].

Another possible direction of research is to investigate the equation for Ψ , Eq. (2.86), which is the combination of Einstein's equations into a single one. It would certainly be interesting to solve it numerically. Even analytically, this should allow oneself to probe the modifications of gravity in a regime where the quasistatic approximation starts to break down. Bellini and Sawicki have started to look into this recently [6], where they show that in general the quasistatic regime breaks down at the sound horizon, $kc_s \sim aH$. I think there are still much information that can be extracted from this equation, in particular concerning relativistic effects.

The exploration of theories beyond Horndeski is just at its beginning. The goal would be to find a necessary and sufficient condition for Lorentz invariant scalar-tensor theories to be stable, that can be checked straightforwardly from the action. Requiring second-order EOM does not fulfill all these requirements since I showed in Chap. 3 that it is not necessary. The Hamiltonian analysis in unitary gauge of Sect. 3.4 also falls short, since it is not a Lorentz invariant proof. Doing it from the covariant Lagrangian, i.e. without choosing a specific gauge, is bound to be an extremely cumbersome computation, which cannot be classified as straightforward. The existence of field redefinitions that map the theory to a stable one, on top of not

being necessary, cannot qualify as a straightforward check either, since one has in general to guess a specific transformation for each theory. Our proposal sparked a renewed interest in defining well posed theories, improving on the methods that we used [7–12].

Concerning more particularly our proposal, G^3 , people have started to look at its non linear behavior [13]. It was shown that contrarily to the Horndeski case, where non linearities allow to fully recover GR on small scales (through Vainshtein screening), in G^3 the gravitational potentials differs from that of GR inside sources, such as stars. This was latter used in [14] to study the evolution of stars for a specific G^3 Lagrangian. In [15], we derived the very general modification due to this non standard behavior in the Lane-Emden equation [16], that governs the profile of stars for a polytropic fluid. In particular, we found a generic bound on the parameter α_H of Chap. 2 for the existence of physical solutions to this equation. The effects of the breaking of Vainshtein screening in G^3 theories in stars has been further studied in [17–19].

Let me end with some considerations on consistency relations. The theoretical community has really shown a frank enthusiasm regarding these relations, as seen by the number of authors that have recently published on the subject [20–23]. It has been proposed to test the origin of magnetic fields [24], and as a mean to compute higher order corrections to the linear power spectrum [25]. What I think would be interesting is to check these relations in N-body simulations, where one is not limited to equal times correlators, but can actually look at the r.h.s. of Eq. (5.13).

References

1. **XXX Collaboration** Collaboration, P. Ade et al., Planck 2015 results. XIV. Dark energy and modified gravity. 1502.01590
2. L. Amendola, Coupled quintessence. Phys. Rev. D **62**, 043511 (2000). astro-ph/9908023
3. M. Zumalacárregui, T. Koivisto, D. Mota, P. Ruiz-Lapuente, Disformal scalar fields and the dark sector of the universe. JCAP **1005**, 038 (2010). 1004.2684
4. J. Gleyzes, D. Langlois, M. Mancarella, F. Vernizzi, Effective theory of interacting dark energy. JCAP, **1508**(08), 054 (2015). 1504.05481
5. J. Gleyzes, D. Langlois, M. Mancarella, F. Vernizzi, Effective theory of dark energy at redshift survey scales. JCAP **1602**(02), 056 (2016). 1509.02191
6. I. Sawicki, E. Bellini, Limits of quasistatic approximation in modified-gravity cosmologies. Phys. Rev. **D92**(8), 084061 (2015). 1503.06831
7. C. Deffayet, G. Esposito-Farese, D.A. Steer, Counting the degrees of freedom of generalized Galileons. Phys. Rev. **D92**, 084013 (2015). 1506.01974
8. D. Langlois, K. Noui, Degenerate higher derivative theories beyond Horndeski: evading the Ostrogradski instability. JCAP **1602**(02) 034 (2016). 1510.06930
9. D. Langlois, K. Noui, Hamiltonian analysis of higher derivative scalar-tensor theories. 512.06820
10. M. Crisostomi, M. Hull, K. Koyama, G. Tasinato, Horndeski: beyond, or not beyond? JCAP **1603**(03) 038 (2016). 1601.04658
11. J.B. Achour, D. Langlois, K. Noui, Degenerate higher order scalar-tensor theories beyond Horndeski and disformal transformations. 1602.08398

12. M. Crisostomi, K. Koyama, G. Tasinato, Extended Scalar-Tensor Theories of Gravity. 1602.03119
13. T. Kobayashi, Y. Watanabe, D. Yamauchi, Breaking of Vainshtein screening in scalar-tensor theories beyond Horndeski. Phys. Rev. **D91**(6) 064013 (2015). 1411.4130
14. K. Koyama, J. Sakstein, Astrophysical Probes of the vainshtein mechanism: stars and galaxies. Phys. Rev. **D91**, 124066 (2015). 1502.06872
15. R. Saito, D. Yamauchi, S. Mizuno, J. Gleyzes, D. Langlois, Modified gravity inside astrophysical bodies. JCAP **1506**, 008 (2015). 1503.01448
16. S. Chandrasekhar, *An Introduction to the Study of Stellar Structure III* (The University of Chicago Press, Chicago, 1939)
17. J. Sakstein, Testing gravity using dwarf stars. Phys. Rev. **D92**, 124045 (2015). 1511.01685
18. J. Sakstein, K. Koyama, Testing the Vainshtein mechanism using stars and galaxies. Int. J. Mod. Phys. **D24**(12), 1544021 (2015)
19. R.K. Jain, C. Kouvaris, N.G. Nielsen, White Dwarf Critical Tests for Modified Gravity. 1512.05946
20. A. Joyce, J. Khoury, M. Simonović, Multiple soft limits of cosmological correlation functions. JCAP **1501**(01), 012 (2015). 1409.6318
21. A. Kehagias, A.M. Dizgah, J. Noreña, H. Perrier, A. Riotto, A consistency relation for the observed galaxy bispectrum and the local non-gaussianity from relativistic corrections. JCAP **1508**(08), 018 (2015). 1503.04467
22. B. Horn, L. Hui, X. Xiao, Lagrangian space consistency relation for large scale structure. JCAP **1509**(09), 068 (2015). 1502.06980
23. T. Nishimichi, P. Valageas, Redshift-space equal-time angular-averaged consistency relations of the gravitational dynamics. Phys. Rev. **D92**(12), 123510 (2015). 1503.06036
24. R.K. Jain, M.S. Sloth, Consistency relation for cosmic magnetic fields. Phys.Rev. **D86**, 123528 (2012). 1207.4187
25. C. Wagner, F. Schmidt, C.T. Chiang, E. Komatsu, The angle-averaged squeezed limit of non-linear matter N-point functions. JCAP **1508**(08), 042 (2015). 1503.03487

Curriculum Vitae

Jérôme Gleyzes

Postdoctoral Scholar at JPL
Office 169-237, JPL, 4800 Oak Grove Drive
91109 Pasadena, CA, USA
jerome.L.gleyzes@jpl.nasa.gov



Education

- 2012–2015** **Doctorate**, *Institut de Physique Théorique-CEA Saclay*, Paris, (with distinctions)
- 2010–2012** **Master**, *Ecole Normale Supérieure*, Paris, (with distinctions)
Specialty: Theoretical Physics
- 2009–2010** **Bachelor of Science**, *Ecole Normale Supérieure*, Paris, (with distinctions)

Ph.D (2012–2015)

Title *Dark Energy and the Large Scale Structure of the Universe*
Supervisor Dr. Filippo Vernizzi

List of Publications

- [1] **Essential Building Blocks of Dark Energy**, JCAP 1308 (2013) 025, [[arXiv:1304.4840](#)], J. Gleyzes, D. Langlois, F. Piazza, F. Vernizzi.
- [2] **Single-Field Consistency Relations of Large Scale Structure. Part II: Resummation and Redshift Space**, JCAP 1402 (2014) 051, [[arXiv:1311.0290](#)], P. Creminelli, J. Gleyzes, M. Simonović, F. Vernizzi.
- [3] **Single-Field Consistency Relations of Large Scale Structure. Part III: Test of the Equivalence Principle**, JCAP 1406 (2014) 009, [[arXiv:1312.6074](#)], P. Creminelli, J. Gleyzes, L. Hui, M. Simonović, F. Vernizzi.
- [4] **Healthy theories beyond Horndeski**, Phys. Rev. Lett. 114 (2015) no. 21, 211101, [[arXiv:1404.6495](#)], J. Gleyzes, D. Langlois, F. Piazza, F. Vernizzi
- [5] **Resilience of the standard predictions for primordial tensor modes**, Phys. Rev. Lett. 113 (2014) no. 23, 231301, [[arXiv:1407.8439](#)], P. Creminelli, J. Gleyzes, J. Noreña, F. Vernizzi.
- [6] **Exploring gravitational theories beyond Horndeski**, JCAP 1502 (2015) 018, [[arXiv:1408.1952](#)], J. Gleyzes, D. Langlois, F. Piazza, F. Vernizzi.
- [7] **A unifying description of dark energy**, Int.J.Mod.Phys. D23 (2015) no. 13, 1443010, [[arXiv:1411.3712](#)], J. Gleyzes, D. Langlois, F. Vernizzi.
- [8] **Modified gravity inside astrophysical bodies**, JCAP 1506 (2015) 008, [[arXiv:1503.01448](#)], R. Saito, D. Yamauchi, S. Mizuno, J. Gleyzes, D. Langlois.
- [9] **Effective Theory of Interacting Dark Energy**, JCAP 1508 (2015) no. 08, 054, [[arXiv:1504.05481](#)], J. Gleyzes, D. Langlois, M. Mancarella, F. Vernizzi.
- [10] **Effective Theory of Dark Energy at Redshift Survey Scales**, JCAP 1602 (2016) no. 02, 056, [[arXiv:1509.02191](#)], J. Gleyzes, D. Langlois, M. Mancarella, F. Vernizzi.

Talks

26/11/14	ITP, Heidelberg, Germany	<i>Healthy theories beyond Horndeski</i>
19/11/14	ITF, Utrecht, the Netherlands	<i>Uniting theories and observations: the Essential Building Blocks of Dark Energy</i>
03/11/14	IAP, Paris, France	<i>Uniting theories and observations: the Essential Building Blocks of Dark Energy</i>
10/09/14	Columbia University, NYC, USA	<i>Healthy theories beyond Horndeski</i>
08/09/14	UPenn, Philadelphia, USA	<i>Healthy theories beyond Horndeski</i>

03/09/14	CWRU, Cleveland, OH	<i>Healthy theories beyond Horndeski</i>
02/07/14	LPT, Orsay, France	<i>Healthy theories beyond Horndeski</i>
24/05/14	APC, Paris, France	<i>Healthy theories beyond Horndeski</i>
16/04/14	PONTC conference, Avignon, France	<i>Consistency relations for the large scale structures</i>
12/06/13	ICG, Portsmouth, UK	<i>The Effective Field Theory of Dark Energy</i>
11/06/13	DAMTP, Cambridge, UK	<i>The Effective Field Theory of Dark Energy</i>
10/06/13	University of Oxford, UK	<i>The Effective Field Theory of Dark Energy</i>

Conferences

25/08/14–29/08/14	COSMO 2014, Chicago.
14/07/14–18/07/14	Non-Linear Structure in the Modified Universe, Lorentz Center, Leiden, the Netherlands.
04/08/14–08/08/14	Summer school on Cosmology at the International Center for Theoretical Physics, Trieste.
10/07/14–13/07/14	Cosmological Frontiers in Fundamental Physics 2014, laboratoire APC, Paris.
08/07/13–04/08/13	Les Houches summer school “Post Planck Cosmology”, France.
14/03/13–15/03/13	Cosmological Tests of Gravity, Oxford.
07/02/13–08/02/13	Workshop Dark Energy Phenomenology, at Astroparticule et Cosmologie (APC), Paris.
16/07/12–02/08/12	Summer school on Cosmology at the International Center for Theoretical Physics, Trieste.

References

Filippo Vernizzi	Institut de Physique Théorique, CEA Saclay	filippo.vernizzi@cea.fr
David Langlois	Laboratoire APC, Paris VII	langlois@apc.univ-paris7.fr
Paolo Creminelli	International Center for Theoretical Physics, Trieste	creminel@ictp.it
Federico Piazza	Centre de Physique Théorique, Marseille	Federico.Piazza@cpt.univ-mrs.fr
Pedro Ferreira	University of Oxford	p.ferreira1@physics.ox.ac.uk
Andrew Tolley	Case Western Reserve University, Cleveland	andrew.j.tolley@case.edu